STUDIES ON GRAVITATIONAL WAVES

AND

STARS WITH NEUTRON CORES

Thesis by

Mark Edward Zimmermann

In Partial Fulfillment of the Requirements

for the Degree of

Doctor of Philosophy

California Institute of Technology

Pasadena, California

1980

(Submitted December 10, 1979)

ACKNOWLEDGEMENTS

The individual chapters in this thesis acknowledge separately much of the financial and scientific aid which enabled me to get this work done. Here, I would like to thank the Schlumberger Corporation, the State of California, and the California Institute of Technology for supporting me as a graduate student.

I lack the words to properly express my gratitude for my advisor and the help he has given me. The best I can do is to quote from Murray Rothbard's preface to his treatise on economic principles, Man, Economy, and State (1970, Nash Publishing, Los Angeles), in which Dr. Rothbard speaks of his advisor, Ludwig von Mises. I have changed only a few nouns:

> Apart from my intellectual debt to Professor Kip S. Thorne, I can never fully express my personal debt. His wisdom, insight, kindness, enthusiasm, and unflagging encouragement of even the slightest signs of productivity among his students have been a continuous inspiration to all who know him. He is one of the great teachers of physics, as well as one of the great physicists, and I am grateful to have had the opportunity of studying for many years in his theoretical astrophysics and relativity group at the California Institute of Technology.

ABSTRACT

This thesis reports on investigations in two major areas: astrophysics and relativity. It is divided into six independent chapters.

Chapter I contains estimates of the astrophysically-likely amplitude of gravitational radiation emitted by the Crab and Vela pulsars. For my analysis, I model the pulsars as rapidly-rotating, freely-precessing, rigid or elastic solid bodies. I find that the Crab is likely to produce gravitational waves at Earth with dimensionless amplitude $10^{-27\pm2}$, and that Vela is likely to give waves one or two orders of magnitude larger.

Chapters II and III study the gravitational radiation produced by an idealized rotating and freely-precessing rigid body in the weak-field, slow-motion, small-stresses, quadrupole-moment formalism. Chapter II gives the results for axisymmetric objects and for arbitrarily shaped objects undergoing small-angle precession. In that chapter, I also discuss the application of my results to neutron stars in nature, and I describe in detail how to analyze the incoming waves and extract information about their source. Chapter III extends the analysis of Chapter II to the general case of an arbitrary rigid body undergoing large-angle precession.

Chapter IV considers all astrophysically-reasonable sources of gravitational waves. Based on a minimal set of "cherished beliefs" about the universe and about gravitation, I give general upper limits to the expected intensity of gravitational radiation at the earth, at various frequencies and from a variety of sources.

Chapter V examines a "natural" coordinate system which might be set

up by a rotating and accelerating observer. I expand the metric through second-order terms in distance from the origin of the coordinates; from the metric, I derive the equations of motion for test particles. I identify many forces and pseudoforces in the equations of motion, and I discuss how my results may be used to analyze some laboratory gravitational experiments.

Chapter VI of this thesis is a report on my results in studying nucleosynthesis in stars with neutron-star cores. I was not able to generate any self-consistent models with a total mass of 16 $M_\odot$, core mass of 1 $M_\odot$, and core radius of 10 km; nuclear reactions fell short of producing the needed luminosity by a factor of 25 or more. I describe in detail my modeling procedures and the reasons for the failure of nucleosynthesis, and I point out extensions and modifications of my models which may be more successful.

TABLE OF CONTENTS

INTRODUCTION

Two subjects, astrophysics and relativity, are combined in different proportions in the six papers included in this dissertation. Some of the work which I describe is almost "pure" general relativity; the astrophysical universe supplies only a motivation or an application for the mathematical problem being investigated. Other papers are much more oriented toward the astrophysical; relativity appears, at most, in a weak-field, slow-motion approximation. In either case, relativity and astrophysics act synergistically, so that in their collaboration the whole is more than the sum of the separate parts. On a larger scale, beyond this thesis, the same phenomenon has occurred in modern astronomy. Man's understanding of the universe has been enriched by the influx of ideas from general relativity, especially as they have been applied to "violent" events such as quasars, collapses to form black holes, and the birth of the universe itself. Theoretical relativity has its very raison d'être grounded in astronomically-observed fact, and much of the development of the field has been guided and nurtured by problems posed by astrophysics. More cross-fertilization between the two subjects will certainly follow the first confirmed observation of gravitational radiation.

So, the partnership between astrophysics and relativity which appears in many of these papers is not a new one. The specific object in which that partnership is frequently embodied, the neutron star, is also not new. Speculation about and theoretical work on the structure of neutron stars

has a forty-five-year history, and the evidence accumulated during more than a decade of pulsar observations has both solidified and extended the theoretically-acquired knowledge. The human mind, however, always seems to to retain a fascination with extremes: the highest, the hottest, the smallest, the fastest, etc. As (probably) the densest material objects in the universe, neutron stars have a natural attraction, and they have repaid the attention given them by yielding a stream of discoveries. As central as neutron stars have been to a variety of fields in modern astrophysics, it is fitting that they should supply a central core for several of the investigations reported here.

* * * * * * *

Each of the six chapters in this dissertation is a separate, self-contained paper. In the remainder of this introduction, I will give an overview of the material discussed in each chapter, along with some background information about the research. Four of the six papers have already been published or accepted for publication, a fifth is under consideration by a journal, and the sixth, which is an internal progress report, may eventually form the basis of a published work. Three of the papers were written in collaboration with co-authors; in each case, I did a major part of the work independently and do not hesitate to accept credit (or blame) for the results.

Chapter I, "Revised estimate of gravitational radiation from Crab and Vela pulsars", is a report on an attempt to guess the actual amplitude

of gravitational waves produced by one class of objects: neutron stars, which I idealize as rotating and freely-precessing rigid bodies. The work, which appeared as a letter to Nature, brings up to date some of the estimates made by William Press and Kip Thorne in a more general survey of gravitational-wave sources six years earlier. A major point made by my letter is that the fastest pulsars are not necessarily the strongest sources of gravitational radiation at the Earth; a more slowly rotating neutron star may be closer or may have a larger non-axisymmetry, for example. (More specifically, my best estimates suggest that the Vela pulsar, with period 0.089 s, is likely to produces waves with amplitudes one or two orders of magnitude larger than the Crab pulsar, which has period 0.033 s.) Although this possibility is fairly obvious, it was apparently overlooked or discounted in earlier investigations.

During the preparation of the paper in Chapter I, Roger Blandford pointed out that a quadrupolar electrical charge distribution, rotating at frequency Ω, could emit electromagnetic radiation at frequency Ω as well as at 2Ω. In earlier work on gravitational waves from mechanical systems, it was universally presumed (as far as I have been able to determine) that all of the gravitational quadrupole radiation occurred at frequency 2Ω. This belief is correct for a rigid body rotating about one of its principal axes, but as Roger Blandford suspected, it is not correct in general. Although the astrophysical estimates of gravitational wave amplitudes given in Chapter I turn out to be reasonable in the light of later analyses, the estimates were based on inapplicable formulae and on misconceptions about the nature of the radiation.

Chapters II and III contain the details of the correct analysis of gravitational waves produced by rotating and precessing rigid bodies in the weak-field, slow-motion, small-stresses, quadrupole-moment formalism. Chapter II was written in collaboration with Eugene Szedenits, Jr. He derived the major equations independent of me, checked my results, and kindly and continuously prodded me to get the research finished, written, and published. I am responsible for all of the results and the prose (including all alliteration) in the paper.

Chapter II presents the explicit waveforms radiated by two special cases of freely precessing rigid bodies. The first case is that of an axisymmetric object; the second is that of an arbitrarily-shaped object, precessing with a very small wobble angle. Three new, important results emerge from the calculations for an axisymmetric body: (1) the gravitational radiation comes out at two frequencies, ω and 2ω; (2) the radiation at frequency ω is much stronger than that at frequency 2ω if the wobble angle of the precession is small; and (3) electromagnetic radiation emitted by a point fixed on the surface of the body is seen to arrive in pulses at a frequency Ω differing from the fundamental gravitational frequency ω by the precession frequency. (These three facts also apply, with some modification, to the waves emitted by an asymmetric, rigid, freely precessing body, though that situation is much more complex due to the non-sinusoidal nature of the classical precession.) The new information which Chapter II contains may have important consequences for experimenters (gravitational astronomers) who attempt to observe pulsars as sources of waves. Their task is made harder by the splitting between the electromagnetic and the

gravitational frequencies, since it now is not so clear precisely where they should "listen"; on the other hand, when they begin to detect objects, the gravitational waves will give extensive information about their sources, information which is difficult or impossible to derive from electromagnetic observations. Chapter II discusses how to extract this information from the incoming waves.

Chapter III extends the analysis of Chapter II to the case of a freely precessing rigid body with an arbitrary moment-of-inertia tensor (arbitrarily great deviations from axisymmetry). In that chapter, I present plug-in-and-grind algorithms for computing the gravitational power radiated and the waveforms produced by an arbitrary source. For the special case of a nearly-spherical object precessing with a small wobble angle, I give the dominant terms in the expansions of the power and the waveforms. The expansions retain the exact frequency dependence of the waves which are being produced. It is important to determine the frequency of the waves accurately, since a slight error in the frequency will integrate up to be a large phase error; many proposed experimental schemes to observe gravitational waves from pulsars cannot tolerate sizeable phase errors. The exact results of Chapter III also confirm the special cases calculated in Chapter II.

Chapter IV expands my horizon and examines all astrophysically-likely sources of gravitational radiation. This chapter was written in collaboration with Kip Thorne, and has been accepted for publication in a festschrift in honor of Abraham H. Taub, to appear in 1980. Each of the authors deserves approximately equal credit for the contents. In Chapter IV,

we derive very general upper limits on the intensity of gravitational waves bathing the Earth, based on a minimum set of "cherished beliefs" about the astrophysical universe and about the correct theory of gravitation. The results are given as functions of frequency for extragalactic and for galactic sources, and for discrete objects (bursters, transient sources, and continuous-wave monochromatic sources) as well as for an unresolved (stochastic) background. In several frequency bands, gravitational wave detectors are currently approaching sensitivities at which our "cherished beliefs" permit the detection of gravitational waves--

--a heartening prospect!

Chapter V of this dissertation is mainly theoretical; it examines a "natural" coordinate system which might be used by a gravitational experimenter. This paper describes work all of which was done independently by Wei-Tou Ni (National Tsing Hua University, Taiwan) and by me. In the summer of 1977, when Ni visited Caltech, we discovered that we were both in the process of writing up identical results on the same subject, and so we decided to publish together. The paper contains an analysis of the "local coordinates of an observer's proper reference frame" for an observer who may be both rotating and accelerating relative to an inertial coordinate system, and who may be in a region of spacetime through which gravitational waves are passing. We derived the metric, accurate through second order terms in distance from the origin of the coordinates; from the metric, we obtained the equations of motion for test particles in that coordinate frame. We identified a large number of forces in the equations of motion: Coriolis and centripedal pseudoforces,

electric, magnetic, and magnetic-magnetic Riemann (tidal) forces, and special-relativistic corrections to the Newtonian forces. We also described how our calculations could be used to simplify the analysis of some laboratory gravitational experiments.

The final section of this thesis, Chapter VI, is a detailed, unpublished report on progress I have made in the study of nucleosynthesis in stars with degenerate neutron cores. Several years ago, Kip Thorne and Anna Żytkow began an analysis of stars with neutron-star cores and massive, extended envelopes. They found that such objects could support themselves by steady accretion onto the dense central core if the envelope mass was less than about 10 $M_{\odot}$. More massive envelopes required hydrogen-burning nuclear reactions in order to generate their luminosity. Thorne and Żytkow used one approximation to estimate this nucleosynthetic process, but they warned that a more detailed treatment might significantly change their results. I have undertaken such a treatment, initially in collaboration with Michael Newman, Kip Thorne, and Anna Żytkow, and later working alone.

As Chapter VI describes, my results are quite negative. I could not produce any viable stellar models; in the best of circumstances, nuclear reactions fell short of producing the required luminosity by a factor of about 25. I discuss in detail the modeling procedures I used to calculate nucleosynthesis and the convective transport of reaction products in the stellar envelope. I also describe some possible extensions or modifications of my methods which may be able to produce more successful models. New work is in progress at Santa Cruz (Woosley) and elsewhere on the theory

of ultra-high-temperature nucleosynthesis, and perhaps within a year (or a few years) results will be available which will make models possible under conditions in which current theory finds them impossible.

* * * * * * *

The universe is an exciting place! In particular, the hot or fast or dense objects which bring relativistic effects into prominent display are interesting and rewarding subjects for investigation. Most of the work included in this dissertation has its ultimate roots in my personal fascination with astronomy, which began about the time I was six years old and first looked through a small telescope, and which developed during years of reading and asking stupid questions. I've finally understood a few things, at least in part, and have had some fun describing them in the chapters of this thesis. If I am required to give reasons or motivations for all that I've described herein, I must eventually fall back upon the enjoyment that it has given me. I suspect that the joy of discovering and of explaining one's discoveries is fundamental to a lot of people. If what I've done adds to anyone else's pleasure, or suggests something new and amusing for them to ponder, that's an unexpected bonus!

CHAPTER I

GRAVITATIONAL RADIATION FROM THE CRAB AND VELA PULSARS--A REVISED ESTIMATE

This chapter is a paper which appeared in Nature, Vol. 271, No. 5645, February 9, 1978, pages 524-525. It is reprinted by permission of the publisher, Macmillan Journals Ltd. The research reported in this chapter was supported in part by the National Science Foundation [AST76-80801].

ABSTRACT

A survey of the recently published literature on pulsars yields plausible values for the non-axisymmetric part of the moment of inertia of the Crab and Vela neutron stars. The resulting gravitational radiation luminosity produces a dimensionless strain at Earth of $h \sim 10^{-27\pm2}$. Such strains may be detectable in the future using supercooled high-Q dielectric crystals.

With recent progress in the development of ultra-high-Q dielectric crystals[1], experimenters in the field of general relativity have begun to consider looking for rotation-induced gravitational radiation from pulsars[2,3]. If one could control the frequency of oscillation of a high-Q crystal, keeping it in phase with the electromagnetic signals observed from a pulsar, one might hope to absorb a measurable amount of (quadrupole) gravitational radiation at twice the pulsar frequency. Press and Thorne[4] in 1972 estimated that the gravitational waves from the Crab pulsar would produce a dimensionless strain in a detector on Earth of $h \sim 10^{-26}$ to 10^{-28}, and that other pulsars would be several orders of magnitude fainter. Additional observational data, and progress in pulsar models during the past five years, make a new estimate desirable. I find that the amplitude of the gravitational waves from the Crab pulsar (PSR0531+21) is likely to be within two orders of magnitude of 10^{-27}, but that the Vela pulsar (PSR0833-45) is likely to produce waves of amplitude a factor 10 to 100 larger.

The waves are produced by the rotation of mass asymmetries in the neutron star. Of all conceivable mass asymmetries, conventional pulsar theory[5,6] points to one as the most likely to dominate the radiation: the neutron star must be rotationally flattened with oblateness

$$\varepsilon_o \equiv \frac{\text{(equatorial radius - polar radius)}}{\text{(mean radius)}} .$$

If the star were to rotate about its polar axis of symmetry, it would not radiate gravitationally. However, the observed "restless" behavior of the Crab and Vela rotation periods P [5,7] makes it seem likely[8-11] that the rotation axis and the symmetry axis are misaligned by a small angle θ_w. Such a misalignment would produce a "Chandler wobble" in the star's rotation[9], and

the wobble-induced strains would produce microquakes that provide an attractive and successful explanation[8,10] for the observed "restlessness". The misalignment would also cause a fraction $\varepsilon \equiv \varepsilon_o \theta_w$ (for small θ_w) of the star's moment of inertia I to radiate as a time-changing quadrupole moment. The resulting luminosity in gravitational quadrupole radiation would be[4]

$$L_{GW} = \frac{32G}{5c^5} \varepsilon^2 I^2 \left(\frac{2\pi}{P}\right)^6 \simeq 5 \times 10^{32} \frac{\text{erg}}{\text{s}} \left(\frac{\varepsilon}{2 \times 10^{-6}}\right)^2 \left(\frac{I}{4 \times 10^{44} \text{g-cm}^2}\right)^2 \left(\frac{P}{0.033\text{s}}\right)^{-6}$$

Of the crucial parameters, P is determined by radio and optical observations[7] to great precision. The distances to the pulsars are less well known, but the association with supernova remnants yields distance estimates of 2000 pc and 500 pc for the Crab and Vela respectively, good to within about 25% [7,12]. Neutron-star moments of inertia depend both upon the assumed mass of the star and upon the equation of state of matter at high densities. However, since the stellar radius tends to decrease as mass increases, I is somewhat buffered; early equations of state gave[5] $7 \times 10^{43} \lesssim I \lesssim 7 \times 10^{44}$ g-cm^2, but more recent work suggests[13] $3 \times 10^{44} \lesssim I \lesssim 3 \times 10^{45}$ g-cm^2. Within this range, the original Pines and Shaham[8] "crustquake" explanation of the Crab pulsar glitches agrees with the spindown power output ($I\Omega\dot{\Omega}$) required to drive the nebula[5,14] and implies $I \sim 4 \times 10^{44}$ g-cm^2 (though Pandharipande, Pines, and Smith (PPS) for their 1.33 $M_\odot$ Crab model[13] find $I \sim 2 \times 10^{45}$ g-cm^2). The Vela pulsar, which has experienced at least three "giant" speedups within the past 8 years[7,15] is modelled as a more massive, solid-core object[18] with moment of inertia[13] $I \sim 2$ to 3×10^{45} g-cm^2.

The oblateness of the star, ε_o, is predicted by standard starquake theory and by calculations of the critical strain which the crust (for the

Crab) or the core (for Vela) can withstand before fracturing. The resulting values are, for the Crab[5,8,11], $\varepsilon_o = 1$ to 2×10^{-4} (though the PPS 1.33 $M_\odot$ model[13] has $\varepsilon_o \simeq 3.5\times10^{-4}$), and for Vela[11,13,16], $\varepsilon_o \sim 10^{-2}$ to 10^{-3}. The fraction of this oblateness which is effective in producing gravitational radiation is θ_w, the wobble angle. The microquake theories suggest that θ_w is limited by starquakes to values of the order of 10^{-1} radians[8,10,11]; however, the lack of observed wobble[7] (and in particular, the constancy and sharpness of the optical Crab light curve) suggests that 10^{-1} be taken as an extreme upper bound, and that θ_w probably lies between 10^{-3} and 10^{-2} radians. The wobble question is the most uncertain part of this analysis; see Pines and Shaham[9] for comments and references.

The most probable values for the vital parameters in determining the gravitational luminosity are summarized in Table 1, for the standard Crab model, the PPS[13] (stiff equation of state) 1.33 $M_\odot$ Crab, and for Vela. The resulting gravitational wave luminosity L_{GW}, the energy flux at Earth $\mathcal{F} \equiv L_{GW}/4\pi R^2$, and the wave amplitude (strain, or metric perturbation)[17] $h \equiv (16\pi G\mathcal{F}/c^3\omega_{GW}^2)^{1/2}$, are given, together with their probable ranges using the parameter estimates described above. The errors have been added coherently, not by quadrature, so the range covered is rather large; most of the uncertainty comes from the uncertainty in θ_w.

It is possible, of course, that something is radically wrong with the above assumptions. On the other hand, if internal toroidal magnetic fields exist with $B \gtrsim 10^{15}$G [6,9], they could produce an oblateness $\varepsilon_o \sim 10^{-35}\,(B/1\text{ Gauss})^2$ comparable to or larger than the fluid oblateness. If the protons in the neutron star form a type-II superconductor[18,19] with critical field $H_{c1} = (4 \text{ to } 8)\times10^{14}$G, then in the low-flux-density limit ($B \ll H_{c1}$)

$\varepsilon_o \sim 10^{-35}$ B H_{cl} and so somewhat smaller internal fields may begin to cause a significant oblateness. In both cases, the internal fields may tend to align themselves perpendicular to the spin axis of the star[19] (effectively $\theta_w = 90°$) and would thus be maximally efficient in producing gravitational radiation. An internal field of 10^{15}G would make a wave of amplitude $h \sim 5\times 10^{-27}$ from the Crab's distance; a field of 10^{12}G in a type-II superconductor would produce $h \sim 2\times 10^{-30}$. So it is improbable that h is much less than the minimum estimates (2×10^{-29} for the Crab, and 1×10^{-27} for Vela) which starquake theory suggests.

The wave amplitude h could, however, be larger. Mountains or other local inhomogeneities in the crust or core could conceivably produce a net nonaxisymmetric oblateness of the same order of magnitude as the materials' shearing strengths[5,13], several orders of magnitude larger than the starquake models predict. An extreme upper bound on L_{GW} can be set by requiring that gravitational radiation account for the entire observed slowdown of the pulsars. That limit yields[7] for the Crab, $L_{GW} \lesssim 2\times 10^{38}$ erg/s, $\mathcal{F} \lesssim 7\times 10^{-7}$ erg/cm^2-s, $h \lesssim 8\times 10^{-25}$, and for Vela, $L_{GW} \lesssim 2\times 10^{37}$ erg/s, $\mathcal{F} \lesssim 1\times 10^{-6}$ erg/cm^2-s, $h \lesssim 3\times 10^{-24}$, which coincidentally agrees with the upper-bound estimate for Vela on the basis of maximum credible oblateness (Table 1).

To detect the quadrupole radiation at frequencies ω_{GW} of 380 s^{-1} for the Crab and 140 s^{-1} for Vela, some experimenters envision using large monocrystals, probably of sapphire or silicon[1,2]. For crystals of effective length ℓ and effective mass m, the change in amplitude of oscillation due to absorption of gravitational waves in phase with the crystal's oscillation during a measurement time $\hat{\tau}$ is (assuming $\hat{\tau} \ll \tau^*$, the damping time):

$$\Delta X_{GW} = \frac{\hat{\tau}\,\omega h \ell}{2} \quad .$$

Brownian motion at temperature T in a crystal with damping time τ^* ($\tau^* \equiv 2Q/\omega$) produces an amplitude change

$$\langle \Delta X^2_{Brownian} \rangle^{1/2} = \left(\frac{2\hat{\tau}\, kT}{m\omega^2 \tau^*}\right)^{1/2}$$

where k is Boltzmann's constant.

For a reasonable signal-to-noise ratio[20] of 10, the minimum detectable wave has amplitude

$$h \gtrsim 10\left[\frac{2kT}{mQ\,\omega^3 \ell^2\,\hat{\tau}}\right]^{1/2} \simeq 7\times 10^{-28}\left(\frac{T}{10^{-3}K}\right)^{1/2} \cdot \left(\frac{10^5 g}{m}\right)^{1/2} \cdot \left(\frac{10^{14}}{Q}\right)^{1/2} \cdot \left(\frac{380 s^{-1}}{\omega_{GW}}\right)^{3/2}$$

$$\cdot \left(\frac{10^2 cm}{\ell}\right)\left(\frac{10^7 s}{\hat{\tau}}\right)^{1/2}$$

It is straightforward to verify that detection of this signal would not require a "quantum non-demolition sensor"[20,21], though the construction of the required sensor would be a nontrivial task. The minimum detectable wave amplitude for Vela is a factor of 4 higher, due to its lower frequency. The values of T, m, Q, ℓ, and $\hat{\tau}$ assumed above are not entirely unreasonable goals for the next 5 to 10 years of experimental effort[22]. It thus appears that, if the Crab or Vela pulsars are as strong as the best estimates indicate, they may be borderline-detectable by gravitational astronomers within the 1980's.

I would like to thank Carlton M. Caves, Peter Goldreich, Kip S. Thorne and David Douglass for helpful conversations or correspondence on this subject.

Table 1 Estimated pulsar gravitational radiation

	Standard Crab	PPS[13] Crab	Vela
P(s)	.033	.033	.089
$\omega_{GW}(s^{-1})$	380	380	140
R (pc)	2000	2000	500
I ($g\text{-}cm^2$)	4×10^{44}	2×10^{45}	2×10^{45}
ε_o	2×10^{-4}	4×10^{-4}	3×10^{-3}
θ_w	10^{-2}	10^{-2}	10^{-2}
L_{GW}(erg/s)	5×10^{32}	4×10^{34}	1×10^{34}
max	1×10^{35}	1×10^{37}	2×10^{37}
min	3×10^{29}	8×10^{31}	9×10^{30}
$\mathcal{F}$ ($erg/cm^2\text{-}s$)	1×10^{-12}	9×10^{-11}	4×10^{-10}
max	4×10^{-10}	4×10^{-8}	1×10^{-6}
min	4×10^{-16}	1×10^{-13}	2×10^{-13}
h	1×10^{-27}	9×10^{-27}	5×10^{-26}
max	2×10^{-26}	2×10^{-25}	3×10^{-24}
min	2×10^{-29}	3×10^{-28}	1×10^{-27}

REFERENCES

1. Bagdasarov, Kh. S., Braginsky, V. B. & Mitrofonov, V. P., results reported at International Symposium on Experimental Gravitation, Pavia, Italy, September 1976 (unpublished).
2. Douglass, D. H., results reported at International Symposium on Experimental Gravitation, Pavia, Italy, September 1976 (unpublished).
3. Douglass, D. H., "Occasional Notes" No. D12 and D17, unpublished (1976).
4. Press, W. H. & Thorne, K. S., Ann. Rev. Astron. & Astrophys., 10, 335-374 (1972).
5. Ruderman, M., Ann. Rev. Astron. & Astrophys., 10, 427-476 (1972).
6. Rees, M. J., Astrophys. Space Sci., 39, 3-7 (1976).
7. Groth, E. J., "Observational Properties of Pulsars," from Gursky, H. & Ruffini, R., Neutron Stars, Black Holes, and Binary X-ray Sources (D. Reidel, Holland, 1975), pp. 119-174.
8. Pines, D. & Shaham, J., Nature Phys. Sci., 235, 43-49 (1972).
9. Pines, D. & Shaham, J., Comm. Astrophys. Space Phys., 2, 37-44 (1974).
10. Pines, D. & Shaham, J., Nature, 248, 483-485 (1974).
11. Pines, D., "Observing Neutron Stars: Information on Stellar Structure from Pulsars and Compact X-Ray Sources," in Proceedings 16th Solvay Conference on Physics (Editions de l'Universite Bruxelles, 1974).
12. ter Harr, D., Phys. Rep. 3C, 57-126 (1972).
13. Pandharipande, V. R., Pines, D. & Smith R. A., Astrophys. J., 208, 550-566 (1976).
14. Baym, G. & Pethick, C., Ann. Rev. Nucl. Sci., 25, 27-77 (1975).
15. Manchester, R. N., Goss, W. M. & Hamilton, P. A., Nature, 259, 291-292 (1976).

16. Pines, D., Shaham, J. & Ruderman, M., Nature Phys. Sci., 237, 83, 84, 96 (1972).

17. Misner, C. M., Thorne, K. S., & Wheeler, J. A., Gravitation (W. H. Freeman & Co., San Francisco, 1973).

18. Easson, I., Pethick, C. J., "The stress tensor of cosmic and laboratory type II superconductors," preprint, 1977.

19. Jones, P. B., Astrophys. Space Sci., 33, 215-230 (1975).

20. Braginsky, V. B. & Manukin, A. B., Measurement of Weak Forces in Physics Experiments, English translation ed. by D. Douglass (University of Chicago Press, Chicago, 1977).

21. Giffard, R. P., Phys. Rev. D14, 2478-2486 (1976).

22. Braginsky, V. B., Caves, C. M. & Thorne, K. S., Phys. Rev. D15, 2047-2068 (1977).

CHAPTER II

GRAVITATIONAL WAVES FROM ROTATING AND PRECESSING RIGID BODIES: SIMPLE MODELS AND APPLICATIONS TO PULSARS

This chapter is a paper by Mark Zimmermann and Eugene Szedenits, Jr. It was published in the 1979 July 15 issue of Physical Review D, Volume 20, pages 351-355.

PHYSICAL REVIEW D VOLUME 20, NUMBER 2 15 JULY 1979

Gravitational waves from rotating and precessing rigid bodies: Simple models and applications to pulsars

Mark Zimmermann and Eugene Szedenits, Jr.*
W. K. Kellogg Radiation Laboratory, California Institute of Technology, Pasadena, California 91125
(Received 29 January 1979)

An axially symmetric, torque-free rigid body, rotating and precessing, emits gravitational quadrupole radiation at two frequencies, ω and 2ω, corresponding to the $l = 2$, $m = 1,2$ spherical harmonics. We present explicitly the waveforms of the two polarizations at both frequencies. From observations of gravitational waves, one can derive information about the body's orientation and its precession amplitude. Electromagnetic radiation emitted by a spot fixed on the surface of the body arrives in pulses at a mean frequency Ω which is typically different from ω. If the body is not axially symmetric but the amplitude of the precession is small, the gravitational radiation at the lower frequency ω is split into two frequencies on either side of the electromagnetic pulse frequency. We present explicit waveforms for the two polarizations in this case also.

I. INTRODUCTION

Pulsars are widely interpreted as rotating, rather rigid neutron stars.[1] Some of the nearer, more rapidly spinning pulsars might be good sources of gravitational waves.[2-6] Experimental searches for these waves have already been made,[7,8] so far with negative results. In these experiments and in theoretical discussions of gravitational waves from pulsars, it has generally been assumed that the gravitational radiation is emitted at precisely twice the observed pulsar frequency. We point out here that this assumption is typically incorrect. The simplest pulsar model, an axially symmetric rigid body undergoing free precession, emits gravitational quadrupole radiation at two frequencies, ω and 2ω. The frequency ω and the radio pulsation frequency Ω differ by the precession frequency Ω_p; hence an attempt to resonate a high-Q gravitational-wave antenna with the pulsar's emissions, in order to build up a detectable signal, may fail if the radio pulses are used as a guide and if radio measurements have failed to determine the precession frequency. Also the gravitational radiation at frequency 2ω is usually much weaker than that at frequency ω.

In this paper we present explicit gravitational radiation waveforms for two of the simplest imaginable pulsar models: (1) a rigid, axisymmetric body undergoing free precession, and (2) a rigid asymmetric body, freely precessing with small wobble angle. Future papers will discuss more general models.

Section II of this paper outlines the assumptions and methods used here. Section III gives the results for the axisymmetric model and explains how a gravitational astronomer can deduce a pulsar's spin orientation, inclination, wobble angle, and ellipticity, from gravitational-wave observations. That section also explains the reasons for the difference between the fundamental gravitational-wave frequency and the electromagntic pulsar frequency. Section IV presents waveforms for the asymmetric model rotating with small mean wobble angle $\bar{\theta}$, and discusses how a gravitational astronomer can deduce information about a pulsar's orientation, oblateness, etc. in this case. Finally, Sec. V summarizes and reviews these results and other recent work on gravitational radiation from rigid bodies. That section also points out an error in Zimmermann's estimates[6] of gravitational luminosities for the Crab and Vela pulsars and gives corrected estimates.

II. METHOD

For the purposes of this paper, we model pulsars as torque-free, rigidly rotating bodies. Actually, radiation reaction, accretion, and other torques certainly exist, but simple estimates of their size suggest that their effects are likely to be small compared to the free precession.[9] Therefore we ignore them. Also, solid neutron-star matter is not perfectly rigid, so the precession rate calculated for a rigid body needs to be reduced somewhat, depending on the shear modulus and structure of the specific model being investigated. Fortunately the precessional equations of motion for a nonrigid body are isomorphic to the rigid-body equations, in the limit that the body's oblateness and wobble angle are small, and provided that the body acts as an elastic solid on precessional time scales.[9,10] The rigid-body gravitational radiation waveforms calculated below should therefore be correct for a nonrigid body, if the actual reduced precession rate is used in place of the theoretical rigid-body rate. Liquid-core neutron-star models typically precess slower than

rigid bodies by factors ranging from 10^2 to 10^1; solid-core models of more massive neutron stars typically precess within a factor of 2 of the perfectly rigid precession rate.[9,11] Precession periods of ~20 hours for the Crab and of a few minutes for a solid-core Vela neutron star have been estimated.[11]

We take, as our theory of gravitation and mechanics, standard Newtonian theory (the weak-field, slow-motion, small-stress approximation to general relativity), augmented by the quadrupole-moment formalism for gravitational-wave generation.[12] (This formalism is discussed in most textbooks on general relativity; see, for example, Misner, Thorne, and Wheeler,[13] whose notation and conventions we use in this paper.) We are fairly sure, and shall attempt to prove in a subsequent paper, that the strong-field, slow-motion approximation[14] to general relativity (which is more nearly valid for neutron stars where $GM/Rc^2 \sim 0.2$) will give precisely the same waveform predictions as the weak-field formalism we use. The only difference to be expected is in the expressions for the body's moment of inertia and quadrupole-moment tensors as integrals over the body's mass and stress distributions.[14,15]

In our analysis the only relevant parameters from stellar structure are the three principal moments of inertia of the body and the wobble angle θ between the total angular momentum vector $\vec{J}$ and the body's third principal axis $\hat{x}_3$.

III. AXISYMMETRIC MODEL: WAVEFORMS AND ANALYSIS

We first consider a symmetric rigid body with moments of inertia $I_1 = I_2 \neq I_3$. The free precession of such an object in Newtonian theory is discussed in most classical mechanics texts.[16-18] It is straightforward to plug the resulting time-changing quadrupole-moment tensor into the gravitational radiation equations[13] and grind out the waves produced.

Suppose that the object's conserved angular momentum $\vec{J}$ has an "inclination angle" i relative to the plane of the observer's sky. (Inclination angle i is defined as astronomers do for binary star systems: $i = 0°$ means that $\vec{J}$ points toward the observer, $i = 90°$ means that $\vec{J}$ is perpendicular to the line of sight, $i = 180°$ means that $\vec{J}$ points away from the observer.) For an object at distance r, we find that the two polarizations[13] of gravitational waves have dimensionless amplitudes:

$$h_+ = \frac{2I_1\omega^2\epsilon \sin\theta}{r}[(1+\cos^2 i)\sin\theta\cos 2\omega t + 2\cos i \sin i \cos\theta \cos\omega t],$$

$$h_\times = \frac{2I_1\omega^2\epsilon \sin\theta}{r}(2\cos i \sin\theta \sin 2\omega t + \sin i \cos\theta \sin\omega t), \quad (1)$$

where the frequency is $\omega = J/I_1$, the ellipticity is $\epsilon = (I_3 - I_1)/I_1$, and we set $c = G = 1$.

A particular choice of coordinate axes and of the origin of time, $t = 0$, was made by the observer to yield the above wave amplitudes: If $\hat{v}$ and $\hat{w}$ are orthogonal unit vectors chosen transverse to the direction of wave propagation, with $\hat{v} \times \hat{w} =$ (direction toward observer), then

$$h_+ = h^{TT}_{vv} = -h^{TT}_{ww} = (-1/r)(\ddot{I}_{vv} - \ddot{I}_{ww})$$

and

$$h_\times = h^{TT}_{vw} = (-2/r)\ddot{I}_{vw},$$

where TT refers to the "transverse-traceless" gauge, dots are time derivatives evaluated at the retarded time $t - r$, and the minus signs come from our use of

$$I_{ab} \equiv \int \rho(r^2\delta_{ab} - x_a x_b)\, d^3x$$

instead of the

$$\mathcal{I}_{ab} \equiv \int \rho(x_a x_b - \tfrac{1}{3}\delta_{ab} r^2)\, d^3x$$

of Ref. 13.

The observer can get into our "preferred" orientation by rotating his transverse axes $\hat{v}$ and $\hat{w}$ so as to maximize the observed ratio $|h_{+,2\omega}|/|h_{\times,2\omega}|$ (where $h_{+,2\omega}$ means the amplitude of h_+ at frequency 2ω, with its $\cos 2\omega t$ time dependence factored out, etc.). The same orientation of $\hat{v}$ and $\hat{w}$ must also maximize the independently observable ratio $|h_{\times,\omega}|/|h_{+,\omega}|$ if the waves come from a freely precessing, axially symmetric body. In this orientation, the projection of $\vec{J}$ into the plane of the sky lies along one of the directions $\hat{v}$, $\hat{w}$, $-\hat{v}$, or $-\hat{w}$. The quadrupole nature of the waves makes this 90° ambiguity unavoidable.

In Eqs. (1) the observer's origin of time $t = 0$ is chosen so as to make the component of $h_\times$ at frequency ω proportional to $+\sin\omega t$, with a positive constant of proportionality. The same choice of $t = 0$ must make the piece of $h_\times$ at 2ω proportional to $+\cos 2\omega t$ and

$$(h_+ \text{ at } \omega) \propto (\pm\cos\omega t),$$

$$(h_\times \text{ at } 2\omega) \propto (\pm\sin 2\omega t),$$

with the sign determined by the sign of $\cos i$. With this choice of time origin, it turns out that at (retarded time) $t = 0$, the body's symmetry axis $\hat{x}_3$ lies in the plane defined by $\vec{J}$ and the direction

to the observer. If the body's ellipticity ϵ is positive (oblate spheroid), $\hat{x}_3$ is at its farthest from the observer at $t=0$; if $\epsilon<0$ (prolate spheroid), $\hat{x}_3$ is at its nearest to the observer. (We use the convention that the constant of the motion $\hat{x}_3\cdot\vec{J}=J\cos\theta$ is positive; in other words, θ lies between 0° and 90°. During free precession, $\hat{x}_3$ moves around $\vec{J}$ at angular rate ω.)

With his transverse axes aligned and his origin of time selected in the above manner, the observer can read off from his measured waveforms and Eqs. (1) the inclination and wobble angle of the gravitational wave source. The independent ratios $h_{\times,\omega}/h_{+,\omega}$ and $h_{\times,2\omega}/h_{+,2\omega}$ determine the inclination i in the range 0° to 180°; given i, the ratios $h_{+,2\omega}/h_{+,\omega}$ and $h_{\times,2\omega}/h_{\times,\omega}$ determine the wobble angle θ between 0° and 90°. Finally, the overall amplitude of the signals determines

$$|I_1\epsilon/r| = |(I_3-I_1)/r| .$$

If the distance r is known by other means, then a direct measure of the nonaxisymmetry $|I_3-I_1|$ follows. Note that gravitational observations alone cannot distinguish an oblate from a (perhaps improbable) prolate spheroid.

To compare the gravitational radiation waveforms with the electromagnetic pulsar signals, one needs a simple pulsar model. Suppose that something fixed on the surface of the neutron star (a magnetic pole, for example) at colatitude λ relative to the $\hat{x}_3$ body axis is associated with radio, optical, or other pulses observed once per turn of the star. The apparent rate of pulsation seen by a distant observer varies during the body's precession and depends on the precessional motion, on λ, and on the details of the pulsar radiation beam. Free precession would produce periodic peregrinations in the perceived pulse period, the mean pulse profile, and other pulsar parameters, such as pulse polarization.

Electromagnetic observations of pulsars have shown no evidence for precession.[19,20] In particular, any precession with a period between about 2 and 150 days must have an amplitude less than a few degrees[20] in the observed cases.

There are two scenarios which could explain the absence of observable precession. First, if the angle λ (between a pulsar's $\hat{x}_3$ body axis and the source of the radiation beam) were small compared to the wobble angle θ, then a pulse would be seen whenever the $\hat{x}_3$ pulsar axis passed sufficiently close to the observer's line of sight. The mean observed electromagnetic pulse frequency Ω would thus equal the gravitational-wave frequency $\omega=J/I_1$. But during the body's precession time

$$2\pi/\Omega_p = 2\pi I_3/\omega(I_1-I_3)\cos\theta ,$$

the observer would pass through the pulsar radiation beam from many different directions. For the precession to be invisible, the pulsar beam would have to be not only nearly axisymmetric, but also would have to be without observable linear polarization. Any net linear polarization would rotate through 360° during a precession time; this has not been observed.[1,21]

The second and much more plausible scenario to explain the lack of electromagnetic precession observations is that the pulsar's beam source is at an arbitrary angle λ, but that the wobble angle θ is small. In this case, the body-frame precessional angular velocity Ω_p adds to the inertial-space $\hat{x}_3$ angular velocity ω to give a mean electromagnetic pulse frequency $\Omega=\omega+\Omega_p$ different from the gravitational-wave frequency. (For an oblate body, $\Omega<\omega$.) The observer always passes through the pulsar beam from approximately the same direction, so no significant changes in pulse profile or polarization would be expected. A simple knife-beam model of the pulsar radiation pattern gives the result (for small θ) that during a precession time pulses arrive early and late by a phase of up to $\theta/\tan\lambda$, with sinusoidally varying phase shift.

Small (but nonzero) values of θ have been suggested in order to explain pulsar "glitches" (speed ups) and timing "noise" in terms of precession- and spin-down-induced starquakes.[11,22,23] Although the estimated fractional frequency difference between the electromagnetic pulses and the gravitational radiation is small, probably in the range 10^{-3} to 10^{-10} (Refs. 6, 11, 20, and 23), the fact that a difference may exist is critical for some gravitational-wave experiments. For instance, it has been suggested[6] that by controlling the frequency of a high-Q crystal to follow the radio pulsar emission, one might mechanically integrate up an observable gravitational-wave signal. Other proposals (Ref. 24 and references cited therein) involve heterodyne techniques to mechanically convert a monochromatic pulsar signal to zero frequency. These schemes clearly will fail for the simple freely precessing model described here, if the integration time needed to produce a measurable signal exceeds the reciprocal of the body-frame precession frequency. A more sophisticated broadband method of gravitational-wave detection is required. Any splitting between the gravitational and electromagnetic frequencies is a potential difficulty, but as compensation it provides another measure of the object's oblateness, including its sign (oblate vs prolate).

IV. TRIAXIAL MODEL WITH SMALL WOBBLE ANGLE: WAVEFORMS AND ANALYSIS

If the object lacks axial symmetry but its wobble angle is small enough, then its free precession and the resulting gravitational waves can still be expressed simply. Following a classical mechanics text,[16] let the body have principal moments of inertia $I_1 < I_2 < I_3$. Define two (not necessarily small) eccentricity parameters

$$e_1 = [2(I_3 - I_1)/I_1]^{1/2}$$

and

$$e_2 = [2(I_3 - I_2)/I_2]^{1/2}.$$

The mean ellipticity is $\epsilon = \frac{1}{2} e_1 e_2$. Let the precession amplitude be small, with $\vec{J}$ always near the $\hat{x}_3$ body axis and with mean wobble angle $\bar{\theta}$. To first order in $\bar{\theta}$, the mean electromagnetic pulsation frequency (from a spot fixed on the body, far from the $\hat{x}_3$ axis) is $\Omega = J/I_3$ and the precessional frequency is $\Omega_p \equiv \epsilon\Omega$. Define the small parameter $a \equiv 2\bar{\theta}/(e_1^2 + e_2^2)^{1/2}$. [Note that $\bar{\theta}$ must be much less than $\max(e_1, e_2)$ for a to be small and for this approximation to hold.] Then by plugging into the quadrupole radiation formulas,[13] we obtain

$$h_+ = \frac{2}{r}(1+\cos^2 i)(I_1 - I_2)\Omega^2 \cos 2\Omega t + \frac{\epsilon a \sin 2i}{2\sqrt{2}\,r}\left[(e_1 I_1 + e_2 I_2)\omega_+^2 \cos\omega_+ t + (e_1 I_1 - e_2 I_2)\omega_-^2 \cos\omega_- t\right],$$

$$h_\times = \frac{4}{r}\cos i (I_1 - I_2)\Omega^2 \sin 2\Omega t + \frac{\epsilon a \sin i}{\sqrt{2}\,r}\left[(e_1 I_1 + e_2 I_2)\omega_+^2 \sin\omega_+ t + (e_1 I_1 - e_2 I_2)\omega_-^2 \sin\omega_- t\right], \tag{2}$$

where $\omega_\pm \equiv (1 \pm \epsilon)\Omega$.

The above h_+ and $h_\times$ are defined using the same choice of transverse $\hat{v}$ and $\hat{w}$ vectors discussed following Eqs. (1). To get into the orientation and time origin of the waveforms (2), an observer can rotate his transverse axes to maximize $|h_{+,2\Omega}|/|h_{\times,2\Omega}|$. The same orientation will maximize $|h_{\times,\omega_+}|/|h_{+,\omega_+}|$ and $|h_{\times,\omega_-}|/|h_{+,\omega_-}|$, if the object producing the gravitational waves is indeed a precessing triaxial body with small wobble angle. An additional check is that the frequency of the 2Ω radiation must equal the sum of the frequencies of the other two components of the radiation (plus corrections of order $\bar{\theta}^2$). As before, one of the transverse axes $\hat{v}$, $\hat{w}$, $-\hat{v}$, or $-\hat{w}$ lies along the projection of $\vec{J}$ into the sky, but gravitational observations cannot resolve the 90° ambiguity. The choice of $t = 0$ to make the time dependence of the measured h's agree with Eqs. (2) corresponds, as for the symmetric case earlier, to the body $\hat{x}_3$ axis lying in the plane defined by $\vec{J}$ and the direction toward the observer, with $\hat{x}_3$ at $t = 0$ as far from the observer as it ever gets.

The object's inclination angle i is again defined unambiguously and redundantly by the ratios of the components of h_+ and $h_\times$ at the three frequencies. However, in making the small-$\bar{\theta}$ approximation, we have sacrificed the information $[O(\bar{\theta}^2)]$ necessary to derive the mean wobble angle $\bar{\theta}$ itself from the observations. The splitting between the various frequency components of the gravitational waves does enable one to measure the mean ellipticity ϵ. The relative amplitudes of the waves then give a variety of nonlinear combinations of the three moments of inertia and the wobble angle. If the distance to the object, r, is known by other means (so that the 2ω radiation gives a value for $I_1 - I_3$), then the observations are sufficient to determine all of the unknowns: I_1, I_2, I_3, and $\bar{\theta}$.

We view the results of the triaxial-rigid-body case [Eqs. (2) for small $\bar{\theta}$ and the waveforms for arbitrary $\bar{\theta}$ in a subsequent paper] not necessarily as predictions of actual gravitational waveforms to be expected, but as indications of the probable complexity and high information content of gravitational waves from astrophysical sources. Pulsars in nature are not perfectly rigid, and they are subject to significant electromagnetic radiation-reaction torques, accretion of matter, glitches, timing noise of uncertain origin, and other effects which we have omitted. Gravitational astronomy may be a powerful way to get a handle on the details of those effects.

V. CONCLUSIONS

Previous investigators have derived the correct energy and angular momentum loss equations for rigid rotating bodies in general relativity.[4,25-27] For the case $I_1 = I_2$, their result for the gravitational-wave luminosity is, in our notation

$$L_{GW} = \tfrac{2}{5}\epsilon^2 I_1^2 \omega^6 \sin^2\theta (16\sin^2\theta + \cos^2\theta),$$

where the $16\sin^2\theta$ term is from 2ω radiation and the $\cos^2\theta$ term is from ω radiation. To our knowledge, the fact that ω radiation exists and is significant has never been clearly pointed out. (Perhaps it has been overlooked because it vanishes when an object rotates about a principal axis.) For small wobble angles $\theta \ll 90°$, the radiation at frequency ω is in fact larger than the 2ω radiation for a sufficiently symmetric object. [The

reason is simple: A body, such as an American football, wobbling by a small angle about its symmetry axis, has a large time-changing piece that "looks like itself" after a time $2\pi/\omega$, but only a small piece that "looks like itself" after time π/ω. In contrast, a football tumbling end-over-end ($\theta \sim 90°$) "repeats itself" every half revolution, and radiates gravitational waves most strongly at 2ω.] The possible difference between the frequency of the gravitational radiation (produced by the body's inertia tensor) and the mean electromagnetic pulsar frequency (produced by a spot fixed to the body's surface) is also significant.

A recent estimate by one of us (Zimmermann) of the actual astrophysical amplitude of the waves produced by pulsars, such as the Crab and Vela, found $h \sim 10^{-24}$ to 10^{-29} (Ref. 6) at frequency 2ω. Energy conservation, balancing spin-down and gravitational-wave luminosity, means that neither of these objects can have h at frequency ω much over 10^{-24}. But we must point out here that the formulas used for this estimate[6] are in error. For small θ, the gravitational luminosities (erg sec^{-1}) calculated in Ref. 6 are too high by a factor of 16 and the bulk of the luminosity occurs at frequency ω, not 2ω. The actual mean wave amplitude h at frequency ω is a factor of 2 smaller than the values quoted; at frequency 2ω, the actual h is smaller by a factor of $\theta^{-1} \sim 100$, if θ is as small as estimated. (These errors are smaller than the astrophysically induced uncertainties in the estimates of Ref. 6.)

It is conceivable that experiments sensitive enough to detect sources with $h \sim 10^{-24}$ will be running within the next decade. Gravitational astronomers who do such experiments should be aware of the likelihood that the strongest radiation will be near but not at the radio pulsar frequency. Successful observations of these gravitational waves will yield new information about pulsar structure and spin alignment, information probably not obtainable by any other means.

ACKNOWLEDGMENTS

We would like to thank Roger Blandford, Carlton M. Caves, and Kip S. Thorne for valuable comments and suggestions. This work was supported in part by NASA Grant No. NGR05-002-256 and a grant from PACE. We also gratefully acknowledge the help of MACSYMA in checking Eqs. (1) and (2). [MACSYMA and the MIT Mathlab Group are supported in part by ERDA Contract No. E(11-1)-3070 and by NASA Grant No. NSG-1323.] The work of M. Z. was partially supported by a Robert A. Millikan Fellowship.

---

*On leave of absence from Caltech; current address: 3053 Lakehaven Court, Ann Arbor, Michigan 48105.

[1]J. H. Taylor and R. N. Manchester, Annu. Rev. Astron. Astrophys. 15, 19 (1977).

[2]J. P. Ostriker and J. E. Gunn, Astrophys. J. 157, 1395 (1969).

[3]H. J. Melosh, Nature (London) 224, 781 (1969).

[4]W. Y. Chau, Nature (London) 228, 655 (1970).

[5]W. H. Press and K. S. Thorne, Annu. Rev. Astron. Astrophys. 10, 335 (1972).

[6]M. Zimmermann, Nature (London) 271, 524 (1978).

[7]H. Hirakawa, K. Tsubono, and M-K. Fujimoto, Phys. Rev. D 17, 1919 (1978).

[8]D-J. Lu and J-G. Gao, Acta Phys. Sin. 25, 181 (1976).

[9]P. Goldreich, Astrophys. J. 160, L11 (1970).

[10]W. H. Munk and G. J. F. MacDonald, *The Rotation of the Earth* (Cambridge University Press, Cambridge, England, 1960), especially Sec. 6.2.

[11]V. R. Pandharipande, D. Pines, and R. A. Smith, Astrophys. J. 208, 550 (1976).

[12]A. Einstein, Sitzungsber. Preuss. Akad. Wissenschaften, p. 154 (part 1, 1918).

[13]C. W. Misner, K. S. Thorne, and J. A. Wheeler, *Gravitation* (Freeman, San Francisco, 1973), Chap. 36.

[14]K. S. Thorne, Rev. Mod. Phys. (to be published); also available as Cornell University Reports Nos. CRSR 663 (unpublished) and CRSR 664 (unpublished).

[15]J. R. Ipser, Astrophys. J. 166, 175 (1971).

[16]L. D. Landau and E. M. Lifshitz, *Mechanics* (Pergamon, London, 1976), 3rd ed., Secs. 33–37.

[17]H. Goldstein, *Classical Mechanics* (Addison-Wesley, Reading, Mass. 1950), Chap. 5.

[18]J. B. Marion, *Classical Dynamics of Particles and Systems* (Academic, New York, 1970), Chap. 12.

[19]G. R. Huguenin, J. H. Taylor, and D. J. Helfand, Astrophys. J. 181, L139 (1973).

[20]D. J. Helfand, Ph.D. thesis (University of Massachusetts, 1977) (unpublished), especially Chap. III.

[21]P. A. Hamilton, P. M. McCulloch, J. G. Ables, and M. M. Komesaroff, Mon. Not. Roy. Astron. Soc. 180, 1 (1977).

[22]D. Pines and J. Shaham, Nature (London), Phys. Sci. 235, 43 (1972).

[23]D. Pines and J. Shaham, Comm. Astrophys. Space Phys. 2, 37 (1974).

[24]V. B. Braginsky and V. N. Rudenko, Phys. Rep. 46C, 165 (1978).

[25]W. Y. Chau and R. N. Henriksen, Astrophys. J. 161, L137 (1970).

[26]B. Bertotti and A. M. Anile, ESRIN Report No. 126, 1971 (unpublished).

[27]B. Bertotti and A. M. Anile, Astron. Astrophys. 28, 429 (1973).

CHAPTER III

GRAVITATIONAL WAVES FROM ROTATING AND PRECESSING RIGID BODIES: II. GENERAL SOLUTIONS AND COMPUTATIONALLY USEFUL FORMULAE

This chapter is a paper which has been submitted for publication to Physical Review D.

Gravitational Waves from Rotating and Precessing Rigid Bodies: II. General Solutions and Computationally Useful Formulae

Mark Zimmermann

W. K. Kellogg Radiation Laboratory

California Institute of Technology, Pasadena, California 91125

ABSTRACT

A rigid, freely-precessing Newtonian body emits gravitational radiation. In this paper I review the classical-mechanics results for free precession which are needed in order to calculate the weak-field, slow-motion, quadrupole-moment gravitational waves. Within that formalism, I give algorithms for computing the exact gravitational power radiated and waveforms produced by arbitrary rigid-body freely-precessing sources. I also present the dominant terms in series expansions of the waveforms for the case of an almost-spherical object precessing with a small wobble angle. These series expansions, which retain the precise frequency dependence of the waves, may be useful for gravitational astronomers when freely-precessing sources begin to be observed.

I. INTRODUCTION

In this paper I analyze the quadrupole gravitational radiation emitted by a freely-precessing, rigid, Newtonian body. An earlier work[1] (hereinafter referred to as Paper I) presented the solutions for axisymmetric objects and, in the small-wobble-angle limit, an approximate solution for nonaxisymmetric bodies. Paper I also discussed some astrophysical applications of those calculations to neutron stars as sources of gravitational waves. Here, I give algorithms for computing the exact results for the gravitational power radiated and waveforms produced by an arbitrary rigid Newtonian object, rotating free of external torques, in the standard quadrupole moment formalism. I also give computationally useful formulae for the interesting case of an almost-spherical object precessing with a small wobble angle. These series expansions retain the precise frequency dependence of the waves — an important point for observers who may have to integrate over long times in order to see a signal. The results are compared with the simpler, approximate waveforms of Paper I. Since that paper discussed at length the application of these calculations to astrophysical systems, only a few remarks on that topic are included here.

Section II of this paper reviews some of the classical Newtonian-mechanics results for free precession, defines the coordinate system and terminology used herein, and presents formulae useful for calculations of the power radiated in gravitational waves by a rotating rigid body. That section also gives the dominant terms in the gravitational luminosity for an object with small wobble angle, small oblateness, and small nonaxisymmetry, and interprets those terms. Section III reviews more of the classical free-precession results, and uses them to derive formulae for the gravitational waveforms $h_+(t)$ and $h_\times(t)$. That section also presents

explicitly the dominant terms, with their exact frequency dependences, for the same astrophysically-relevant limit as in Sec. II. The waveforms are interpreted and compared with the approximate results of Paper I. Figures 1 and 2 show the exact results for h_+ and $h_\times$ as calculated according to the algorithm discussed in Sec. III.C., in two specific cases, for a variety of observer inclinations relative to the precessing body. Finally, Sec. IV summarizes the conclusions of this paper.

II. POWER RADIATED IN GRAVITATIONAL WAVES

A. Review of classical free precession results and specification of coordinate system

Throughout this paper, I shall use the physical conventions of Landau and Lifshitz[2] in describing rigid body motions, and the mathematical notation of Abramowitz and Stegun[3] for elliptic functions and integrals. Much of the material necessarily repeated here in the course of specifying the problem is taken directly from Ref. 2. I work in units where $G = c = 1$.

A rigid, Newtonian object in flat space has its inertial properties completely specified by its mass and by a symmetric tensor $\overleftrightarrow{I}$ with components $I_{ij} \equiv \int \rho(\delta_{ij} r^2 - x_i x_j) d^3x$. In some noninertial coordinate system called the "body frame" $\overleftrightarrow{I}$ is diagonalized, with diagonal components I_1, I_2, I_3, and the center of mass of the object is stationary at the origin. Choose the body-frame unit basis vectors $\vec{e}_1$, $\vec{e}_2$, $\vec{e}_3$ to form a right-handed coordinate system such that $I_1 < I_2 < I_3$. (If any two of the principal moments of inertia are equal, the analysis in Paper I applies.) I shall use Latin subscripts for components of tensors evaluated in the inertial-space reference frame, and Greek subscripts in the body frame. When specific components are referred to explicitly, the letters x, y, and z

are used in the inertial frame and the digits 1, 2, and 3 in the body frame.

The components of a tensor (such as $\overleftrightarrow{I}$) in the body frame and in the inertial frame are related by the "rotation matrix" $R_{j\mu} \equiv \vec{e}_j \cdot \vec{e}_\mu$. At any moment, the body frame's instantaneous angular velocity may be described by a vector $\vec{\Omega}$. The total angular momentum of the body is $\vec{J} = \overleftrightarrow{I} \cdot \vec{\Omega}$, a constant (if gravitational radiation-reaction torques are ignored). Choose the coordinate system of the inertial frame so that $\vec{J} = J\,\vec{e}_z$.

The orientation of the body frame relative to the inertial system is described by three Euler angles: θ is the angle between $\vec{e}_z$ and $\vec{e}_3$, φ is the longitude of the ascending node (that is, the angle between $\vec{e}_x$ and the line of nodes formed by the intersection of the $\vec{e}_x$-$\vec{e}_y$ plane and the $\vec{e}_1$-$\vec{e}_2$ plane), and ψ is the angle in the $\vec{e}_1$-$\vec{e}_2$ plane between the line of nodes and $\vec{e}_1$. (See Sec. 35 of Ref. 2 for illustrations and comments.)

Choose the origin of time and the orientation of $\vec{e}_x$ and $\vec{e}_y$ such that at $t = 0$, θ is at its maximum value, $\psi = \pi/2$, and $\varphi = 0$; that is, $\vec{e}_2$ lies in the $\vec{e}_x$-$\vec{e}_y$ plane and $\vec{e}_1$ and $\vec{e}_3$ lie in the $\vec{e}_y$-$\vec{e}_z$ plane. (This completes the specification of the two coordinate systems, and results in formulae which agree with the conventions of Paper I and Ref. 2.)

If the components of $\vec{\Omega}$ in the body frame are denoted by Ω_1, Ω_2, and Ω_3, then the body has rotational energy $E = \frac{1}{2}\,(I_1\Omega_1^{\,2} + I_2\Omega_2^{\,2} + I_3\Omega_3^{\,2})$ and angular momentum $J \equiv |\vec{J}| = (I_1^{\,2}\Omega_1^{\,2} + I_2^{\,2}\Omega_2^{\,2} + I_3^{\,2}\Omega_3^{\,2})^{\frac{1}{2}}$. Now, for specificity, make one additional assumption about the precession: assume that $J^2 > 2EI_2$. This is equivalent to assuming that, in the body frame, the apparent precessional motion of $\vec{J}$ is a closed curve around the $\vec{e}_3$ axis. (If $J^2 = 2EI_2$, the motion of $\vec{J}$ is along a curve passing through the $\vec{e}_2$ axis and the solutions for the gravitational radiation may be

obtained as a limit of the equations given below. If $J^2 < 2EI_2$, the motion of $\vec{J}$ is along a closed curve around the $\vec{e}_1$ axis, and by consistently interchanging the indices "1" and "3" below, the correct solutions appear.)

The components of $\vec{\Omega}$ in the body frame are simple elliptic functions of time. Define the initial-value constants $a \equiv \Omega_1(t=0)$ and $b \equiv \Omega_3(t=0)$, and the dimensionless time variable τ according to the equation

$$\tau = bt \left[\frac{(I_3 - I_2)(I_3 - I_1)}{I_1 I_2}\right]^{\frac{1}{2}} \tag{1}$$

Then:

$$\Omega_1 = a \text{ cn } \tau$$

$$\Omega_2 = a \left[\frac{I_1(I_3 - I_1)}{I_2(I_3 - I_2)}\right]^{\frac{1}{2}} \text{ sn } \tau \tag{2}$$

$$\Omega_3 = b \text{ dn } \tau \ .$$

The parameter m of the elliptic functions in Eqs. (2) is

$$m = \frac{(I_2 - I_1)\ I_1\ a^2}{(I_3 - I_2)\ I_3\ b^2} \ . \tag{3}$$

As $m \to 0$, sn $\tau \to \sin \tau$, cn $\tau \to \cos \tau$, dn $\tau \to 1$, and the solutions reduce to the symmetric-object solutions of Paper I. The elliptic functions are periodic in their argument τ, with period $4K$ where $K(m)$ is the "complete elliptic integral of the first kind" defined and tabulated in Ref. 3.

B. Derivation of equations useful for the quadrupole-moment formalism calculation

The quadrupole-moment formalism[4] says that the total energy radiated per unit time in gravitational waves is $\frac{1}{5}\langle \dddot{\mathcal{I}}_{jk} \dddot{\mathcal{I}}_{jk} \rangle$ where $\mathcal{I}_{jk} \equiv \int \rho (x_j x_k - \frac{1}{3}\delta_{jk} r^2) d^3x$ and $\dddot{\mathcal{I}}_{jk} \equiv \frac{d^3}{dt^3}\mathcal{I}_{jk} = -\frac{d^3}{dt^3} I_{jk}$. The angle-brackets denote a time-average over a few periods.

The solution for the body's precessional motion is much simpler in the body frame than in the inertial frame, so it is profitable to work in the body frame as much as possible. In evaluating the total power radiated in gravitational waves, in fact, one can work entirely in the body frame, and I shall do so.

Since $I_{jk} = R_{j\mu} R_{k\nu} I_{\mu\nu}$ and the body-framed $I_{\mu\nu}$ is constant, simple differentiation with respect to time gives

$$\dddot{I}_{jk} = I_{\mu\nu} (\dddot{R}_{j\mu} R_{k\nu} + 3\ddot{R}_{j\mu} \dot{R}_{k\nu} + 3\dot{R}_{j\mu} \ddot{R}_{k\nu} + R_{j\mu} \dddot{R}_{k\nu}).$$

The derivatives of the rotation matrices are:

$$\begin{aligned}
\dot{R}_{j\mu} &= \varepsilon_{jk\ell} \Omega_k R_{\ell\mu} = \varepsilon_{\nu\mu\gamma} \Omega_\nu R_{j\gamma} \\
\ddot{R}_{j\mu} &= \varepsilon_{\nu\mu\gamma} \dot{\Omega}_\nu R_{j\gamma} + \Omega_\mu \Omega_\nu R_{j\nu} - |\vec{\Omega}|^2 R_{j\mu} \qquad (4) \\
\dddot{R}_{j\mu} &= \left[\varepsilon_{\mu\gamma\beta} (\ddot{\Omega}_\beta - |\vec{\Omega}|^2 \Omega_\beta) + 2\Omega_\mu \dot{\Omega}_\gamma + \dot{\Omega}_\mu \Omega_\gamma \right] R_{j\gamma} - 3\Omega_\beta \dot{\Omega}_\beta R_{j\mu} .
\end{aligned}$$

Taking Eqs. (4) and plugging into the equation for $\dddot{I}_{jk}$ yields $\dddot{I}_{jk} = R_{j\mu} R_{k\nu} B_{\mu\nu}$ where the body-frame quantity $B_{\mu\nu}$ is:

$$B_{\mu\nu} \equiv -6\Omega_\gamma \dot{\Omega}_\gamma I_{\mu\nu} + I_{\gamma\nu}\left[\varepsilon_{\gamma\mu\epsilon}(\ddot{\Omega}_\epsilon - 4|\vec{\Omega}|^2\Omega_\epsilon) + 2\Omega_\gamma\dot{\Omega}_\mu + \dot{\Omega}_\gamma\Omega_\mu\right] +$$

$$+ I_{\mu\gamma}\left[\varepsilon_{\gamma\nu\epsilon}(\ddot{\Omega}_\epsilon - 4|\vec{\Omega}|^2\Omega_\epsilon) + 2\Omega_\gamma\dot{\Omega}_\nu + \dot{\Omega}_\gamma\Omega_\nu\right] + \tag{5}$$

$$+ 3\, I_{\gamma\delta}\Omega_\epsilon\left[\Omega_\gamma(\varepsilon_{\epsilon\delta\nu}\Omega_\mu + \varepsilon_{\epsilon\delta\mu}\Omega_\nu) + \dot{\Omega}_\eta\,(\varepsilon_{\epsilon\delta\nu}\varepsilon_{\eta\gamma\mu} + \varepsilon_{\epsilon\delta\mu}\varepsilon_{\eta\gamma\nu})\right].$$

The problem of calculating the total power radiated, P, thus reduces to the problem of evaluating $P = \frac{1}{5}\langle \dddot{I}_{jk}\dddot{I}_{jk}\rangle = \frac{1}{5}\langle B_{\mu\nu}B_{\mu\nu}\rangle$.

The terms of $B_{\mu\nu}$ are not really as complicated as they may appear to be when written in tensorial notation. Using the fact that $I_{\mu\nu}$ is diagonal in the body frame, one finds:

$$B_{11} = 6\left\{\Delta_2\Omega_2\dot{\Omega}_2 - \Delta_3\Omega_3\dot{\Omega}_3 - \Delta_1\Omega_1\Omega_2\Omega_3\right\} \tag{6}$$

where

$$\Delta_1 \equiv I_2 - I_3,\ \Delta_2 \equiv I_3 - I_1,\ \Delta_3 \equiv I_1 - I_2. \tag{7}$$

The other diagonal components of $B_{\mu\nu}$ follow by cycling the indices $1\to2\to3\to1$. For the off-diagonal terms,

$$B_{12} = \Delta_3(\ddot{\Omega}_3 - 4|\vec{\Omega}|^2\Omega_3) + \dot{\Omega}_1\Omega_2(2\Delta_1 - \Delta_2) -$$

$$- \dot{\Omega}_2\Omega_1(2\Delta_2 - \Delta_1) - 3\Omega_1^2\Omega_3\Delta_2 - 3\Omega_2^2\Omega_3\Delta_1 \tag{8}$$

and the other components of $\overleftrightarrow{B}$ follow by cycling the indices and by symmetry ($B_{\mu\nu} = B_{\nu\mu}$).

Equation (5) is quite general and in fact can be used to calculate for any time-varying rotation rate $\vec{\Omega}(t)$ the inertial-frame time derivatives of any rank-2 tensor $\overleftrightarrow{I}$ which is constant in the body frame. For our special case, where $\vec{\Omega}$ is that of free precession and $\overleftrightarrow{I}$ is the inertia

tensor, the equations of motion and their derivatives determine the derivatives of Ω_μ:

$$\begin{aligned}
\dot{\Omega}_\mu &= I^{-1}_{\mu\beta}\, \varepsilon_{\beta\gamma\delta} I_{\gamma\epsilon} \Omega_\epsilon \Omega_\delta \\
\ddot{\Omega}_\mu &= I^{-1}_{\mu\beta}\, \Omega_\beta \Omega_\gamma I_{\gamma\delta} \Omega_\delta - |\vec{\Omega}|^2 \Omega_\mu + \\
&\quad + I^{-1}_{\mu\beta}\, \varepsilon_{\beta\gamma\delta} I_{\gamma\epsilon} \Omega_\epsilon I^{-1}_{\delta\eta}\, \varepsilon_{\eta\kappa\sigma} I_{\kappa\chi} \Omega_\sigma \Omega_\chi \,.
\end{aligned} \tag{9}$$

Using these identities to remove the derivatives of $\vec{\Omega}$ from $B_{\mu\nu}$ gives:

$$\begin{aligned}
B_{11} &= 6\Omega_1\Omega_2\Omega_3 \left(- \Delta_1 + \frac{\Delta_2^2}{I_2} - \frac{\Delta_3^2}{I_3} \right) \\
B_{12} &= - 4\Omega_3 |\vec{\Omega}|^2 \Delta_3 + \\
&\quad + \Delta_1 \Omega_2^2 \Omega_3 \left(\frac{\Delta_3^2}{I_1 I_3} + \frac{2\Delta_1 - \Delta_2}{I_1} - 3 \right) + \\
&\quad + \Delta_2 \Omega_1^2 \Omega_3 \left(\frac{\Delta_3^2}{I_2 I_3} - \frac{2\Delta_2 - \Delta_1}{I_2} - 3 \right) .
\end{aligned} \tag{10}$$

The other components follow by symmetry and by cyclically permuting subscripts.

In order to evaluate the actual power radiated in gravitational waves, it is necessary to know the average values over a cycle of $sn^2\ \tau$, $sn^4\ \tau$, $sn^6\ \tau$, etc. These can be expressed in terms of the complete elliptic integrals of the first and second kinds, K(m) and E(m) (see Ref. 3). The results of time-averaging over a cycle are[5]:

$$\langle \mathrm{sn}^2\ \tau\rangle = \frac{K-E}{mK} = \tfrac{1}{2} + \frac{m}{16} + \frac{m^2}{32} + \frac{41m^3}{2048} + \cdots$$

$$\langle \mathrm{sn}^4\ \tau\rangle = \langle \mathrm{sn}^2\ \tau\rangle \left[\frac{2(1+m)}{3m}\right] - \frac{1}{3m}$$

$$= \frac{3}{8} + \frac{m}{16} + \frac{35m^2}{1024} + \cdots \qquad (11)$$

$$\langle \mathrm{sn}^6\ \tau\rangle = \langle \mathrm{sn}^4\ \tau\rangle \left[\frac{4(1+m)}{5m}\right] - \langle \mathrm{sn}^2\ \tau\rangle \left[\frac{3}{5m}\right]$$

$$= \frac{5}{16} + \frac{15m}{256} + \cdots$$

The identities $\mathrm{cn}^2\ \tau = 1 - \mathrm{sn}^2\ \tau$ and $\mathrm{dn}^2\ \tau = 1 - m\ \mathrm{sn}^2\ \tau$ which relate other elliptic functions to sn τ enable all of the other averages to be calculated from the above ones. From these averages, the exact power cutput in gravitational radiation is straightforward to write out.

C. Exact quadrupole-moment gravitational luminosity

The total power P radiated in gravitational waves depends on the parameters I_1, I_2, and I_3 (principal moments of inertia of the rigid body), and a and b (initial values of the components of the body's angular velocity along the $\vec{e}_1$ and $\vec{e}_3$ body axes).

To compute the total gravitational luminosity for any choice of these parameters, one can proceed as follows: (1) evaluate the elliptic-function parameter m from Eq. (3); (2) evaluate the averages over a cycle $\langle \mathrm{sn}^6\ \tau\rangle$, $\langle \mathrm{sn}^2\ \tau\ \mathrm{cn}^4\ \tau\rangle$, $\langle \mathrm{sn}^2\ \tau\ \mathrm{cn}^2\ \tau\ \mathrm{dn}^2\ \tau\rangle$, etc. of the various combinations of even powers of sn τ, cn τ, and dn τ with exponents adding up to 6, using Eqs. (11) and the elliptic function identities which follow them; (3) evaluate the averages $\langle B_{\mu\nu}{}^2\rangle$ for μ, ν running 1 through 3, using

Eqs. (2), (7), (10), and the averages calculated in step (2); (4) add up the results of step (3) and divide by 5 to get $P \equiv \frac{1}{5}\langle B_{\mu\nu}B_{\mu\nu}\rangle$, the quadrupole-moment formalism result for the luminosity in gravitational waves.

D. Series expansions for small wobble angle, small oblateness, and near-axisymmetry

Because the gravitational power radiated P must be invariant under a reversal of the direction of rotation ($\vec{\Omega} \to -\vec{\Omega}$), P contains only even powers of Ω_1, Ω_2, and Ω_3. Define coefficients F_μ, G, and $H_{\mu\nu}$ for each of the types of terms in $\vec{\Omega}$ by:

$$P \equiv \frac{1}{5}\left(F_\mu\langle\Omega_\mu^{\,6}\rangle + G\langle\Omega_1^{\,2}\Omega_2^{\,2}\Omega_3^{\,2}\rangle + H_{\mu\nu}\langle\Omega_\mu^{\,4}\Omega_\nu^{\,2}\rangle_{\mu\neq\nu}\right) \quad . \tag{12}$$

One can expand F_μ, G, and $H_{\mu\nu}$ for the interesting case of small oblateness, where the differences between the principal moments of inertia are small compared to the principal moments themselves. The results are simple; through order $\Delta_\mu^{\,2}$:

$$\begin{aligned} F_\mu &= 32\ \Delta_\mu^{\,2} \\ G &= 100\ (\Delta_1^{\,2}+\Delta_2^{\,2}+\Delta_3^{\,2}) + 84\ (\Delta_1\Delta_2+\Delta_1\Delta_3+\Delta_2\Delta_3) \\ H_{\mu\nu} &= 2\ (13\ \Delta_\mu+\Delta_\nu)(5\ \Delta_\mu+\Delta_\nu) \qquad \text{for} \qquad \mu \neq \nu \\ H_{11} &= H_{22} = H_{33} \equiv 0. \end{aligned} \tag{13}$$

The equation $F_\mu = 32\ \Delta_\mu^{\,2}$ is, in fact, exact to all orders in Δ_μ. The "F_μ terms" in P, which are proportional to a sixth power of a single

body-frame angular velocity, are precisely $(32/5)(I_2 - I_3)^2\langle\Omega_1{}^6\rangle$, $(32/5)(I_3 - I_1)^2\langle\Omega_2{}^6\rangle$, and $(32/5)(I_1 - I_2)^2\langle\Omega_3{}^6\rangle$. These are familiar from the case of rotation about a principal axis, where there are no other terms.

The expression for P in terms of F_μ, G, and $H_{\mu\nu}$ still contains unevaluated averages of angular velocities. In the astrophysically relevant case of small wobble angle, small oblateness, and near-axisymmetry those averages can be conveniently expanded. Small wobble angle means that the ratio of the body-frame angular velocities $\Omega_1(0)/\Omega_3(0) = a/b \ll 1$. Small oblateness implies that $(I_3 - I_1)/I_3 \ll 1$ (since $I_1 < I_2 < I_3$, there is no need to mention I_2 here). Near-axisymmetry causes $(I_2 - I_1)/(I_3 - I_1) \ll 1$; that is, the equatorial moments of inertia are close to each other compared to their difference from the polar moment. If equal weights are given to all three of these small parameters, the power radiated by a freely precessing rigid body can be expanded to give, at lowest order:

$$P \approx \frac{32}{5}\, b^6\, (I_2 - I_1)^2 + \frac{2}{5}\, a^2 b^4\, (I_3 - I_{1:2})^2, \qquad (14)$$

where $I_{1:2}$ is some average of I_1 and I_2, the precise nature of which is irrelevant to this order.

This simple result for the gravitational luminosity is also quite reasonable. The first term, $(32/5)\, b^6\, (I_2 - I_1)^2$, is the standard result for a rigid body freely-rotating about its principal axis I_3 at angular velocity b. The second term is the small-wobble-angle limit of the energy radiated by a freely-rotating axisymmetric rigid body,[1] with equatorial moments of inertia $I_1 = I_2$.

III. GRAVITATIONAL WAVEFORMS FROM FREE PRECESSION

A. Further review of classical free precession results

The calculation of the waveforms radiated by a precessing object is both simpler and more complex than the calculation of the total power radiated by that body. It is simpler in that only two time derivatives occur, instead of three, and that only terms linear in $\overleftrightarrow{I}$ occur, instead of terms quadratic. It is more complex in that the Euler angles of the body appear explicitly. It is also complicated somewhat by the appearance of one more parameter, the observer's inclination angle "i" relative to the invariant $\vec{J}$ direction.

The components Ω_1, Ω_2, and Ω_3 of $\vec{\Omega}$ in the body frame are periodic in time, with period

$$T \equiv \frac{4K}{b}\left[\frac{I_1 I_2}{(I_3 - I_2)(I_3 - I_1)}\right]^{\frac{1}{2}} \tag{15}$$

[see Eqs. (1), (2), and (3)].

The Euler angles θ and ψ are also periodic, with period $T/2$:

$$\begin{aligned} \cos\theta &= \frac{I_3 b}{J}\,\mathrm{dn}\,\tau \\ \tan\psi &= \left[\frac{I_1(I_3 - I_2)}{I_2(I_3 - I_1)}\right]^{\frac{1}{2}} \frac{\mathrm{cn}\,\tau}{\mathrm{sn}\,\tau}\ . \end{aligned} \tag{16}$$

Here and throughout I use the notation and initial-value choices of Sec. II.A and of Ref. 2, wherein the classical free-precession results which I quote are derived. Note that if the oblateness of the body is small, the period T is very long. As $I_1 \to I_2$ and the object approaches axisymmetry, $m \to 0$, $\Omega_3(t) \to$ constant, and $T \to 2\pi I_1/[\Omega_3(I_3 - I_1)]$, the

usual free precession period of a symmetric body. Note also that for precession around the $\vec{e}_3$ axis, $\dot{\psi} < 0$.

The Euler angle φ, unfortunately, is complicated; if it is written as a sum, $\varphi \equiv \varphi_1 + \varphi_2$, then the function φ_1 can be expressed by

$$\exp(2i\varphi_1(t)) = \frac{\vartheta_4\left(\frac{2\pi t}{T} - i\pi\alpha\right)}{\vartheta_4\left(\frac{2\pi t}{T} + i\pi\alpha\right)} \tag{17}$$

where α is a solution of $\mathrm{sn}(2i\alpha K) = iI_3 b/(I_1 a)$ and ϑ_4 is a theta-function in the notation of Ref. 3. (Because of the common periodicity of the elliptic functions and the theta-functions, all solutions α are equivalent.) If $K'(m) \equiv K(1-m)$ and $q \equiv \exp(-\pi K'/K)$, then a useful series expansion of φ_1 can be written:

$$\varphi_1(t) = \sum_{n=1}^{\infty} \frac{-2q^n}{n(1-q^{2n})} \sin\left(\frac{4n\pi t}{T}\right) \sinh(2n\pi\alpha). \tag{18}$$

The function $\varphi_1(t)$ is periodic in t with period $T/2$. The other part of φ is a linear function of time: $\varphi_2(t) = 2\pi t/T'$, where

$$\frac{2\pi}{T'} \equiv \frac{J}{I_1} - \frac{2i}{T}\frac{\vartheta_4'(i\pi\alpha)}{\vartheta_4(i\pi\alpha)}$$

$$= \frac{J}{I_1} + \frac{2b}{K}\left[\frac{(I_3 - I_2)(I_3 - I_1)}{I_1 I_2}\right]^{\frac{1}{2}} \sum_{n=1}^{\infty} \frac{q^n}{1-q^{2n}} \sinh(2n\pi\alpha). \tag{19}$$

Thus, $\cos(\varphi_2(t))$ has a period T' not, in general, commensurate with T, and so the body's motion typically is nonperiodic. The period $T' \to 2\pi I_1/J$ as the body becomes axisymmetric.

B. Derivation of equations for the quadrupole-moment waveform calculation

The general expression for the waveforms radiated is a simple one: in the transverse-traceless gauge of Ref. 4, the dimensionless gravitational-wave amplitudes are

$$h_+ \equiv h^{TT}_{\hat{v}\hat{v}} = - h^{TT}_{\hat{w}\hat{w}} = \frac{-1}{r} \left(\ddot{I}_{\hat{v}\hat{v}} - \ddot{I}_{\hat{w}\hat{w}}\right)$$

$$h_\times \equiv h^{TT}_{\hat{v}\hat{w}} = \frac{-2}{r} \ddot{I}_{\hat{v}\hat{w}} \quad . \tag{20}$$

In these equations, r is the distance from the observer to the source of the radiation, and $\hat{v}$ and $\hat{w}$ are unit vectors transverse to the waves' direction of propagation. Specifically, for a source at the origin of the inertial frame and a distant observer in the $\vec{e}_y$-$\vec{e}_z$ plane at colatitude i from the $\vec{e}_z$ axis, the vectors $\hat{v}$ and $\hat{w}$ may be defined as $\hat{v} \equiv \vec{e}_y \cos i - \vec{e}_z \sin i$ and $\hat{w} = -\vec{e}_x$. Such an observer would, in the usual astronomical convention, define the body's "inclination" to be angle i.

As in Sec. II, it is advantageous to work as much as possible in the body frame. Using the relation $\ddot{I}_{jk} = I_{\mu\nu}(\ddot{R}_{j\mu}R_{k\nu} + 2\dot{R}_{j\mu}\dot{R}_{k\nu} + R_{j\mu}\ddot{R}_{k\nu})$, and substituting the results for $\dot{R}_{j\mu}$ and $\ddot{R}_{j\mu}$ from Sec. II.B, Eqs. (4), I obtain:

$$\ddot{I}_{jk} = R_{j\mu}R_{k\nu}A_{\mu\nu}$$

where

$$A_{\mu\nu} \equiv -2|\vec{\Omega}|^2 I_{\mu\nu} + (\epsilon_{\delta\gamma\mu}\dot{\Omega}_\delta + \Omega_\gamma\Omega_\mu)I_{\gamma\nu} +$$
$$+ (\epsilon_{\delta\gamma\nu}\dot{\Omega}_\delta + \Omega_\gamma\Omega_\nu)I_{\mu\gamma} + 2\epsilon_{\delta\gamma\mu}\epsilon_{\eta\chi\nu}\Omega_\delta\Omega_\eta I_{\gamma\chi} \tag{21}$$

is defined completely in terms of body-frame quantities. Combining Eqs. (20) and (21) with the definitions of $\hat{v}$, $\hat{w}$, and inclination i, I obtain

$$h_+ = \frac{-1}{r}\Big[(\cos i\, R_{y\mu} - \sin i\, R_{z\mu})(\cos i\, R_{y\nu} - \sin i\, R_{z\nu}) - \\ - R_{x\mu} R_{x\nu}\Big] A_{\mu\nu} \tag{22}$$

$$h_\times = \frac{2}{r}(\cos i\, R_{y\mu} - \sin i\, R_{z\mu})\, R_{x\nu}\, A_{\mu\nu}$$

where the explicit components of $A_{\mu\nu}$ are

$$A_{11} = 2\,(\Delta_2 \Omega_2^{\,2} - \Delta_3 \Omega_3^{\,2})$$

$$A_{12} = (\Delta_1 - \Delta_2)\Omega_1\Omega_2 + \Delta_3\dot{\Omega}_3 \tag{23}$$

$$= \left(\Delta_1 - \Delta_2 + \frac{\Delta_3^2}{I_3}\right)\Omega_1\Omega_2$$

and symmetry and cyclic index permutation give the rest.

The components of the rotation matrix $R_{j\mu}$ in terms of the Euler angles θ, φ, and ψ are reproduced here for convenient reference. They are

$$R = \begin{matrix} \\ j \\ \downarrow \end{matrix} \begin{matrix} \xrightarrow{\qquad\qquad \mu \qquad\qquad} \\ \end{matrix} \begin{pmatrix} \cos\psi\cos\varphi - \cos\theta\sin\psi\sin\varphi & -\sin\psi\cos\varphi - \cos\theta\cos\psi\sin\varphi & \sin\theta\sin\varphi \\ \cos\psi\sin\varphi + \cos\theta\sin\psi\cos\varphi & -\sin\psi\sin\varphi + \cos\theta\cos\psi\cos\varphi & -\sin\theta\cos\varphi \\ \sin\theta\sin\psi & \sin\theta\cos\psi & \cos\theta \end{pmatrix} \tag{24}$$

C. Exact quadrupole-moment gravitational waveforms

The gravitational wave amplitudes radiated by a freely-precessing, Newtonian, rigid body depend on the parameters I_1, I_2, and I_3 (principal moments of inertia of the body), a and b (initial values of the components of the body's angular velocity along the $\vec{e}_1$ and $\vec{e}_3$ body axes), i (inclination angle of the observer relative to the invariant $\vec{J}$ direction of the body), and time t.

To compute the gravitational waveforms h_+ and $h_\times$ for any choice of these parameters, one can proceed as follows: (1) evaluate the elliptic function parameter m from Eq. (3); (2) evaluate the constant α defined by $\mathrm{sn}(2i\alpha K(m)) = iI_3 b/(I_1 a)$ [following Eq. (17)]; (3) evaluate the time parameter τ using Eq. (1), the angular velocities Ω_1, Ω_2, and Ω_3 at "time" τ using Eqs. (2), and the Euler angles θ, φ, and ψ using Eqs. (15)-(19); (4) evaluate the components of $A_{\mu\nu}$ and $R_{j\mu}$ using Eqs. (23) and (24); (5) plug the results of the preceding evaluations evaluations into Eqs. (22) to compute $h_+(t)$ and $h_\times(t)$. This algorithm was used to calculate the waveforms shown in Figs. 1 and 2, which are discussed in the following subsection.

D. Series expansions for small wobble angle, small oblateness, and small nonaxisymmetry

While arbitrarily-accurate values for h_+ and $h_\times$ may be computed using the algorithm described above, for many purposes it may be more useful to have available the first terms of a series expansion of the gravitational waveforms. In making these expansions, one must be careful not to lose the correct, exact frequency dependence of the waves. Experiments to detect nearly-monochromatic gravitational radiation often

need to integrate for long times in order to build up an observable signal. Hence, "small" errors in the calculated power spectrum are dangerous. There also may exist several closely-spaced frequency components in the radiation, which will be confused and confounded by a series expansion that fails to preserve the correct frequency spectrum.

To make the expansions possible, in addition to demanding small elliptic function parameter m, it is also convenient to demand that the wobble angle be small and that the parameter

$$\delta \equiv 1 - \left[\frac{I_1(I_3 - I_2)}{I_2(I_3 - I_1)}\right]^{\frac{1}{2}}$$

be small. This allows expansion of cos ψ. The assumption of small δ is equivalent to the assumption that the body's nonaxisymmetry is not too large.

The resulting expansions of the cosines of the Euler angles are:

$$\cos\theta = \frac{bI_3}{J}\left[1 + \frac{m}{4}(\cos 2\nu - 1) + \mathcal{O}(m^2)\right]$$

$$\cos\psi = \sin\nu\left[1 + (\delta + \frac{m}{4})\cos^2\nu + \mathcal{O}(\delta^2, m^2, m\delta)\right] \qquad (25)$$

$$\cos\varphi = \cos\frac{2\pi t}{T'} + \frac{m}{8}\sinh(2\pi\alpha)\sin\frac{2\pi t}{T'}\sin 2\nu + \mathcal{O}(m^2)$$

where $\nu \equiv \pi\tau/(2K) = 2\pi t/T$.

One may now plug in and grind these explicit Euler angles through the equations for h_+ and $h_\times$. The results are simple and interesting for the astrophysically important case of small wobble angle, small oblateness, and near-axisymmetry discussed in Sec. II:

$$h_+ = \frac{-2}{r}(1+\cos^2 i)(I_2 - I_1)\Omega^2 \cos(2\Omega t) + \\ + \frac{\sin(2i)}{r}(I_3 - I_{1:2})\left(\frac{aI_1}{bI_3}\right)\left(\frac{2\pi}{T'}\right)^2 \cos\left(\frac{2\pi t}{T'}\right)$$

$$h_\times = \frac{-4}{r}\cos i\,(I_2 - I_1)\Omega^2 \sin(2\Omega t) + \\ + \frac{2}{r}\sin i\,(I_3 - I_{1:2})\left(\frac{aI_1}{bI_3}\right)\left(\frac{2\pi}{T'}\right)^2 \sin\left(\frac{2\pi t}{T'}\right) \qquad (26)$$

where $\Omega \equiv (2\pi/T') - (2\pi/T)$ and $I_{1:2}$ is an average of I_1 and I_2 (as before). These are the dominant terms in the radiation; corrections are of higher order in m, δ, $aI_1/(bI_3)$, $(I_3 - I_1)/I_3$, and $(I_2 - I_1)/(I_3 - I_1)$. Eqs. (26) do, however, retain the exact frequency dependence of the dominant parts of the waves in the period T'. (The cost is that T' obeys a messy transcendental equation.) The results here agree with Eqs. (2) of Paper I, where a simpler expansion was made which only gave the waves' approximate frequencies.

As was the case in Sec. II, the dominant components of h_+ and $h_\times$ [Eqs. (26)] have a simple physical interpretation. The waves at frequency 2Ω with strength independent (to this order in the expansion) of the wobble angle are from the differing moments of inertia I_1 and I_2. They are identical in strength, frequency, and angular distribution to the waves produced by a simple rigid rotor (a spinning dumbbell, for example). The waves at frequency $2\pi/T'$ are the small-wobble-angle limit of the waves produced by a freely-precessing, axisymmetric ($I_1 = I_2$) object [Eqs. (1) of Paper I]. As in that case, the mean frequency of pulses seen from a spot fixed on the body's surface is not equal to the gravitational-wave frequency; the two differ by the precession frequency $2\pi/T$. As discussed in

Paper I, this frequency splitting may cause difficulties for some gravitational-wave detectors which rely on a high-Q system, mechanically synchronized with a pulsar's electromagnetic pulses, to integrate up an observable signal. On the other hand, if the frequency splitting can be observed, it will provide a direct measurement of a pulsar's oblateness. Other details of the gravitational waveforms give information about wobble angle, inclination, and nonaxisymmetry — information difficult or impossible to obtain by electromagnetic means. See Paper I for a detailed discussion.

Figure 1 shows the computed waveforms h_+ and $h_\times$ for a freely-precessing, nearly-axisymmetric body ($I_1/I_3 = 0.99$, $I_2/I_3 = 0.991$) moving with a fairly small wobble angle ($a/b = 0.1$). The exact solution as graphed agrees with the first terms in the series expansion [Eqs. (26)] to within the expected accuracy of $\sim 10\% \sim |a/b| \sim \delta$. The particular choice of initial conditions at $t = 0$ used in this paper, and the location of the observer in the $\vec{e}_y - \vec{e}_z$ plane, produces the particular phase relationship between h_+ and $h_\times$ evident near $t = 0$. At later times, the frequency splitting due to the (in this case slow) body-frame precession changes the relative phases of the two wave polarizations. The $\sim 10\%$ contributions from terms not retained in Eqs. (26) also cause slow (timescale T) amplitude variations of the waves; the variations are especially visible at $i = 0$. The frequencies of the dominant Fourier components as calculated in Eqs. (26) are exact.

In Fig. 2, the waves emitted at various angles by a highly-oblate ($I_1/I_3 = 1/3$, $I_2/I_3 = 2/3$) body precessing with a large wobble angle ($a/b = 1$) are shown. In this case the two timescales T and T' are of comparable magnitudes, and the waveforms at all inclinations i exhibit a wealth of information about their source.

IV. CONCLUSIONS AND OPEN QUESTIONS

The results given in Secs. II and III of this paper for the power and waveforms produced by a freely precessing, rigid, Newtonian body are simple applications of the quadrupole-moment formalism to one specific physical system. As discussed in Paper I, these idealized calculations may be applicable to the astrophysically realistic case of a rapidly rotating neutron star. The sensitivities of gravitational experiments are improving at a rapid rate; it is conceivable that some precessing-body sources will be detectable within the next decade. The results presented here may then help save others some computational labor.

Papers I and II have only dealt with weak-field, slow-motion, small-stress sources (the standard Newtonian approximation to general relativity). Neutron stars have rather strong fields, since $GM/rc^2 \sim 0.2$ in typical models. I suspect, but have not proved, that the strong-field, slow-motion approximation to general relativity will give precisely the same waveform predictions as does the weak-field formalism, if the moment of inertia and quadrupole moment tensors of the body are properly redefined. This topic might be worth further investigation. It might also be interesting to calculate more realistic models of precessing neutron stars, where the assumptions of infinite rigidity and zero external torques are relaxed. (Paper I, Sec. II, suggests but does not prove that such realistic models will typically not differ significantly from the models calculated here, except for having a longer precession timescale T.) Finally, more work on the interpretation of the gravitational waveforms might be valuable; Paper I discussed how to deduce information about the source from the waves, but only for the cases of axisymmtric bodies and of small-wobble-angle precession for triaxial bodies.

ACKNOWLEDGMENTS

I would like to thank MACSYMA, an algebraic-symbol-manipulation computer system developed by the MIT Mathlab group, for aid in deriving and checking many of the equations in this paper. (MACSYMA is supported in part by ERDA under contract number E(11-1)-3070 and by NASA grant NSG 1323.) This work was supported in part by the National Aeronautics and Space Administration [NGR 05-002-256] and a grant from PACE; I am also grateful for support from the California Institute of Technology's Robert A Millikan Fellowship.

REFERENCES

[1] M. Zimmermann and E. Szedenits, Jr., "Gravitational waves from rotating and precessing rigid bodies: simple models and applications to pulsars," Phys. Rev. D 20, 351 (1979).

[2] L. D. Landau and E. M. Lifshitz, Mechanics, translated by J. B. Sykes and J. S. Bell (Pergamon Press, Oxford, 1976) (3rd edition), §§ 33-37.

[3] M. Abramowitz and I. A. Stegun, Handbook of Mathematical Functions (National Bureau of Standards, U.S. Government Printing Office, Washington, D.C., 1972) (10th printing), Chaps. 16 & 17 (by L. M. Milne-Thomson).

[4] C. M. Misner, K. S. Thorne, and J. A. Wheeler, Gravitation (W. H. Freeman & Co., San Francisco, 1973) Chap. 36.

[5] I. S. Gradshteyn and I. M. Ryzhik, Table of Integrals, Series, and Products (Academic Press, New York, 1965) (4th edition), § 5.13.

FIGURE CAPTIONS

Fig. 1. Gravitational radiation waveforms h_+ (solid lines) and $h_\times$ (dashed lines) measurable by observers at inclinations $i = 0^\circ$, 30°, 60°, and 90° relative to the $\vec{J}$ of the freely precessing, rigid, Newtonian source. The algorithm and equations of Sec. III were applied to a body with principal moments of inertia $I_1/I_3 = 0.99$ and $I_2/I_3 = 0.991$, rotating with initial values of its angular velocities $\Omega_1(0)/\Omega_3(0) \equiv a/b = 0.1$. For this case, solution of the equations of motion gave elliptic function parameter $m = 1.1 \times 10^{-3}$, $\alpha = 0.94893$, period $T' = 6.18906b$, and precession period $T = 656.19b$. The dimensionless "units" in terms of which h is plotted are

$$\frac{G}{c^4}\frac{I_3 b^2}{r} = 1.1 \times 10^{-21}\left(\frac{I_3}{10^{45}\ \text{g-cm}^2}\right)\left(\frac{b}{200\ \text{rad s}^{-1}}\right)^2\left(\frac{1\ \text{Kpc}}{r}\right).$$

Fig. 2. Gravitational radiation waveforms h_+ (solid lines) and $h_\times$ (dashed lines) measurable by observers at inclinations $i = 0^\circ$, 30°, 60°, and 90° relative to the $\vec{J}$ of the freely precessing, rigid, Newtonian source. In this case, $I_1/I_3 = 1/3$, $I_2/I_3 = 2/3$, $\Omega_1(0)/\Omega_3(0) \equiv a/b = 1$, $m = 1/3$, $\alpha = 0.429786$, $T' = 1.79069\,b$, and $T = 6.93566\ b$. As in Fig. 1, the dimensionless "units" in terms of which h is plotted are GI_3b^2/rc^4.

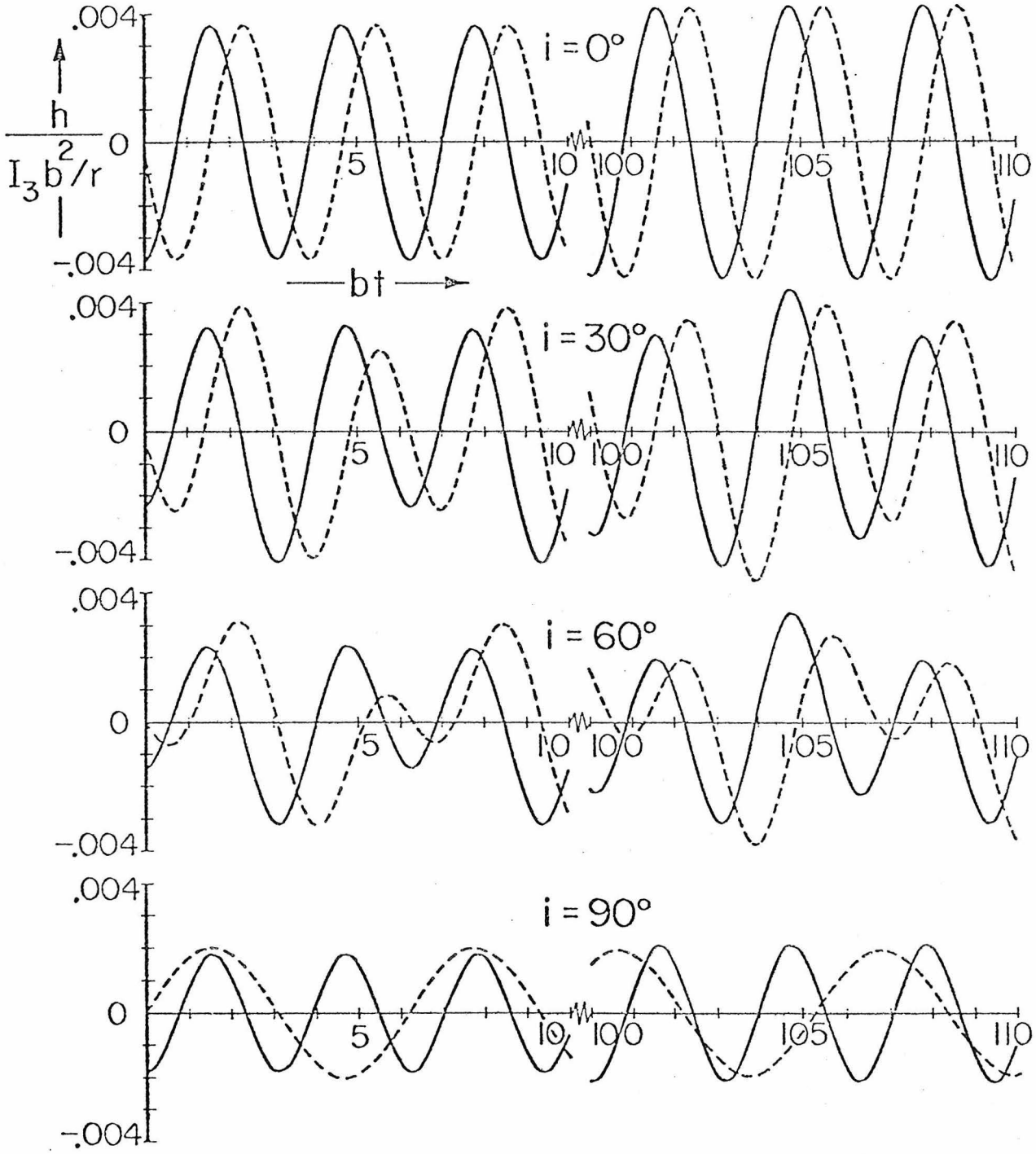

Fig. 1

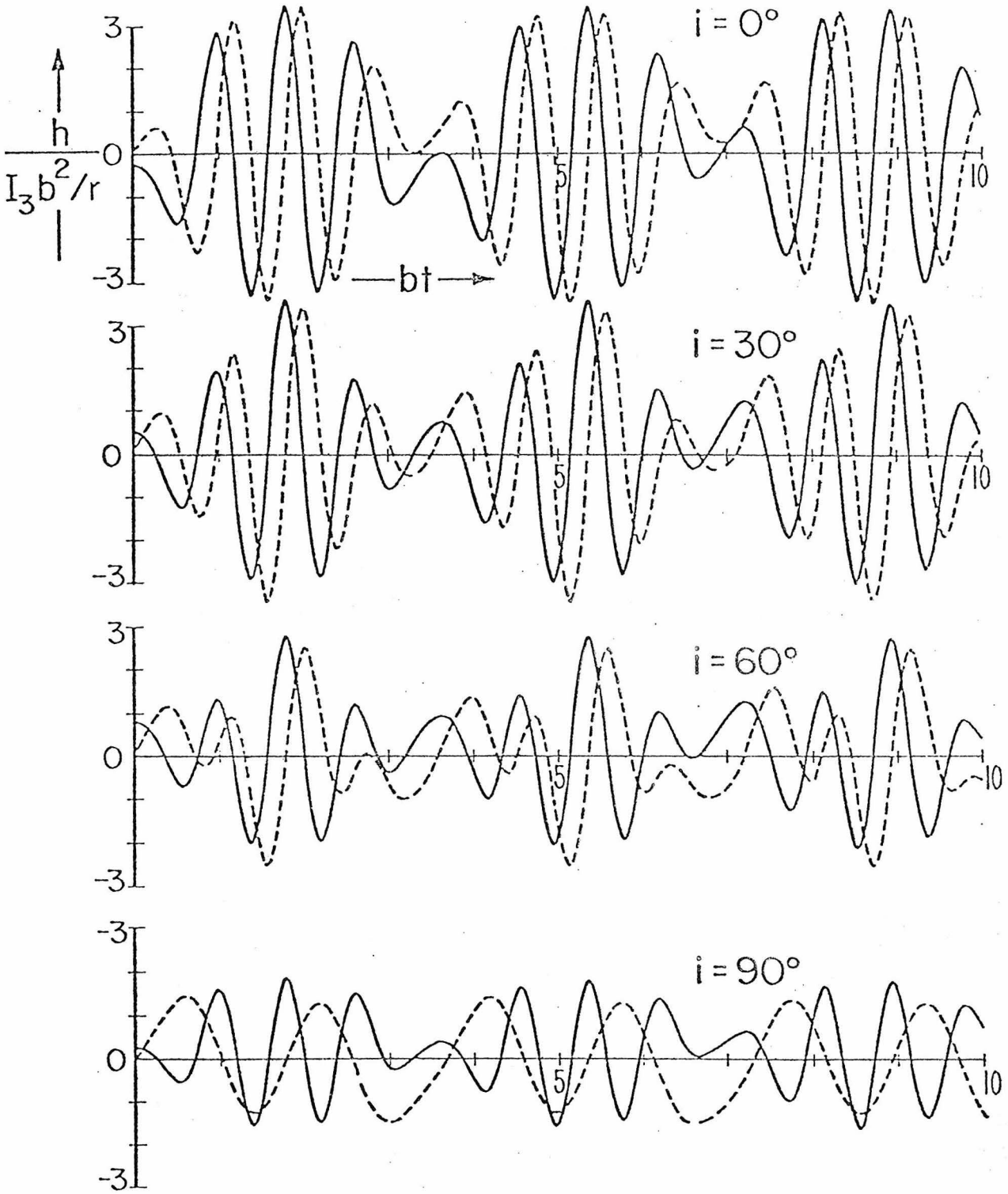

Fig. 2

CHAPTER IV

THE GRAVITATIONAL WAVES THAT BATHE THE EARTH: UPPER LIMITS BASED ON THEORISTS' CHERISHED BELIEFS

This chapter is a paper by Mark Zimmermann and Kip S. Thorne. It has been accepted for publication in a festschrift in honor of Abraham H. Taub, to be published in 1980.

THE GRAVITATIONAL WAVES THAT BATHE THE EARTH: UPPER LIMITS BASED ON THEORISTS' CHERISHED BELIEFS*†

MARK ZIMMERMANN§ and KIP S. THORNE

W. K. Kellogg Radiation Laboratory

California Institute of Technology, Pasadena, CA 91125 USA

ABSTRACT

On the basis of our cherished beliefs about the structure of the Universe and the theory of gravitation, we derive theoretical upper limits on the strengths of the gravitational waves which bathe the Earth. Separate limits are presented, as functions of frequency, for waves from extragalactic sources and for waves from inside our own Galaxy; and in each case, for discrete sources (bursters, transient sources, and monochromatic sources) and for a stochastic background due to unresolved sources. An observation of gravitational waves exceeding these limits would be disturbing (and exciting), since it would require a modification of one or more generally accepted assumptions about the astrophysical universe or the nature of gravity.

---

*This manuscript is dedicated to our good friend and colleague, Abraham H. Taub, on the occasion of his retirement from the University of California at Berkeley.

†Supported in part by the National Aeronautics and Space Administration [NGR 05-002-256] and by the National Science Foundation [AST76-80801 A02].

§Robert A. Millikan Graduate Fellow.

I. INTRODUCTION

During the past two decades general relativity theory has had an increasingly strong impact on astrophysics — first in the theory of quasars; then in cosmology, pulsars, compact X-ray sources, and the search for black holes. We hope for an even stronger impact in the future, when gravitational waves open up a new "window" onto the Universe — a window in which general relativity will play an absolutely essential role.

The efforts of experimenters to develop gravitational-wave detectors of ever-increasing sensitivity have been described in a number of recent review articles.[1,2,3,4] As these efforts proceed, it is useful to have theoretical "benchmarks" against which to gauge their progress. Such benchmarks are of three major types. The first type, as sensitivities improve, are "nihil obstat" upper limits on the strengths of the waves. An observation of waves above these limits would overturn one or more cherished beliefs about either the structure of the universe or the physical laws governing gravitational radiation. Type two benchmarks are at a level where the best estimates of plausible astrophysical sources indicate that something should be seen. Observations at these sensitivities are sure to give significant astronomical information; even if no waves are detected, many otherwise acceptable models will be eliminated. Type-three benchmarks are the absolute minimum gravitational-wave strengths consistent with other astronomical observations. A failure to see waves below these limits would be as serious a matter as observations of waves above the type-one limits; in either case, something is radically wrong with the theory of gravitation or with conventional astrophysical wisdom.

Type-two and type-three benchmarks have been reviewed in several recent articles.[5,6] The purpose of this article is to set forth benchmarks of the

first type — "cherished-belief" upper limits on gravitational wave strengths.

In §II we list and discuss the cherished beliefs on which our limits are based. In §III we derive, from those cherished beliefs, upper limits on the strength of any stochastic background of gravitational waves which might bathe the Earth — both a limit on waves from unresolved sources in our Galaxy, and a limit on extragalactic waves. We also describe scenarios that could lead to these upper limits. In §IV we derive similar upper limits on waves from discrete sources including bursters, transient sources, and monochromatic sources. Again there are separate upper limits for sources in our own Galaxy and extragalactic sources. For the case of broad-band bursts, we also describe a scenario which could lead to the Galactic upper limits.

Throughout we shall restrict attention to gravitational-wave frequencies in the domain of current experimental interest: 10^{-4} Hz $\lesssim f \lesssim$ 10^{+4} Hz. The lower limit, 10^{-4} Hz, is dictated by the technology of gravitational-wave detectors[1,2,3,4] — in particular, the round-trip radio-wave travel time to spacecraft at reasonable distances (e.g., Jupiter). The upper limit, 10^{+4} Hz, is dictated by our cherished belief[5] that the only highly-efficient sources of gravitational waves in the Universe today are objects near their Schwarzschild radii — neutron stars and black holes of stellar mass and larger — and that these objects cannot radiate significantly at frequencies above $f_{max} \simeq 10^{+4}$ Hz.

The notation used in our discussion is summarized in Box 1. A more detailed discussion of each parameter is given at the point in the text where it is first introduced.

II. CHERISHED BELIEFS

The cherished beliefs, on which we base our limits, are of two types: beliefs about the astrophysical structure of the Universe (§II.A), and beliefs about the physical laws governing gravitational radiation (§II.B).

A. The Structure of the Universe

Our first cherished belief is the "cosmological principle" that we do not live in a special time or place in the Universe — except for being inside a local density enhancement, the Galaxy. The cosmological principle implies that, on the average, sources of gravitational waves are no more luminous now than they have been (and will be) for a Hubble time $T_H = 1 \times 10^{10}$ years, the only timescale available. It also implies that the nearest source is at a typical distance from us, neither fortuitously near nor far. (For objects of number density n in Euclidean 3-space, the mean distance to the nearest one is $0.55396\ldots n^{-1/3}$; over 90% of the time, the nearest is between $0.2\, n^{-1/3}$ and $0.9\, n^{-1/3}$. We will use $0.5\, n^{-1/3}$ as the distance to the nearest source throughout this paper.)

Our next cherished belief is that there is no significant amount of "relict," primordial gravitational radiation bathing the Earth — more precisely, that all the significant sources of gravitational waves are at cosmological redshifts $z \leq 3$. This is as much a simplifying assumption as a cherished belief: Although semi-plausible models of the early Universe give only modest amounts of gravitational radiation[7,8] (amounts well below the upper limits of this paper), we are so ignorant about the early Universe that it is hard to place firm upper limits on the waves from there, except the obvious limit that their total energy density not exceed by much the

density required to close the Universe. The closure limit will follow from our other cherished beliefs without our assuming it explicitly.

The cosmological principle, plus the belief in "no primordial waves," allows us to approximate the universe by a very simple model which is accurate to within an order of magnitude in energies (a factor of 3 in gravitational-wave amplitudes). In this model the expansion of the Universe is ignored, space is regarded as Euclidean, the Universe is regarded as extending outward from Earth in all directions to a Hubble distance $R_H = c\,T_H = 1 \times 10^{10}$ light years, within this distance the smeared-out mass density of potential gravitational-wave sources is regarded as constant and as equal to the "closure density" $\rho_u = (c^2/G)(3/8\pi)R_H^{-2} = 2 \times 10^{-29}$ g/cm^{-3}, and outside R_H the density drops to zero (cosmological cutoff on sources). Our use of the closure density for ρ_u does not mean that we believe in this value, but rather that this is a reasonable upper limit and will thus give rise to the largest possible limits on gravitational-wave strengths. The Galaxy we shall model as a region of constant, enhanced mean mass density, $\rho_g = 2 \times 10^{-24}$ g/cm^3 (no radial structure), and of spherical shape with radius $R_g = 60{,}000$ light years and with the Earth located (roughly) at its center. The numbers for our Galaxy take account of a now popular galactic halo with total mass $M_g = (4\pi/3)\,R_g^{\,3}\rho_g \simeq 1 \times 10^{12}\,M_\odot$ and radius $R_g \simeq 60{,}000$ light years.[9,10,11]

Our third cherished belief is that within our Galaxy no single, coherently radiating object has mass in excess of $M_{max} \simeq 10^8\,M_\odot$.[12] This is a very generous upper limit. We make no assumption about the maximum mass of extragalactic objects.

Our fourth cherished belief is that the dominant sources of gravitational waves have no significant beaming of their radiation. In principle, strong beaming can occur — e.g., in waves from ultrarelativistic collisions of

astrophysical objects,[13,14] in waves from sources with gravitational lens properties,[15,16] and in waves from carefully contrived directional antennas.[17] However, we do not know of any type of hypothetical strong-beaming source that is likely to make up a significant fraction of the mass density of the Galaxy or Universe. Moreover, our limits are fairly insensitive to the no-beaming assumption: a simple geometrical analysis in flat space shows that, if sources beam their energy into a solid angle $\Omega < 4\pi$, and if the Earth is located randomly relative to the beams, then the expected energy flux from the nearest visible object increases only as $(\Omega/4\pi)^{-1/3}$, and the expected total flux from all sources out to some fixed cutoff radius remains constant. (On the other hand, as Lawrence,[15] Misner,[18] Jackson,[16] and others have argued, there could be an object at the center of our Galaxy which preferentially beams its radiation into the Galactic plane, where we lie. Our no-beaming assumption rules this out.)

Our fifth cherished belief is that narrow-band sources of gravitational waves ($\Delta f \ll f$) have their frequencies f distributed randomly over a bandwidth $\Delta f \gtrsim f$.

B. The Physical Laws Governing Gravitational Radiation

We take our cherished beliefs about gravitational-wave theory from general relativity — though most other relativistic theories of gravity would lead to similar beliefs. Our beliefs are expressed in order-of-magnitude form.

Consider a source of mass M, which radiates gravitational waves coherently. (Examples: A pulsating star, a binary star system, two colliding black holes.) If small parts of the source produce waves which superpose incoherently, those parts must be regarded as separate sources. (Example:

for the thermal bremsstrahlung radiation produced by collisions of electrons and ions inside the Sun, the source is not the entire Sun but rather a single colliding electron-ion pair.) Let f be a frequency at which the source radiates significantly. Our first cherished belief is an upper limit on the frequency f, for a given source mass M:[5]

$$f \leqslant \frac{c^3/G}{2\pi M} \simeq \frac{30000 \text{ Hz}}{M/M_\odot} \quad . \tag{1}$$

This limit corresponds to a belief that the characteristic timescale $(2\pi f)^{-1}$ of the coherent waves must exceed the light-travel time across half the Schwarzschild radius of the source, GM/c^3. This limit can be violated in sources with significant beaming — e.g., sources with ultrarelativistic internal velocities;[13,14] but we have ruled out such sources. We strongly doubt that coherent, nonbeaming sources can violate this limit. For example, typical events involving black holes (births, collisions, infall of matter) produce waves of frequency $f \sim 10000 \text{ Hz } (M/M_\odot)^{-1}$,[19,20,21,5] with a very rapid falloff of intensity above $f = 30000 \text{ Hz } (M/M_\odot)^{-1}$.

In general relativity and other similar theories, a source with negligible beaming gives rise predominantly to quadrupole radiation. The luminosity of such a source is given by Einstein's[22] quadrupole formula

$$L = \frac{1}{5} (G/c^5)\Big(\sum_{j,k} \partial^3 I_{jk}/\partial t^3\Big)^2 \quad ,$$

where the third time derivative of the quadrupole moment, expressed in terms of the coherent source's mass M, radius R, and frequency f, is

$$\partial^3 I_{jk}/\partial t^3 \leqslant MR^2(2\pi f)^3 \leqslant 2\pi M f c^2 \quad .$$

Here we have used the relation, for a coherent source,

$$(2\pi fR) \simeq (\text{internal velocity of source}) \leqslant c \quad .$$

Combining these relations we obtain a cherished belief about the maximum luminosity that a source of mass M and frequency f can produce:

$$L \leqslant \frac{G}{c}(2\pi Mf)^2 \simeq (4 \times 10^{50} \text{ erg/sec}) \left(\frac{M}{M_\odot}\right)^2 \left(\frac{f}{1 \text{ Hz}}\right)^2 \quad . \tag{2}$$

Note that when $f = f_{max} = (c^3/G)(2\pi M)^{-1}$, then $L \leqslant L_{max} \simeq c^5/G \approx (4 \times 10^{59}$ erg/sec) — a limit which, so far as we know, was first suggested by Dyson.[23]

In our analysis we shall idealize our typical source as radiating gravitational waves in a series of outbursts separated by quiescent periods. Let N denote the total number of outbursts, τ_* the mean duration of each outburst, and L the average luminosity during each outburst. Our next cherished belief is that, in the source's entire lifetime the total energy radiated cannot exceed the total mass-energy Mc^2 of the source:

$$NL\tau_* \leq Mc^2 \quad . \tag{3}$$

In describing the gravitational waves arriving at Earth we shall use, at various times, four different measures of wave strength: First, in describing waves from discrete sources we shall use a mean value h for the dimensionless gravitational-wave amplitude at the frequency f in a bandwidth $\Delta f \simeq f$:

$$h \simeq \langle [h_+(t)]^2 + [h_\times(t)]^2 \rangle^{1/2} \quad .$$

Here the average $\langle \ \rangle$ is over the time τ_* that the source is on; and $h_+(t)$

and $h_\times(t)$ are the dimensionless amplitudes for the two orthogonal modes of polarization, which for a source in the z-direction determine the transverse-traceless part of the metric perturbation via

$$\mathbf{h}^{TT} = h_+(t - z)[\underset{\sim}{e}_x \otimes \underset{\sim}{e}_x - \underset{\sim}{e}_y \otimes \underset{\sim}{e}_y] + h_\times(t - z)[\underset{\sim}{e}_x \otimes \underset{\sim}{e}_y + \underset{\sim}{e}_y \otimes \underset{\sim}{e}_x] \ .$$

We presume that h_+ and $h_\times$ have been sent through a bandpass filter of frequency f and bandwidth $\Delta f \simeq f$. For monochromatic waves, $h_+(t) = A_+ \cos(2\pi ft + \varphi_+)$ and $h_\times(t) = A_\times \cos(2\pi ft + \varphi_\times)$, our definition of h gives $h = [\frac{1}{2}(A_+^2 + A_\times^2)]^{\frac{1}{2}}$. Second, for discrete sources we shall also use the total flux of energy, $\mathcal{F}$, at the frequency f and in the bandwidth $\Delta f \simeq f$. We shall assume (cherished belief!) the general relativistic relationship between $\mathcal{F}$ and h:

$$\mathcal{F} = \frac{c^3}{G} \cdot \frac{\pi}{4} f^2 h^2 = \left(0.03 \frac{\text{erg}}{\text{cm}^2\,\text{s}}\right)\left(\frac{f}{1\ \text{Hz}}\right)^2\left(\frac{h}{10^{-20}}\right)^2 \ . \qquad (4)$$

Third, in describing stochastic background radiation, we shall use the energy flux per unit frequency, $\mathcal{F}_f$ ("flux density"; ergs cm^{-2} sec^{-1} Hz^{-1}), which our cherished beliefs imply will be independent of the orientation of our unit surface area. Fourth, for the stochastic background we shall also use an amplitude $\tilde{h}(f)$ (dimensions $\text{Hz}^{-1/2}$), which is defined in analogy with Eq. (4) by

$$\mathcal{F}_f = \frac{c^3}{G} \frac{\pi}{4} f^2 \tilde{h}^2 = \left(0.03 \frac{\text{erg}}{\text{cm}^2\ \text{sec Hz}}\right)\left(\frac{f}{1\ \text{Hz}}\right)^2\left(\frac{\tilde{h}}{10^{-20}\ \text{Hz}^{-1/2}}\right)^2 \ . \qquad (5)$$

The square of $\tilde{h}$, roughly speaking, is the spectral density of the gravitational-wave amplitude h(t). The stochastic background will produce in a broad-band gravitational-wave detector a spectral density of strain $(\Delta\ell/\ell)_f^2 = \alpha\,\tilde{h}^2$, where α is a factor of order unity which depends on the detailed construction of the detector.

In relating the strengths of the waves at earth to the luminosity L of a source at distance r, we shall assume energy conservation (cherished belief!)

$$\mathcal{F}_{\text{due to one source}} = L/4\pi r^2 \quad , \tag{6}$$

and we shall assume that gravitational waves propagate at the speed of light (cherished belief!).

III. UPPER LIMITS ON STOCHASTIC BACKGROUND

From the cherished beliefs of § II one can derive the upper limits on a stochastic background of gravitational radiation shown in Figure 1. In § A we explain the origin of the limit for extragalactic radiation; in § B we explain the Galactic limit.

A. Extragalactic Radiation

Consider a specific frequency f at which the background is strong, and let Δf be the bandwidth about f over which the specific flux $\mathcal{F}_f$ is roughly constant. For a background due to broad-band sources, by definition of "broad-band," we have $\Delta f \gtrsim f$. For a background due to superposed narrow-band sources, the last cherished belief of § II.A ("frequencies distributed randomly over a bandwidth $\gtrsim$ f") implies $\Delta f \gtrsim f$. Thus, in either case the background is roughly constant over $\Delta f \gtrsim f$, but it can drop off fairly rapidly at both ends of this band.

An upper limit on $\mathcal{F}_f$, for extragalactic background, follows from our cherished beliefs that (i) the total energy radiated by all sources cannot exceed the sum of the masses of those sources; and (ii) we do not live at a special place or time, so that the total gravitational-wave energy must be spread roughly uniformly over the entire universe and the energy density at Earth must be roughly the same as the average energy density in the universe. These beliefs imply a total energy density in background radiation at Earth less than or of order the total mass-energy density of the universe:

$$\begin{pmatrix}\text{background}\\ \text{energy density}\end{pmatrix} = 4\mathcal{F}_f \Delta f/c \leqslant \rho_u c^2 \quad .$$

(The factor 4 comes from integrating over all directions.) Combining this with the bandwidth requirement $\Delta f \gtrsim f$, we obtain the limit

$$\mathcal{F}_f \leq \frac{1}{4}(\rho_u c^3/f) \simeq \left(100 \frac{\text{erg}}{\text{cm}^2 \text{ sec Hz}}\right)\left(\frac{f}{1 \text{ Hz}}\right)^{-1} , \qquad (7a)$$

which corresponds to a wave amplitude

$$f^{1/2} \tilde{h} \leq 6 \times 10^{-19} (f/1 \text{ Hz})^{-1} \qquad (7b)$$

(cf. Eq. 5). These limits are shown in Figure 1.

These extragalactic limits are widely accepted and often discussed in the astrophysical literature — see, e.g., reference 24.

The upper limit (7) can be achieved, within the framework of our cherished beliefs, in a variety of ways. For example, at any frequency $f \leq 10000$ Hz the following scenario is allowed, though not likely: Early in the evolution of the Universe a sizable fraction of the Universe's mass might have gone into black-hole binary systems of mass $M \sim (c^3/G)(2\pi f)^{-1}$. Under the action of gravitational radiation reaction the holes in each binary will spiral together, releasing a sizable fraction of their mass M in a final burst of broad-band radiation of frequency f and duration $\tau_* \sim (2\pi f)^{-1}$. These bursts must be randomly distributed over the volume of the universe and over the Hubble time, so that the average number of bursts occurring at any given time is

$$\eta = \frac{(4\pi/3)\ \rho_u R_H^3}{M}\ \frac{\tau_*}{T_H} \sim 1$$

(cf. relations in §A of Box 1). This is also the average number of bursts passing Earth at each moment of time: and these bursts give rise to background radiation near the upper limit (7).

One can also achieve these upper limits by a superposition of many bursts with lower individual intensities and longer individual durations.

B. Galactic Radiation

For Galactic background radiation, as for extragalactic, the bandwidth over which $\mathcal{F}_f$ is large must be $\Delta f \gtrsim f$. The radiation must be spread roughly uniformly over the interior of the Galaxy ("no special place"), so that the total radiation energy in the Galaxy is $(4\mathcal{F}_f \Delta f)(4\pi/3)(R_g^3/c)$. This radiation energy will escape from the Galaxy in a time R_g/c and must be replenished by source emission in that time. The total energy emitted during the Hubble time T_H is thus $(cT_H/R_g) \times$ (energy density now in Galaxy); and this cannot exceed the total mass-energy of the Galaxy, $(4\pi/3)R_g^3 \rho_g c^2$. Combining these constraints we obtain the upper limit

$$\mathcal{F}_f \leq \frac{1}{4} \frac{R_g \rho_g c^2}{f T_H} \simeq 100 \frac{\text{erg}}{\text{cm}^2 \text{ sec Hz}} \left(\frac{f}{1 \text{ Hz}}\right)^{-1} , \tag{8a}$$

which corresponds to a wave amplitude

$$f^{1/2} \tilde{h} \leq 6 \times 10^{-19} \, (f/1 \text{ Hz})^{-1} . \tag{8b}$$

Note that this is the same order-of-magnitude limit as we obtained for extragalactic radiation! It is the same by virtue of the coincidence (or is it a coincidence?) that the closure density ρ_u and Hubble distance $R_H = cT_H$ of the Universe, and the density ρ_g and radius R_g of the Galaxy satisfy

$$\rho_u \sim \rho_g (R_g/R_H) .$$

The upper limit (8) can be achieved, within the framework of our cherished beliefs, by putting the bulk of the mass of our Galaxy into objects of mass $\sim M$ [with $M \leq (c^3/G)(2\pi f)^{-1}$ and $M \leq M_{max} = 10^8 M_\odot$], which radiate away all their mass in bursts of mean frequency f, duration τ_*, and luminosity $L = Mc^2/\tau_*$ [with $L \leq (G/c)(2\pi Mf)^2$ and $\tau_* \leq T_H$]. The locations of these objects

and the epoch of their emission must be randomly distributed through the Galaxy; so the number of "on" sources contributing to $\mathcal{F}_f$ at Earth at any given time will be $\eta \simeq (M_g/M)(\tau_*/T_H)$ [where $\eta \gtrsim 1$ so that experimenters will see a background rather than individual events]. The mass M and burst duration τ_* can be chosen in accord with our cherished-belief constraints (items in square brackets above) so long as

$$f \gtrsim f_{min} \simeq \left(\frac{c^3/G}{4\pi^2 M_{max} T_H} \right)^{1/2} \simeq 1 \times 10^{-11} \text{ Hz} \quad ; \tag{9}$$

and thus for these frequencies our cherished beliefs cannot give any limit tighter than (8). Note that $f \gtrsim f_{min}$ includes all frequencies of experimental interest. At lower frequencies, objects of mass $M \leqslant M_{max} = 10^8 M_\odot$ radiating with luminosities $L \leqslant (G/c)(2\pi Mf)^2$ cannot radiate away all their mass-energy Mc^2 in a time τ_* less than the age of the Universe T_H; and, consequently, the maximum Galactic flux density and wave amplitude are reduced from the limit (8) to

$$\mathcal{F}_f \leqslant \frac{1}{4} \frac{R_g \rho_g c^2}{f T_H} \left(\frac{f}{f_{min}} \right)^2 \simeq 10^{13} \frac{\text{erg}}{\text{cm}^2 \text{ sec Hz}} \left(\frac{f}{f_{min}} \right) \quad , \tag{10a}$$

$$f^{1/2} \tilde{h} \leqslant 6 \times 10^{-19} \, (f/1 \text{ Hz})^{-1} \, (f/f_{min}) \simeq 6 \times 10^{-8} \tag{10b}$$

for

$$f \lesssim f_{min} \simeq 1 \times 10^{-11} \text{ Hz} \quad .$$

However, this range of frequencies is outside the domain of interest for the present discussion (10^{-4} Hz $\leqslant f \leqslant 10^{+4}$ Hz).

IV. UPPER LIMITS ON WAVES FROM DISCRETE SOURCES

We turn now to gravitational waves from discrete (resolved) sources, including broad-band bursts (duration $\tau_* \sim 1/2\pi f$); transient sources ($1/2\pi f \ll \tau_* < \hat{\tau}$, where $\hat{\tau}$ is the total observation time, i.e., the total time that the experimenter searches for gravitational waves); and permanent sources ($\tau_* \gtrsim \hat{\tau}$). The transient sources and permanent sources can be either broad-band ($\Delta f \gtrsim f$) or narrow-band ($\Delta f \ll f$). Our characterization of the waves by their flux $\mathcal{F}$ and amplitude h pays no attention to the bandwidth of the source. Since the experimenter can never know the total "on time" τ_* of the source unless $\tau_* < \hat{\tau}$, and since our cherished beliefs allow stronger waves the shorter is τ_*, we can restrict attention to the case $\tau_* \leq \hat{\tau}$.

For discrete sources our upper limits answer the following question: "An experimenter searches, with total observation time $\hat{\tau}$, for a gravitational-wave event of duration $\tau_* \leq \hat{\tau}$ at frequencies $f > (2\pi\tau_*)^{-1}$ in a bandwidth $\Delta f \simeq f$. What is the flux $\mathcal{F}$ and amplitude h of the strongest single event he can hope to see within the constraints of our cherished beliefs?" The upper limits that answer this question are shown in Figure 2. These limits are derived and discussed, for extragalactic sources, in §A below, and for Galactic sources in §B.

A. Extragalactic Sources

Let the frequency f, event duration τ_*, and observation time $\hat{\tau}$ be given. The waves will be strongest if the bulk of the mass of the Universe resides in sources of some optimally chosen mass M [with $M \leqslant (c^3/G)(2\pi f)^{-1}$], each of which produces some optimal luminosity L during its "on time" τ_* [where $L \leqslant (G/c)(2\pi Mf)^2$], and each of which has some optimal number N of "on events" during the Hubble time T_H [with $NL\tau_* \leq Mc^2$].

The number density of sources is $n \simeq \rho_u/M$, and the probability that a given source will turn on during the observation time $\hat{\tau}$ is $P = N\hat{\tau}/T_H$. Consequently, the nearest source that turns on during $\hat{\tau}$ is at a distance

$$r \simeq \frac{1}{2}(nP)^{-1/3} = \frac{1}{2}\left(\frac{MT_H}{\rho_u N\hat{\tau}}\right)^{1/3} ;$$

and the flux produced at Earth by this nearest (and thus strongest) source is

$$\mathcal{F} = \frac{L}{4\pi r^2} = \frac{1}{\pi}\left(\frac{N^2L^3}{M^2}\right)^{1/3}\left(\frac{\rho_u\hat{\tau}}{T_H}\right)^{2/3} .$$

This flux is maximized, subject to our cherished-belief constraints (square brackets above) by setting $N = 1$, $M \simeq (c^3/G)(2\pi f)^{-1}$, and $L \simeq Mc^2/\tau_*$ [corresponding to $L \simeq (2\pi f\tau_*)^{-1}\,(G/c)(2\pi Mf)^2 \leqslant (G/c)(2\pi Mf)^2$]. The resulting upper limit is

$$\mathcal{F} \leqslant \left(\frac{1}{2\pi f\tau_*}\right)\left(\frac{c^3}{\pi G^{1/3}}\right)\left(\frac{\rho_u 2\pi f\hat{\tau}}{T_H}\right)^{2/3}$$

$$\simeq \left(\frac{1\times 10^{7}\ \text{erg cm}^{-2}\ \text{sec}^{-1}}{2\pi f\tau_*}\right)\left(\frac{f}{1\ \text{Hz}}\right)^{2/3}\left(\frac{\hat{\tau}}{10^6\ \text{sec}}\right)^{2/3} , \qquad (11a)$$

which corresponds to an amplitude

$$h \leqslant \frac{2\times 10^{-16}}{(2\pi f\tau_*)^{1/2}}\left(\frac{f}{1\ \text{Hz}}\right)^{-2/3}\left(\frac{\hat{\tau}}{10^6\ \text{sec}}\right)^{1/3} . \qquad (11b)$$

The factors $2\pi f\tau_*$ are of order 1 for the most abrupt bursts; slower bursts are constrained to contain the same total energy $Mc^2 = 4\pi r^2\mathcal{F}\tau_*$ and so produce a lower flux $\mathcal{F} \propto 1/\tau_*$.

B. Galactic Sources

Let the frequency f, event duration τ_*, and observation time $\hat{\tau}$ be given. At sufficiently high frequencies an argument identical to that for extragalactic sources (§A) gives the same answer, but with ρ_u replaced by ρ_g: It is optimal for the bulk of the mass of the Galaxy to be put into objects of mass $M \simeq (c^3/G)(2\pi f)^{-1}$, which radiate all their mass-energy Mc^2 in single bursts of duration τ_* and luminosity $L = Mc^2/\tau_*$. The strongest burst seen in time $\hat{\tau}$ has flux $\mathcal{F}$ and amplitude h at the upper limit of the inequalities

$$\mathcal{F} \leqslant \left(\frac{1}{2\pi f\tau_*}\right)\left(\frac{c^3}{\pi G^{1/3}}\right)\left(\frac{\rho_g 2\pi f\hat{\tau}}{T_H}\right)^{2/3}$$

$$\simeq \left(\frac{2 \times 10^{10} \text{ erg cm}^{-2} \text{ sec}^{-1}}{2\pi f\tau_*}\right)\left(\frac{f}{1 \text{ Hz}}\right)^{2/3}\left(\frac{\hat{\tau}}{10^6 \text{ sec}}\right)^{2/3} , \tag{12a}$$

$$h \leqslant \frac{1 \times 10^{-14}}{(2\pi f\tau_*)^{1/2}}\left(\frac{f}{1 \text{ Hz}}\right)^{-2/3}\left(\frac{\hat{\tau}}{10^6 \text{ sec}}\right)^{1/3} , \tag{12b}$$

$$\text{for} \quad f \gtrsim f_{crit} \text{ (defined below).}$$

As one moves to lower and lower frequencies, the optimal scenario corresponds to the strongest event being farther and farther from Earth — at a distance

$$r \simeq \frac{1}{2}\left(\frac{MT_H}{\rho_G\hat{\tau}}\right)^{1/3} = \frac{1}{2}\left[\frac{(c^3/G)\ T_H}{\rho_g 2\pi f\hat{\tau}}\right]^{1/3} .$$

Ultimately, at critical frequency

$$f_{crit} \simeq \frac{1}{12}\ \frac{c^3}{G}\ \frac{T_H}{M_g\hat{\tau}} \simeq \frac{5\text{kHz}}{(\hat{\tau}/10^6 \text{ sec})} , \tag{13}$$

the distance r has grown to the galactic radius R_g. At frequencies $f < f_{crit}$, r exceeds R_g and our optimal scenario is no longer valid.

In the low-frequency regime $f < f_{crit}$ it is optimal to have just one emission event in the entire Galaxy during the observation time $\hat{\tau}$, with a mean distance $r \simeq 3R_g/4$ and a luminosity $L \simeq (M_g c^2/\tau_*)(\hat{\tau}/T_H)$ so large that the entire mass of the Galaxy will be exhausted in the time T_H. These events correspond to a flux and amplitude at the upper limit of the inequalities

$$\mathcal{F} \leqslant \frac{4}{9\pi} \frac{M_g c^2 \hat{\tau}}{R_g^2 T_H \tau_*} = \left(\frac{2 \times 10^9 \text{ erg cm}^{-2} \text{ sec}^{-1}}{2\pi f \tau_*}\right)\left(\frac{f}{1 \text{ Hz}}\right)\left(\frac{\hat{\tau}}{10^6 \text{ sec}}\right) , \tag{14a}$$

$$h \leqslant \frac{2 \times 10^{-15}}{(2\pi f \tau_*)^{1/2}} \left(\frac{f}{1 \text{ Hz}}\right)^{-1/2} \left(\frac{\hat{\tau}}{10^6 \text{ sec}}\right)^{1/2} \tag{14b}$$

$$\text{for} \quad f \leqslant f_{crit} .$$

Our cherished beliefs permit these events to be produced by objects of mass M anywhere in the range

$$M \leqslant \left(\frac{c^3/G}{2\pi f}\right) \simeq 4 M_\odot \left(\frac{f}{f_{crit}}\right)^{-1} \left(\frac{\hat{\tau}}{10^6 \text{ sec}}\right) ,$$

$$M \gtrsim L\tau_*/c^2 \simeq M_g \hat{\tau}/T_H \simeq 4 M_\odot (\hat{\tau}/10^6 \text{ sec})$$

$$M \gtrsim \left(\frac{1}{2\pi f}\right)\left(\frac{cL}{G}\right)^{1/2} \simeq \left(\frac{c^3/G}{2\pi f \tau_*} \frac{M_g \hat{\tau}}{2\pi f T_H}\right)^{1/2} \simeq \frac{4 M_\odot}{(2\pi f \tau_*)^{1/2}} \left(\frac{f}{f_{crit}}\right)^{-1/2} \left(\frac{\hat{\tau}}{10^6 \text{ sec}}\right) .$$

In this optimal scenario each source must experience $N \simeq Mc^2/L\tau_*$ outbursts in its lifetime. As the frequency decreases far below f_{crit}, it ultimately reaches a limiting value

$$f_{lim} \simeq \left[\frac{(c^3/G) M_g \hat{\tau}}{(2\pi M_{max})^2 \tau_* T_H}\right]^{1/2} \simeq (1 \times 10^{-9} \text{ Hz})(\hat{\tau}/\tau_*)^{1/2} \tag{15}$$

at which our optimal scenario requires source masses in excess of $M_{max} = 10^8 M_\odot$. Below this frequency the flux and amplitude limits (14) are no longer valid — but this ultralow-frequency regime is outside our domain of interest, and we shall ignore it.

An attractive (albeit not highly likely) scenario for producing broad-band bursts, $\tau_* \sim 1/f$, at kilohertz frequencies, with amplitude h near the upper limit (12b), (14b) is the following: It is fashionable to speculate[25] that before galaxies formed, a sizable fraction of the mass of the Universe may have condensed into massive stars ($M \sim 2$ to $20\ M_\odot$), conventionally called stars of "Population III." A significant fraction of these stars, like stars today, might have formed in close binaries which produce, after the stars have exhausted their nuclear fuel (in $\Delta t \leqslant 1$ billion years), black-hole and/or neutron-star binary systems. When our Galaxy condensed out of the intergalactic medium, such binaries would have snuggled down around the Galaxy[26] to form a massive halo of the type for which there is strong empirical evidence.[9,10,11] The orbital parameters of these compact binaries in our halo could perfectly well be such that the mean time for the two stars or holes to spiral together due to gravitational radiation reaction is of order the Hubble time T_H. At the end of its inward spiral, such a binary will emit a sizable fraction of its rest mass ($\sim$ 2 to 20 percent) in a broad-band burst of gravitational waves at kilohertz frequencies.[20,27,28] These bursts could be the events of our optimal Galactic scenario.

V. DISCUSSION

It is interesting to compare the cherished-belief upper limits of Figures 1 and 2 with the sensitivities of gravitational-wave detectors — past, present, and future.

The first-generation Weber-type bars (1968-1976) were capable of detecting broad-band bursts occurring once in $\hat{\tau} \simeq 10^6$ sec with frequencies $f \simeq 1000$ Hz and amplitudes $h \gtrsim 3 \times 10^{-16}$. This sensitivity was a little worse than our cherished-belief upper limits (Fig. 2) — which explains why theorists could account for Weber's observed events[29] only by invoking unconventional hypotheses (strong beaming by sources near the galactic center;[15,16,18] or today being a very special time in the evolution of the Galaxy[30]).

Second-generation detectors of the bar type and laser-interferometer type (1979-82) are designed to have sensitivities $h \gtrsim 10^{-18}$ for events occurring once in $\hat{\tau} \simeq 10^6$ sec with frequencies $f \simeq 100$ to 1000 Hz. Such sensitivities are considerably better than our cherished-belief limits (Fig. 2). Thus, although conventional scenarios do not predict waves at this level (sensitivity worse than "type-two benchmarks"), a discovery of waves by second-generation detectors is prefectly possible within the framework of our cherished beliefs.

At much lower frequencies, $f \sim 10^{-3}$ Hz, Doppler tracking of spacecraft is being used to search for gravitational waves. The best sensitivities yet achieved, using the Viking spacecraft,[31] correspond to an rms noise level $h_{rms} \sim 3 \times 10^{-14}$ and a sensitivity to $\hat{\tau} = 10^6$ sec bursts of $h \sim 2 \times 10^{-13}$. These sensitivities are slightly worse than our cherished-belief limits. However, future experiments using the Solar Polar spacecraft (1983) and improved tracking technology are projected to have amplitude sensitivities a

factor ~10 better than Viking's, and a proposed Solar Probe spacecraft (~1986) might do a factor ~100 better.[32] Such sensitivities would be somewhat better than our cherished-belief upper limits.

In conclusion, the technology of gravitational-wave detection is now crossing over our cherished-belief benchmarks. Near-future experiments will be in a realm where it is not irrational to hope for positive results!

The question answered by this paper was posed to us by Ronald W. P. Drever and Ranier Weiss. We thank them.

REFERENCES

1. J. A. Tyson and R. P. Giffard, Ann. Rev. Astron. Astroph., 16, 521 (1978).
2. V. B. Braginsky and V. N. Rudenko, Physics Reports, 46, 165 (1978).
3. D. H. Douglass and V. B. Braginsky, in Gravitational Theories Since Einstein, edited by S. W. Hawking and W. Israel (Cambridge England: Cambridge University Press, 1979).
4. R. Weiss, in Sources of Gravitational Radiation, edited by L. Smarr (Cambridge England: Cambridge University Press, 1979).
5. K. S. Thorne, in Theoretical Principles in Astrophysics and Relativity, edited by N. R. Lebovitz, W. H. Reid, and P. O. Vandervoort (Chicago: University of Chicago Press, 1978).
6. R. Epstein and J. P. A. Clark, in Sources of Gravitational Radiation, edited by L. Smarr (Cambridge England: Cambridge University Press, 1979).
7. L. P. Grischuck, Pis'ma Zh. Eksp. Teor. Fiz., 23, 326 (1976); English translation: Soviet Physics—JETP Letters, 23, 293 (1976); and references therein.
8. B. Bertotti and B. J. Carr, submitted to Astron. Astroph. (1979); also available as a Caltech Orange-Aid Preprint.
9. J. P. Ostriker and P. J. E. Peebles, Astrophys. J., 186, 467 (1973).
10. J. Bardeen, in Proc. IAU Symposium No. 69, Dynamics of Stellar Systems, edited by A. Hayli (Dordrecht Holland: Reidel, 1975), p. 297.
11. A. Toomre, Ann. Rev. Astron. Astroph., 15, 437 (1977).
12. J. H. Oort, Ann. Rev. Astron. Astroph., 15, 295 (1977).
13. C. M. Misner, in Colloques Internationaux du CNRS No. 220, Ondes et radiations gravitationelles, edited by Y. Choquet-Bruhat (Paris: Editions du CNRS, 1974) and references cited therein.

14. S. J. Kovács, Jr. and K. S. Thorne, Astrophys. J., 224, 62 (1978).

15. J. K. Lawrence, Astrophys. J., 171, 483 (1971).

16. J. C. Jackson, Nature, 241, 513 (1973).

17. W. H. Press, Phys. Rev. D, 15, 965 (1977).

18. C. W. Misner, Phys. Rev. Letters, 28, 994 (1972).

19. M. Davis, R. Ruffini, W. H. Press, and R. H. Price, Phys. Rev. Letters, 27, 1466 (1971).

20. S. L. Detweiler and E. Szedenits, Jr., Astrophys. J., in press; also available as Caltech Orange-Aid Preprint 542.

21. C. T. Cunningham, R. H. Price, and V. Moncrief, Astrophys. J., 224, 643 (1978); and Astrophys. J., in press.

22. A. Einstein, Berlin Sitzungsberichte (1918), 154.

23. F. J. Dyson, in Interstellar Communication, edited by A. G. W. Cameron (New York: W. A. Benjamin, 1963).

24. M. Rees, in Colloques Internationaux du CNRS No. 220, Ondes et radiations gravitationelles, edited by Y. Choquet-Bruhat (Paris: Editions du CNRS, 1974), p. 203.

25. J. W. Truran and A. G. W. Cameron, Astrophys. and Space Sci., 14, 179 (1971).

26. J. E. Gunn, Astrophys. J., 218, 592 (1977).

27. J. P. A. Clark and D. M. Eardley, Astrophys. J. (Letters), 215, 311 (1977).

28. S. L. Detweiler, Astrophys. J., 225, 687 (1978).

29. J. Weber, Phys. Rev. Letters, 22, 1302 (1969) and 24, 6 (1970).

30. P. Kafka, Nature, 226, 436 (1970).

31. J. W. Armstrong, R. Woo, and F. B. Estabrook, Astrophys. J., in press.

32. F. B. Estabrook, in A Close-Up of the Sun, edited by M. Neugebauer and R. W. Davies (Pasadena, California: JPL 78-70, 1978), p. 441.

BOX 1

NOTATION

A. Parameters Describing the Structure of the Universe

T_H = Hubble time = 1×10^{10} years = 3×10^{17} seconds

$R_H = cT_H$ = Hubble radius = 1×10^{10} ℓ yr = 9×10^{27} cm

ρ_u = mean mass density of universe = $\frac{3c^2/G}{8\pi R_H^2}$ = 1×10^{-8} $M_\odot/\ell$ yr^3
= 2×10^{-29} g cm^{-3}

R_g = Galaxy radius = 6×10^4 ℓ yr = 6×10^{22} cm

M_g = Galaxy mass = 1×10^{12} $M_\odot$ = 2×10^{45} g

ρ_g = mean mass density of galaxy = $3M_g/4\pi R_g^3$ = 0.001 $M_\odot/\ell$ yr^3
= 2×10^{-24} g cm^3

M_{max} = (maximum mass of coherently radiating object in our Galaxy) = 10^8 $M_\odot$

B. Parameters Describing Gravitational-Wave Sources and their Radiation

M = mass of coherently radiating source

f = mean frequency emitted by source

L = luminosity of source (ergs/sec) in "on" state

τ_* = "on" time for source; burst duration

N = number of "on" events during source's lifetime

n = number of density of sources

r = distance to nearest source

C. Parameters Describing Radiation Arriving at Earth

$\hat{\tau}$ = observation time; experiment duration

$\mathcal{F}$ = flux of energy in gravitational waves (erg cm^{-2} sec^{-1})

h = amplitude of gravitational waves

$\mathcal{F}_f$ = flux density of gravitational-wave background (erg cm^{-2} sec^{-1} Hz^{-1})

$\tilde{h}$ = square root of spectral density of amplitude of background radiation ($Hz^{-1/2}$)

FIGURE CAPTIONS

Figure 1. Upper limits on a stochastic background of gravitational radiation at Earth (Eqs. 7 and 8). The limit for radiation from sources in our Galaxy is approximately the same as the limit for extragalactic radiation. For notation, see Eq. (5) of text and associated discussion.

Figure 2. Upper limits on discrete sources of gravitational waves (Eqs. 11-14). These limits answer the following question: "An Experimenter searches, with total observation time $\hat{\tau}$, for a discrete gravitational-wave event of duration $\tau_* \leq \hat{\tau}$ at frequencies $f > 1/\tau_* \geq 1/\hat{\tau}$ in a bandwidth $\Delta f \simeq f$. What is the flux $\mathcal{F}$ and amplitude h (Eq. 4 and associated discussion) of the strongest single event he can hope to see, within the constraints of our cherished beliefs?"

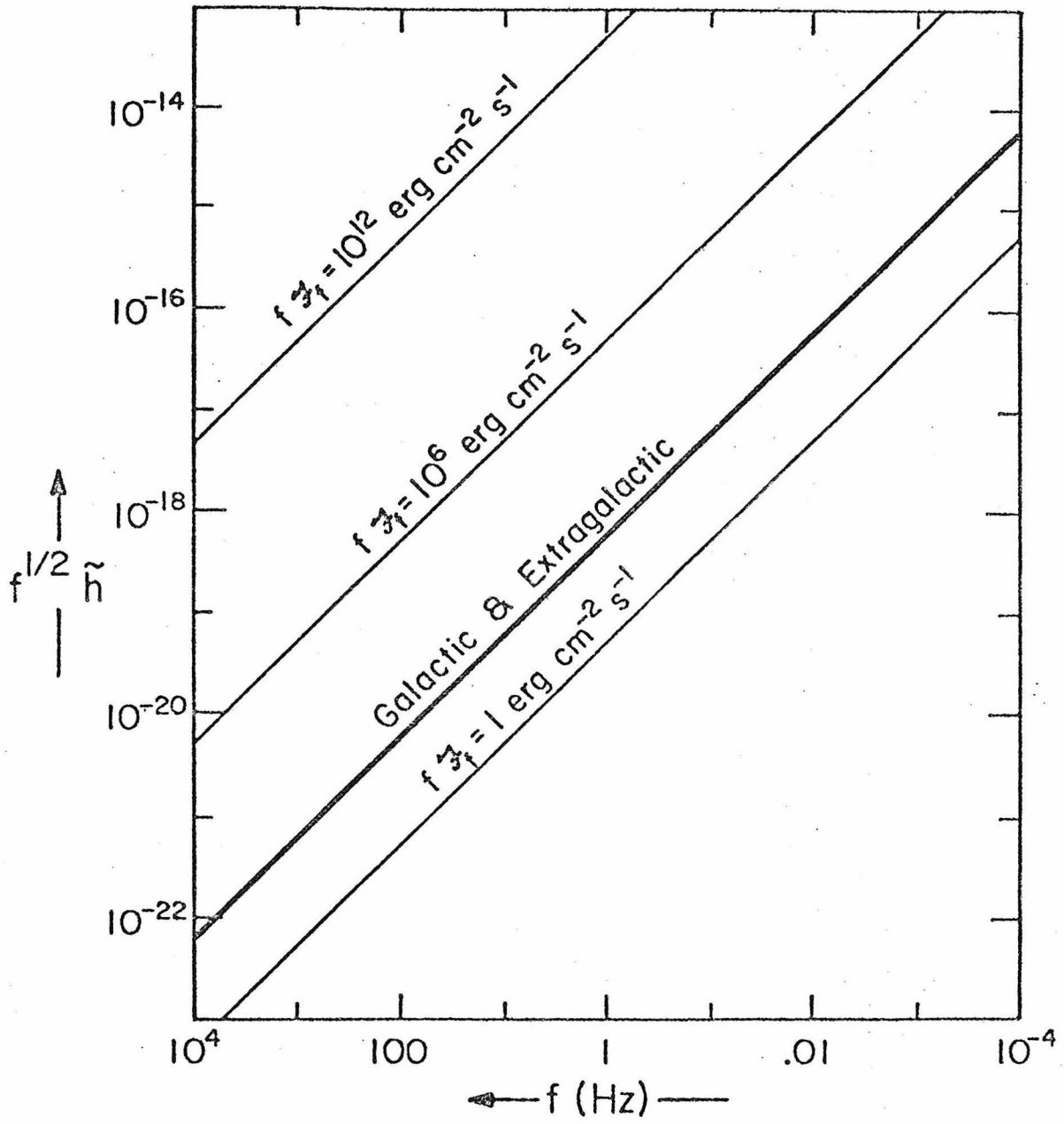
10^{-14}
10^{-16}
10^{-18}
10^{-20}
10^{-22}
$f^{1/2}\,\tilde{h}$
$f\,\mathcal{F}_f = 10^{12}$ erg cm^{-2} s^{-1}
$f\,\mathcal{F}_f = 10^{6}$ erg cm^{-2} s^{-1}
Galactic & Extragalactic
$f\,\mathcal{F}_f = 1$ erg cm^{-2} s^{-1}
10^{4}
100
1
.01
10^{-4}
f (Hz)

Fig. 1

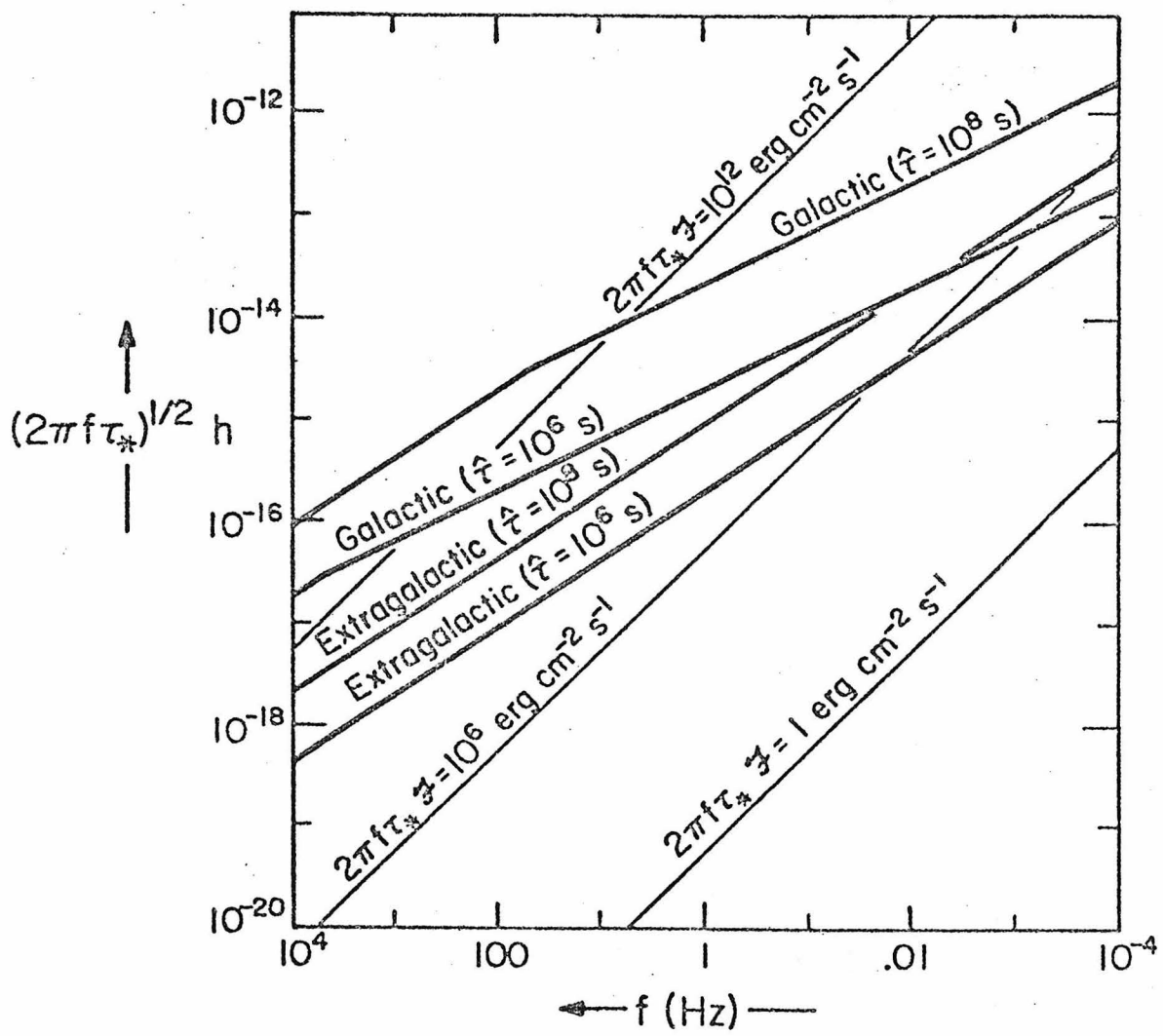
10^{-12}
10^{-14}
10^{-16}
10^{-18}
10^{-20}
$(2\pi f \tau_*)^{1/2}$ h
$2\pi f \tau_* \mathcal{F} = 10^{12}$ erg cm^{-2} s^{-1}
Galactic ($\hat{\tau} = 10^8$ s)
Galactic ($\hat{\tau} = 10^6$ s)
Extragalactic ($\hat{\tau} = 10^9$ s)
Extragalactic ($\hat{\tau} = 10^6$ s)
$2\pi f \tau_* \mathcal{F} = 10^6$ erg cm^{-2} s^{-1}
$2\pi f \tau_* \mathcal{F} = 1$ erg cm^{-2} s^{-1}
10^4
100
1
.01
10^{-4}
f (Hz)

Fig. 2

CHAPTER V

INERTIAL AND GRAVITATIONAL EFFECTS IN THE PROPER REFERENCE FRAME OF AN ACCELERATED, ROTATING OBSERVER

This chapter is a paper by Wei-Tou Ni and Mark Zimmermann. It was published in the 1978 March 15 issue of Physical Review D, Volume 17, pages 1473-1476.

PHYSICAL REVIEW D VOLUME 17, NUMBER 6 15 MARCH 1978

Inertial and gravitational effects in the proper reference frame of an accelerated, rotating observer

Wei-Tou Ni
Department of Physics, National Tsing Hua University, Hsinchu, Taiwan, Republic of China

Mark Zimmermann
W. K. Kellogg Radiation Laboratory, California Institute of Technology, Pasadena, California 91125

(Received 7 September 1977)

Most experimental laboratories accelerate and rotate relative to inertial frames. This paper derives approximate expressions for the general-relativistic metric and the general-relativistic equations of motion of freely falling particles in such a laboratory. The metric is derived accurate to second order in distance from the origin of coordinates; the equations of motion are derived accurate to first order. The equations of motion contain inertial, Coriolis, and centripetal pseudoforces, electric, magnetic, and magnetic-magnetic type forces due to Riemann curvature (inhomogeneous gravity), "gravitational red-shift" corrections to these forces, and velocity-induced special-relativistic corrections.

Synge[1] defined a natural coordinate system for an accelerated observer, which he called the "Fermi coordinates,"[2] and derived integral expressions for the metric and the inertial (coordinate) accelerations about the observer's world line for these coordinates in spacetime with small curvature. Manasse and Misner[3] obtained the second-order coordinate expansion of the metric in the special case of a freely falling observer. Using a somewhat different coordinate system, and a dyadic formalism, Estabrook and Wahlquist[4] derived an equation for the inertial acceleration near an arbitrary world line. Ni[5] and Mashhoon[6] calculated the second-order expansion of the metric and the first-order expansion of the inertial accelerations in these coordinates for an accelerated observer in special and general relativity, respectively.

A natural extension of the Fermi coordinates of Synge to the case of an accelerated *rotating* observer is the "local coordinates of the observer's proper reference frame" defined by Misner, Thorne, and Wheeler (MTW).[7] Such coordinates are important because they are the ones used by real experimenters in real earth-bound laboratories. MTW calculated the first-order expansion of the metric, and obtained the inertial accelerations on the world line of an arbitrarily accelerating and rotating observer. In this paper, we extend their work to obtain the second-order expansion of the metric and the first-order expansion of the inertial accelerations for the case of an arbitrarily accelerating and rotating observer in general relativity and in other metric theories of gravity. To this order, we include centripetal pseudoforces, second-order red-shifts, relativistic corrections, and electric and magnetic Riemann curvature terms.

Consider an observer moving along the world line $P_0(\tau)$ with four-velocity $u(\tau)$ and four-rotation $\omega(\tau)$ in a gravitational field with Riemann tensor $R^{\mu}{}_{\nu\alpha\beta}(\tau)$ along the world line. The orthonormal tetrad $\{e_{\hat{\alpha}}\}$ which the observer carries transports according to[8]

$$\frac{de_{\hat{\alpha}}}{d\tau} = -\vec{\Omega}\cdot e_{\hat{\alpha}}\,, \tag{1}$$

where

$$\Omega^{\mu\nu} \equiv a^{\mu}u^{\nu} - a^{\nu}u^{\mu} + u_{\alpha}\omega_{\beta}\epsilon^{\alpha\beta\mu\nu}\,,^{9} \tag{2}$$

$$a(\tau) \equiv \nabla_u u\,, \tag{3}$$

and τ is the proper time along the world line.

Following Sec. 13.6 of MTW, at any event $P_0(\tau)$ we send out geodesics $P(\tau; n; s)$ orthogonal to $u(\tau)$, where n is the unit vector tangent to a particular geodesic at $P_0(\tau)$, and $n\cdot u(\tau) = 0$. An event a distance s out along any geodesic n is then assigned the coordinates $x^{\hat{0}} \equiv \tau$, $x^{\hat{j}} \equiv sn\cdot e_{\hat{j}}$. These coordinates are called local coordinates.

This coordinate system is good for events near the world line, i.e., for

$$s \ll \min\left\{\frac{1}{|a|}, \frac{1}{|\omega|}, \frac{1}{|R^{\hat{\mu}}{}_{\hat{\nu}\hat{\alpha}\hat{\beta}}|^{1/2}}, \frac{|R^{\hat{\mu}}{}_{\hat{\nu}\hat{\alpha}\hat{\beta}}|}{|R^{\hat{\mu}}{}_{\hat{\nu}\hat{\alpha}\hat{\beta},\hat{\gamma}}|}\right\},$$

since within this distance the geodesics coming out of the world line do not cross ($s \ll 1/|a|$), the "light-cylinder" has not been reached ($s \ll 1/|\omega|$), curvature has not yet caused geodesics to cross ($s \ll 1/|R^{\hat{\mu}}{}_{\hat{\nu}\hat{\alpha}\hat{\beta}}|^{1/2}$), and the Riemann tensor has not yet changed much from its value on the world

line ($s \ll |R^{\hat{\mu}}{}_{\hat{\nu}\hat{\alpha}\hat{\beta}}|/|R^{\hat{\mu}}{}_{\hat{\nu}\hat{\alpha}\hat{\beta},\hat{\gamma}}|$). This last condition is usually the most severe restriction when using this coordinate system in an earth-bound laboratory.

In the local coordinate system we decompose a four-vector V as $V=(V^{\hat{0}}; V^{\hat{i}}) \equiv (V^{\hat{0}}; \vec{V})$. Now defining $b \equiv \nabla_u a$, $\eta \equiv \nabla_u \omega$ and using Eqs. (1) and (2) we have

$$b^{\hat{0}} = \vec{a}\cdot\vec{a}, \quad \vec{b} = \frac{d\vec{a}}{d\tau} + \vec{\omega}\times\vec{a}, \qquad \eta^{\hat{0}} = \vec{\omega}\cdot\vec{a}, \quad \vec{\eta} = \frac{d\vec{\omega}}{d\tau}. \tag{4}$$

Along $P_0(\tau)$, MTW derived the connection coefficients and the first-order partial derivatives to be

$$\left.\begin{aligned} &\Gamma^{\hat{0}}_{\hat{0}\hat{0}} = \Gamma^{\hat{\alpha}}_{\hat{j}\hat{k}} = 0 \\ &\Gamma^{\hat{\delta}}_{\hat{j}\hat{0}} = a^{\hat{j}} \\ &\Gamma^{\hat{j}}_{\hat{k}\hat{0}} = -\omega^{\hat{i}}\epsilon^{\hat{i}\hat{j}\hat{k}} \end{aligned}\right\} \text{ all along } P_0(\tau), \tag{5}$$

$$\left.\begin{aligned} &g_{\hat{\alpha}\hat{\beta},\hat{0}} = g_{\hat{j}\hat{k},\hat{i}} = 0 \\ &g_{\hat{0}\hat{0},\hat{j}} = -2a_{\hat{j}} \\ &g_{\hat{0}\hat{j},\hat{k}} = -\epsilon^{\hat{j}\hat{k}\hat{l}}\omega^{\hat{l}} \end{aligned}\right\} \text{ all along } P_0(\tau). \tag{6}$$

Differentiating Eqs. (5) along the trajectory with respect to τ and using Eqs. (4), we have

$$\left.\begin{aligned} &\Gamma^{\hat{0}}_{\hat{0}\hat{0},\hat{0}} = \Gamma^{\hat{\alpha}}_{\hat{j}\hat{k},\hat{0}} = 0 \\ &\Gamma^{\hat{0}}_{\hat{j}\hat{0},\hat{0}} = b^{\hat{j}}(\tau) + \epsilon^{\hat{j}\hat{k}\hat{l}}a^{\hat{k}}(\tau)\omega^{\hat{l}}(\tau) \\ &\Gamma^{\hat{i}}_{\hat{j}\hat{0},\hat{0}} = -\eta^{\hat{k}}(\tau)\epsilon^{\hat{i}\hat{j}\hat{k}} \end{aligned}\right\} \text{ all along } P_0(\tau). \tag{7}$$

From the definition of the Riemann tensor,

$$\Gamma^{\hat{\alpha}}_{\hat{\mu}\hat{0},\hat{\nu}} = R^{\hat{\alpha}}{}_{\hat{\mu}\hat{\nu}\hat{0}} + \Gamma^{\hat{\alpha}}_{\hat{\mu}\hat{\nu},\hat{0}} + (\Gamma^{\hat{\sigma}}_{\hat{\mu}\hat{\nu}}\Gamma^{\hat{\alpha}}_{\hat{\sigma}\hat{0}} - \Gamma^{\hat{\sigma}}_{\hat{\mu}\hat{0}}\Gamma^{\hat{\alpha}}_{\hat{\sigma}\hat{\nu}}). \tag{8}$$

Combining this equation with Eqs. (5), we find

$$\left.\begin{aligned} &\Gamma^{\hat{0}}_{\hat{0}\hat{0},\hat{i}} = b^{\hat{i}}(\tau) + 2a^{\hat{j}}(\tau)\omega^{\hat{k}}(\tau)\epsilon^{\hat{i}\hat{j}\hat{k}} \\ &\Gamma^{\hat{j}}_{\hat{0}\hat{0},\hat{i}} = R_{\hat{0}\hat{j}\hat{0}\hat{i}} - \eta^{\hat{k}}\epsilon^{\hat{j}\hat{i}\hat{k}} + a^{\hat{i}}a^{\hat{j}} \\ &\qquad + \omega^{\hat{i}}\omega^{\hat{j}} - \delta^{\hat{j}}_{\hat{i}}(\omega^{\hat{l}})^2 \\ &\Gamma^{\hat{0}}_{\hat{j}\hat{0},\hat{i}} = R_{\hat{0}\hat{j}\hat{0}\hat{i}} - a^{\hat{i}}a^{\hat{j}} \\ &\Gamma^{\hat{j}}_{\hat{k}\hat{0},\hat{i}} = R_{\hat{j}\hat{k}\hat{i}\hat{0}} + a^{\hat{k}}\omega^{\hat{l}}\epsilon_{\hat{l}\hat{j}\hat{i}} \end{aligned}\right\} \text{ all along } P_0(\tau). \tag{9}$$

To express $\Gamma^{\hat{\mu}}_{\hat{j}\hat{k},\hat{i}}$ in terms of $R_{\hat{\alpha}\hat{\beta}\hat{\gamma}\hat{\delta}}$, $\vec{a}$, $\vec{b}$, $\vec{\omega}$, and $\vec{\eta}$, we follow the method of Manasse and Misner[3] and use the geodesic deviation equation

$$\frac{d^2N^{\mu}}{ds^2} + 2\frac{dN^{\sigma}}{ds}\Gamma^{\mu}{}_{\sigma\alpha}U^{\alpha} + N^{\sigma}U^{\alpha}U^{\beta}R^{\mu}{}_{\alpha\sigma\beta} + N^{\sigma}U^{\alpha}U^{\beta}(\Gamma^{\mu}_{\sigma\alpha,\beta} + \Gamma^{\tau}{}_{\sigma\alpha}\Gamma^{\mu}{}_{\tau\beta} - \Gamma^{\mu}{}_{\sigma\tau}\Gamma^{\tau}{}_{\alpha\beta}) = 0, \tag{10}$$

where $N = \partial/\partial N$ and $U = \partial/\partial s$ of a one-parameter family of geodesics $\mathcal{G}(N, s)$, and where s is an affine parameter along the geodesic $\mathcal{G}(N, s)$ for N fixed. The family of geodesics we want to consider is $P(\tau; \alpha^{\hat{i}}; s) \equiv P(\tau; n; s)$ where $n = \alpha^{\hat{i}}e_{\hat{i}}$. The case $N = \partial/\partial\tau$ merely leads to part of Eqs. (18). The case $N = \partial/\partial\alpha^{\hat{i}}$ leads to the desired results. In this case $N = \partial/\partial\alpha^{\hat{i}} = s\partial/\partial x^{\hat{i}}$, hence $N^{\hat{i}} = s\delta^{\hat{\mu}}_{\hat{i}}$. Expanding the second term in the geodesic deviation equation in powers of s, we have

$$2\delta^{\hat{\sigma}}_{\hat{i}}\Gamma^{\hat{\mu}}_{\hat{\sigma}\hat{j}}\alpha^{\hat{j}} = 2\lambda\Gamma^{\hat{\mu}}_{\hat{i}\hat{j},\hat{k}}\big|_{P_0(\tau)}\alpha^{\hat{j}}\alpha^{\hat{k}} + O(\lambda^2). \tag{11}$$

Substituting (5) and (11) into (10), dividing (10) by s, and then setting $s=0$, we obtain

$$(3\Gamma^{\hat{\mu}}_{\hat{i}\hat{j},\hat{k}} + R^{\hat{\mu}}_{\hat{j}\hat{i}\hat{k}})\big|_{P_0(\tau)}\alpha^{\hat{j}}\alpha^{\hat{k}} = 0 \tag{12}$$

Since $\alpha^{\hat{j}}$ can be arbitrary, (12) leads to

$$(\Gamma^{\hat{\mu}}_{\hat{i}\hat{j},\hat{k}} + \Gamma^{\hat{\mu}}_{\hat{i}\hat{k},\hat{j}})\big|_{P_0(\tau)} = -\tfrac{1}{3}(R^{\hat{\mu}}_{\hat{j}\hat{i}\hat{k}} + R^{\hat{\mu}}_{\hat{k}\hat{i}\hat{j}})\big|_{P_0(\tau)}. \tag{13}$$

This equation can be solved for $\Gamma^{\hat{\mu}}_{\hat{i}\hat{j},\hat{k}}\big|_{P_0(\tau)}$ by adding to it one cyclic permutation and subtracting another:

$$\Gamma^{\hat{\mu}}_{\hat{i}\hat{j},\hat{k}}\big|_{P_0(\tau)} = -\tfrac{1}{3}(R^{\hat{\mu}}_{\hat{i}\hat{j}\hat{k}} + R^{\hat{\mu}}_{\hat{j}\hat{i}\hat{k}})\big|_{P_0(\tau)}. \tag{14}$$

From the definition of the Christoffel symbols,

$$g_{\mu\nu,\alpha} = g_{\mu\sigma}\Gamma^{\sigma}{}_{\nu\alpha} + g_{\sigma\nu}\Gamma^{\sigma}{}_{\mu\alpha}, \tag{15}$$

we find by differentiation that

$$g_{\hat{\mu}\hat{\nu},\hat{\alpha}\hat{\beta}}\big|_{P_0(\tau)} = \eta_{\hat{\mu}\hat{\sigma}}\Gamma^{\hat{\sigma}}_{\hat{\nu}\hat{\alpha},\hat{\beta}}\big|_{P_0(\tau)} + \eta_{\hat{\sigma}\hat{\nu}}\Gamma^{\hat{\sigma}}_{\hat{\mu}\hat{\alpha},\hat{\beta}}\big|_{P_0(\tau)} + g_{\hat{\mu}\hat{\sigma},\hat{\beta}}\big|_{P_0(\tau)}\Gamma^{\hat{\sigma}}_{\hat{\nu}\hat{\sigma}}\big|_{P_0(\tau)} + g_{\hat{\sigma}\hat{\nu},\hat{\beta}}\big|_{P_0(\tau)}\Gamma^{\hat{\sigma}}_{\hat{\mu}\hat{\alpha}}. \tag{16}$$

Combining Eqs. (5), (6), (7), (9), (14), and (16) we have

$$
\left.
\begin{aligned}
&g_{\hat{\alpha}\hat{\beta},\hat{0}\hat{0}} = 0 \\
&g_{\hat{j}\hat{k},\hat{l}\hat{0}} = 0 \\
&g_{\hat{0}\hat{0},\hat{j}\hat{0}} = -2(b^{\hat{j}} + \epsilon^{\hat{j}\hat{k}\hat{l}} a^{\hat{k}} \omega^{\hat{l}}) \\
&g_{\hat{0}\hat{j},\hat{k}\hat{0}} = -\epsilon_{\hat{j}\hat{k}\hat{l}} \eta^{\hat{l}} \\
&g_{\hat{0}\hat{0},\hat{j}\hat{k}} = -2R^{\hat{0}}{}_{\hat{j}\hat{k}\hat{0}} - 2a^{\hat{j}} a^{\hat{k}} + 2\delta^{\hat{j}}_{\hat{k}} (\omega^{\hat{l}})^2 - 2\omega^{\hat{j}} \omega^{\hat{k}} \\
&g_{\hat{0}\hat{i},\hat{j}\hat{k}} = -\tfrac{2}{3}(R_{\hat{0}\hat{k}\hat{i}\hat{j}} + R_{\hat{0}\hat{j}\hat{i}\hat{k}}) \\
&g_{\hat{i}\hat{m},\hat{i}\hat{j}} = -\tfrac{1}{3}(R_{\hat{i}\hat{l}\hat{j}\hat{m}} + R_{\hat{i}\hat{m}\hat{j}\hat{l}})
\end{aligned}
\right\} \text{ all along } P_0(\tau). \tag{17}
$$

From Eqs. (17), we obtain the second-order expansion of the metric at the point $P(x^{\hat{0}}, x^{\hat{j}})$ as

$$
\begin{aligned}
ds^2 = &-(dx^{\hat{0}})^2[1 + 2a_{\hat{j}} x^{\hat{j}} + (a^{\hat{l}} x^{\hat{l}})^2 + (\omega^{\hat{l}} x^{\hat{l}})^2 \\
&\quad - (\omega)^2 x^{\hat{l}} x^{\hat{l}} + R_{\hat{0}\hat{l}\hat{0}\hat{m}} x^{\hat{l}} x^{\hat{m}}] \\
&+ 2dx^{\hat{0}} dx^{\hat{i}} (\epsilon_{\hat{i}\hat{j}\hat{k}} \omega^{\hat{j}} x^{\hat{k}} - \tfrac{2}{3} R_{\hat{0}\hat{l}\hat{i}\hat{m}} x^{\hat{l}} x^{\hat{m}}) \\
&+ dx^{\hat{i}} dx^{\hat{j}} (\delta_{\hat{i}\hat{j}} - \tfrac{1}{3} R_{\hat{i}\hat{l}\hat{j}\hat{m}} x^{\hat{l}} x^{\hat{m}}) \\
&+ O(dx^{\hat{\mu}} dx^{\hat{\nu}} x^{\hat{l}} x^{\hat{m}} x^{\hat{k}}) ,
\end{aligned} \tag{18}
$$

where $a_{\hat{j}}$, $\omega^{\hat{l}}$, and $R_{\hat{\alpha}\hat{\beta}\hat{\mu}\hat{\nu}}$ are evaluated on the world line at time $x^{\hat{0}}$.

To calculate the coordinate acceleration of a freely falling body, we use the geodesic equation in the form

$$
\frac{d^2 x^{\hat{i}}}{d(x^{\hat{0}})^2} + \left(\Gamma^{\hat{i}}_{\hat{\mu}\hat{\nu}} - \Gamma^{\hat{0}}_{\hat{\mu}\hat{\nu}} \frac{dx^{\hat{i}}}{dx^{\hat{0}}} \right) \frac{dx^{\hat{\mu}}}{dx^{\hat{0}}} \frac{dx^{\hat{\nu}}}{dx^{\hat{0}}} = 0 \tag{19}
$$

and substitute into it the first-order expansion of the Γ's. Defining $w^{\hat{i}} \equiv dx^{\hat{i}}/dx^{\hat{0}}$, the velocity measured by the accelerated rotating observer, the resulting coordinate acceleration is

$$
\begin{aligned}
\frac{d^2 x^{\hat{i}}}{d(x^{\hat{0}})^2} = &-(1 + \vec{a}\cdot\vec{x}) a^{\hat{i}} - (\vec{\omega} \times (\vec{\omega} \times \vec{x}))^{\hat{i}} - (\vec{\eta} \times \vec{x})^{\hat{i}} \\
&- 2(\vec{\omega} \times \vec{w})^{\hat{i}} + 2(\vec{a}\cdot\vec{w})(\vec{\omega} \times \vec{x})^{\hat{i}} \\
&+ w^{\hat{i}} [2\vec{a}\cdot(\vec{\omega} \times \vec{x}) + 2\vec{a}\cdot\vec{w}(1 - \vec{a}\cdot\vec{x}) + \vec{b}\cdot\vec{x}] \\
&- x^{\hat{l}} R_{\hat{0}\hat{i}\hat{0}\hat{l}} - 2x^{\hat{l}} w^{\hat{j}} R_{\hat{i}\hat{j}\hat{l}\hat{0}} \\
&+ \tfrac{2}{3} x^{\hat{l}} w^{\hat{j}} w^{\hat{k}} R_{\hat{i}\hat{j}\hat{k}\hat{l}} + 2x^{\hat{l}} w^{\hat{i}} w^{\hat{j}} R_{\hat{0}\hat{j}\hat{0}\hat{l}} \\
&+ \tfrac{2}{3} x^{\hat{l}} w^{\hat{i}} w^{\hat{j}} w^{\hat{k}} R_{\hat{0}\hat{j}\hat{k}\hat{l}} + O((x^{\hat{l}})^2) .
\end{aligned} \tag{20}
$$

To express $d^2 x^{\hat{i}}/d(x^{\hat{0}})^2$ in terms of the velocity $v^{\hat{i}}$ observed in the local coordinates of an unaccelerated nonrotating observer, we use the relation

$$
\vec{w} = \vec{v}(1 + \vec{a}\cdot\vec{x}) - \vec{\omega} \times \vec{x} + O((x^{\hat{i}})^2) , \tag{21}
$$

which is obtained by integrating Eq. (20).

Substituting Eq. (21) into (20) we obtain

$$
\begin{aligned}
\frac{d^2 x^{\hat{i}}}{d(x^{\hat{0}})^2} = &-(1 + \vec{a}\cdot\vec{x}) a^{\hat{i}} + 2(\vec{a}\cdot\vec{v})(1 + \vec{a}\cdot\vec{x}) v^{\hat{i}} \\
&+ (\vec{b}\cdot\vec{x}) v^{\hat{i}} - 2(1 + \vec{a}\cdot\vec{x})(\vec{\omega} \times \vec{v})^{\hat{i}} + (\vec{\omega} \times (\vec{\omega} \times \vec{x}))^{\hat{i}} \\
&- (\vec{\eta} \times \vec{x})^{\hat{i}} - R_{\hat{0}\hat{i}\hat{0}\hat{l}} x^{\hat{l}} - 2R_{\hat{i}\hat{j}\hat{l}\hat{0}} x^{\hat{l}} v^{\hat{j}} \\
&+ \tfrac{2}{3} R_{\hat{i}\hat{j}\hat{k}\hat{l}} x^{\hat{l}} v^{\hat{j}} v^{\hat{k}} + 2R_{\hat{0}\hat{j}\hat{0}\hat{l}} x^{\hat{l}} v^{\hat{i}} v^{\hat{j}} + \tfrac{2}{3} R_{\hat{0}\hat{j}\hat{k}\hat{l}} x^{\hat{l}} v^{\hat{i}} v^{\hat{j}} v^{\hat{k}} \\
&+ O((x^{\hat{i}})^2) .
\end{aligned} \tag{22}
$$

The various terms in this equation are interpreted in Table I. Notice that to the order calculated there could be no coupling between the Riemannian terms and the a, ω, b, and η terms. Therefore, we can also derive the above results by combining a simpler special-relativistic derivation with the results for a freely falling observer in curved spacetime.

The results presented in this paper may be useful in analysis of tidal deformation of objects due to various types of close encounters, or in analysis of gravitational wave detectors and laboratory experiments where the size of the apparatus is small compared with inhomogeneities in the gravitational fields being observed. A Newtonian physcist can think about the terms in Eq. (22) or Table I as simply Newtonian forces, as described in box 37.1 of MTW. Moreover, a Newtonian physicist can use the equation of motion (20) or (22) to analyze mechanical apparatus in an experimental laboratory. All he needs to do is multiply this equation by the mass of a mass element in his apparatus, and add it linearly onto the forces that would be present if the apparatus were at rest in an inertial reference frame (see, e.g., box 37.1 of MTW).

TABLE I. Various inertial and gravitational effects in coordinate acceleration.

Effect	Term in coordinate acceleration $d^2x^{\hat{i}}/d(x^{\hat{0}})^2$
1. Usual inertial acceleration	$-a^{\hat{i}}$
2. Usual Doppler ("gravitational") red-shift correction to term 1: physical processes "overhead" run fast compared to observer's proper time	$-(\vec{a}\cdot\vec{x})a^{\hat{i}}$
3. Special-relativistic (SR) correction to acceleration [due to $\gamma=1/(1-v^2)^{1/2}$]	$+2(\vec{a}\cdot\vec{v})v^{\hat{i}}$
4. Red-shift correction to term 3	$+2(\vec{a}\cdot\vec{v})(\vec{a}\cdot\vec{x})v^{\hat{i}}$
5. ∂(red-shift)/$\partial\tau$ correction to acceleration	$+(\vec{b}\cdot\vec{x})v^{\hat{i}}$
6. Coriolis acceleration	$-2(\vec{\omega}\times\vec{v})^{\hat{i}}$
7. Red-shift correction to term 6	$-2(\vec{a}\cdot\vec{x})(\vec{\omega}\times\vec{v})^{\hat{i}}$
8. Centripetal acceleration (Ref. 10)	$+[\vec{\omega}\times(\vec{\omega}\times\vec{x})]^{\hat{i}}$
9. Coordinate acceleration if ω changes	$-(\vec{\eta}\times\vec{x})^{\hat{i}}$
10. "Electric-type" (usual) gravitational effect	$-R_{\hat{0}\hat{i}\hat{0}\hat{i}}$
11. SR correction to term 10	$+2R_{\hat{0}\hat{j}\hat{0}\hat{i}}x^{\hat{j}}v^{\hat{j}}$
12. "Magnetic-type" gravitational effect	$-2R_{\hat{i}\hat{j}\hat{i}\hat{0}}x^{\hat{j}}v^{\hat{j}}$
13. SR correction to term 12	$+\frac{2}{3}R_{\hat{0}\hat{j}\hat{k}\hat{i}}x^{\hat{j}}v^{i}v^{j}v^{k}$
14. "Double-magnetic" gravitational effect	$+\frac{2}{3}R_{\hat{i}\hat{j}\hat{k}\hat{i}}x^{\hat{j}}v^{\hat{j}}v^{\hat{k}}$

In actual experiments, while the second-order inertial effects are small, so are the Riemann forces which are being observed. Terms 2, 8, and 9 in Table I, for example, have a dependence on the coordinates similar to the usual $R_{\hat{0}\hat{i}\hat{0}\hat{i}}$ acceleration, term 10; likewise, terms 5 and 7 resemble the "magnetic" Riemann effect, term 12, and term 4 resembles terms 11 and 14. In typical resonant-device experiments, for instance, one might be concerned about noise fluctuations in the acceleration of gravity: If $g=g_0(1+\epsilon\cos\omega t)$, then the second term (red-shift) gives an acceleration which simulates an $R_{\hat{0}\hat{z}\hat{0}\hat{z}}$ of magnitude $2g_0\epsilon$. Thus, one might ask that the dimensionless amplitude (metric perturbation) of the wave h ($h\omega^2 \sim |R_{\hat{0}\hat{i}\hat{0}\hat{i}}|$) be greater than

$$h_{\min}\sim\left(\frac{g_0}{\omega}\right)^2\epsilon\sim 10^{-17}\,\frac{\epsilon}{(\nu/1\ \mathrm{Hz})^2}\ ,$$

where ν is the frequency of the wave. For the Crab pulsar, which is estimated[11] to produce $h\sim 10^{-27}$ at 60 Hz, one thus would want to reduce ϵ below 10^{-7} (or orient the apparatus horizontally). Second-order accelerations due to angular motions may be more serious; there are no good measurements at present of angular seismic noise.[12]

We thank C. M. Caves and K. S. Thorne for helpful comments. This work was supported in part by the National Science Council of the Republic of China, and the National Science Foundation of the United States under Grant No. AST76-80801.

[1] J. L. Synge, *Relativity: The General Theory* (North-Holland, Amsterdam, 1960).

[2] The term "Fermi coordinates" is usually used in a different sense, namely, to describe coordinates such that the affine connections vanish on some curve or other subspace; cf. E. Fermi, Atti R. Accad. Lincei Rend. Cl. Sci. Fis. Mat. Nat. 31, 21 (1922); 31, 51 (1922), and L. O'Raifeartaigh, Proc. R. Irish Acad. 59A, 15 (1958).

[3] F. K. Manasse and C. W. Misner, J. Math. Phys. 4, 735 (1963).

[4] F. B. Estabrook and H. D. Wahlquist, J. Math. Phys. 5, 1629 (1964).

[5] W.-T. Ni, Chin. J. Phys. 15, 51 (1977).

[6] B. Mashhoon, report (unpublished).

[7] C. W. Misner, K. S. Thorne, and J. A. Wheeler, *Gravitation* (Freeman, San Francisco, 1973), cited henceforth as MTW.

[8] Throughout this paper we use MTW notations and conventions.

[9] $\epsilon^{\alpha\beta\mu\nu}$ is the completely antisymmetric tensor with $\epsilon^{0123} = -1$ in an inertial frame.

[10] If we use $\vec{w}$ instead of $\vec{v}$ in the definition of Coriolis acceleration, then the sign of this term flips and we have centrifugal acceleration.

[11] M. Zimmermann, Nature (to be published).

[12] V. B. Braginsky, C. M. Caves, and K. S. Thorne, Phys. Rev. D 15, 2047 (1977).

CHAPTER VI

NUCLEOSYNTHESIS IN STARS WITH NEUTRON-STAR CORES

ABSTRACT

In this paper, I investigate nucleosynthesis in a star of total mass 16 $M_\odot$ with a degenerate neutron core ($M_{core} = 1\ M_\odot$, $R_{core} = 10$ km). Kip Thorne and Anna Żytkow (1975, 1977) performed preliminary analyses of stellar models with neutron-star cores. They found that an object with total mass $\gtrsim 10\ M_\odot$ required nuclear energy generation to support its extended, red-giant-like envelope. Thorne and Żytkow did not, however, study the details of the nucleosynthesis. To do so, I have generated a family of Newtonian stellar envelope models. The envelopes are convective all the way down from the photosphere to just above the central neutron star's surface.

I divide each envelope into two zones: a "burning zone" surrounding the degenerate core, and a "diffusive zone" extending up to the photosphere. The important nuclear reactions occur mainly in the hot, dense "burning zone", which consists of a single convective cell between radii of 10 km and 12.5 km. I treat the cell as a "conveyor belt", which carries matter down and up again to the interface at 12.5 km, where it is mixed with material brought down by higher convective cells. I compute the non-equilibrium nucleosynthesis in the "burning zone" using a program which keeps track of all (24) significant nuclei with $Z \leq 11$ and includes a complete set of (63) reactions for temperatures of under 2×10^9 K.

To follow the convective transport of material in the envelope above the "burning zone's" conveyor belt, I use the Despain (1976) diffusion approximation. In the "diffusive zone", therefore, a set of linear,

second-order, ordinary differential equations coupled by beta decays governs the abundances of the various isotopes as functions of radius. In a young star with a degenerate neutron core, the outer envelope will still have some standard ("cosmic") set of isotopic abundances; as the star evolves, diffusive transport of nuclear reaction products will gradually change those abundances. I solve the system of diffusion equations with boundary conditions given by the "burning zone" at the bottom and the initial envelope abundances at the top of the "diffusive zone".

A self-consistent stellar model must generate enough luminosity by nuclear reactions to support its extended envelope. I found no such models: nuclear reactions never produced more than ~ 0.04 of the required luminosity. Major causes of the low nuclear luminosity are the small amount of mass available in the "burning zone" and the low rate at which convection (diffusion) mixed in "fresh" material to be consumed.

I discuss the possibility that "unconventional" ultra-high-temperature nucleosynthesis (involving significant leakage into nuclei with $Z > 11$) can provide enough luminosity to support self-consistent models. If that possibility fails, then a massive star with a degenerate neutron core is likely to collapse, on a free-fall time scale, to form a black hole.

NUCLEOSYNTHESIS IN STARS WITH NEUTRON-STAR CORES

I. INTRODUCTION

A. The Problem

Kip Thorne and Anna Żytkow (1975, 1977, henceforth referred to as TŻ(L) and TŻ respectively) began an investigation of spherically-symmetric equilibrium models of stars with massive, extended, nondegenerate envelopes surrounding degenerate neutron cores. A somewhat similar problem is that of stars with white-dwarf-like degenerate electron cores. In both cases (electron core and neutron core) solutions for the structures of extended envelopes yield models of red giant or supergiant stars.

The neutron-star-like cores considered by TŻ involve one additional complexity beyond models of ordinary red giants. Gravitation is extremely strong near the degenerate neutron core; the dimensionless Newtonian potential is

$$\frac{G M_{core}}{R_{core} c^2} = 0.15 \left(\frac{M_{core}}{1\ M_\odot} \right) \left(\frac{10\ \text{km}}{R_{core}} \right) .$$

General-relativistic effects therefore have a significant influence on the star's structure. Thorne (1977) derived relativistic equations of stellar structure, including a relativistic generalization of the mixing-length theory for convection. These equations were used in the TŻ work in strong-gravity regions where Newtonian theory became an inaccurate

approximation.

TŻ treated nucleosynthesis and nuclear energy generation in their models using standard formulae and reaction rates (Cox and Giuli, 1968). They pointed out, however, that these formulae and rates might begin to break down and become inapplicable under some of the extreme conditions which occurred in the TŻ models. In particular, in one class of models which critically depend on nuclear burning for their luminosity, TŻ warned that significant changes could result from a more general treatment of nucleosynthesis that included effects omitted from their calculations.

In this paper, I report on my attempt to give the more general treatment called for by TŻ. (I have carried out this work initially in collaboration with Michael Newman, Kip S. Thorne, and Anna Żytkow, and later alone.) In § I.B. of this introduction, I will review the results obtained by TŻ for their stellar models with neutron-star cores. Section I.C. comments on the origin and evolution of these objects, and on possible observational tests of the class of models that I will be studying. In § I.D., I describe the method TŻ used to treat nucleosynthesis in their models; § I.E. discusses my nucleosynthesis approach. Section I.F. summarizes the results which emerge from this work, and mentions several possible future extensions and improvements to my treatment of the problem.

The remainder of this paper presents the details of my analysis. In § II of this work I discuss the Despain (1976) diffusion approximation and its use in modeling the convective mixing of the products of nuclear burning in stars. Section III describes my simple "conveyor belt" method for approximately treating the hot, non-equilibrium nuclear reactions occuring in the bottommost convective cell of my "supergiant" stellar models, just above the surface of the neutron star core. In § IV, I explain the

nucleosynthetic network which I used to compute the energy generation and isotopic abundance evolution rates. Section V presents the results of the diffusion calculations for a variety of models which I worked with. Section VI gives the results of my nucleosynthesis calculations, and § VII contains suggestions for further investigation.

B. Overview of the Thorne-Żytkow (1977) Models

TŻ applied the relativistic equations of stellar structure to the case of a massive star with a neutron core. They sought models with extended, stable envelopes. From the outside, the TŻ solutions look very much like extreme type-M supergiants, with photospheric temperatures of 2500 K to 3200 K and radii of 900 $R_\odot$ to 1300 $R_\odot$. Below the visible layers, the stars have convective atmospheres extending down to near the central neutron-star core.

A model built by TŻ has at its center a core with mass 1 $M_\odot$ and radius 10 km. This core, TŻ calculated, has essentially the same structure as a naked neutron star; the surrounding envelope has almost no effect on the hydrostatic equilibrium solution for the degenerate central mass. TŻ also found that the core is separated from the envelope above it by an "insulating layer" of degenerate-electron matter, which allows $\lesssim 100\ L_\odot$ to leak through. Thus, the degenerate neutron core has a negligible effect on the thermal properties of the surrounding envelope. The only significant coupling between the core and the remainder of the star is via the core's gravitational field.

Around the central object, TŻ placed extended envelopes of various

masses, ranging from 2 $M_\odot$ to 25 $M_\odot$. The models that resulted fell into two distinct classes. One class, which TŻ called "giants", had total masses $\lesssim 10\ M_\odot$ and derived their luminosities mainly from the steady release of gravitational potential energy by gradual accretion onto the central neutron star. The second class, which TŻ named "supergiants", had masses $\gtrsim 10\ M_\odot$ and produced their luminosities mainly by nuclear reactions. Below, I review the characteristics of these two classes of models, as discovered by TŻ.

Figures 1 and 2 illustrate the structure of stars with degenerate neutron cores. (The figures are taken from Thorne and Żytkow (1977).) Consider the features of the stellar interior of a "giant" model shown inside the box of Figure 1. Denote by r_K the radius of the "knee", the abrupt transition between the convective, radiation-pressure dominated, adiabatic "envelope" and the nearly-isothermal "halo" surrounding the central degenerate core. On the right edge of Figure 1 the distance (in meters) above or below r_K is marked; the left edge shows the local density (in g cm^{-3}). The numbers given are for a typical "giant" model.

Moving from the bottom up, one observes first a central isothermal core of degenerate neutron material, surrounded by a thin "insulating layer" which isolates it from the remainder of the star. The insulating layer extends up from the point where neutrons cease to "drip" off the nuclei to the top of the region of electron degeneracy (the "Degenerate-Nondegenerate" line at r_K-40 m). Within the degenerate insulating layer some pycnonuclear reactions (marked "C Shell") occur, but they do not generate a significant amount of luminosity compared to other processes going on in the star.

Above the r_K-40 m line, one moves into the "halo" region of the stellar model. Here, matter is non-degenerate and nearly isothermal; its density ranges from $\sim 10^6$ g cm^{-3} down to ~ 1 g cm^{-3}. The halo is almost identical to the atmosphere of a normal, young neutron star, with a scale height of only a few meters. Within the halo of a "giant" class model there is some nucleosynthesis (in the layers marked "H Shell" and "He Shell") as the matter in the halo slowly settles down toward the core. The energy released by nuclear reactions, however, is small compared to the luminosity due to accretion of gas. That luminosity is mainly created in the layer between r_K and a few scale heights below r_K (marked "Gravitational Energy Release"). Below the region of energy release, there is almost no sign that a massive, extended envelope surrounds the neutron star; if the envelope were removed, the halo would become an atmosphere, and would not be changed significantly.

Above the "knee" at r_K, a fully convective envelope extends up to the photosphere of the star. Figure 2 graphs the run of temperature versus density for two specific envelope models: a 5 $M_\odot$ "giant" and a 12 $M_\odot$ "supergiant". There is one important qualitative difference between models in these classes. A "giant" has a mass in the range of 5 $M_\odot$ to 9 $M_\odot$ and derives $\gtrsim 96$ % of its luminosity from accretion. A "supergiant", on the other hand, has a mass of over 11 $M_\odot$ and gets $\lesssim 7$ % of its luminosity from accretion; the bulk of the "supergiant" star's energy comes from hydrogen burning. (Models of under 5 $M_\odot$ had envelopes unstable against ejection in TŻ's calculations, and will not be discussed further here.) As Figure 2 shows, the "knee" in a "supergiant" model overlaps the "H Shell"

where the bulk of the hydrogen burning occurs. (The significance of that overlap will be discussed in § I.C.)

The luminosities of "giant" models calculated by TŻ range from ~40000 $L_\odot$ to ~60000 $L_\odot$ as the total mass of the model ranges from 5 $M_\odot$ to 9 $M_\odot$. "Supergiant" models have luminosities of ~70000 $L_\odot$ (for an 11.5 $M_\odot$ star) to ~120000 $L_\odot$ (for a 25 $M_\odot$ star). The accretion rate for a "giant" is $\dot{M} \sim 2 \times 10^{-8}\ M_\odot\ yr^{-1}$; for a "supergiant", it is only $\dot{M} \sim 0.15 \times 10^{-8}\ M_\odot\ yr^{-1}$. Photospheric temperatures for "giants" fall in the ~2600 K - 2800 K zone; for "supergiants" the range is ~2900 K - 3100 K.

An interesting and important feature of models of stars with neutron-star cores discovered by TŻ is the existence of a "mass gap"--a zone between the "giant" models ($M_{total} \lesssim 9\ M_\odot$) and the "supergiant" models ($M_{total} \gtrsim 11\ M_\odot$), in which no equilibrium stellar models can be found. The mass gap, as TŻ explain it, occurs because of the behavior of the opacity of the gas at high temperatures. Electron-scattering dominates that opacity; as the temperature increases above 10^7 K, the opacity first falls (due to Klein-Nishina special-relativistic corrections to Thompson scattering) and then, beyond 5×10^8 K, rises abruptly as electron-positron pair production turns on. The Eddington critical luminosity is proportional to 1/(opacity), and for convection to turn off as one moves inward toward the core, it is necessary at some point for the luminosity produced inside that radius to fall below the local critical luminosity. (TŻ include relativistic factors in their definitions of critical luminosity.)

TŻ found two distinct ways for the local luminosity L_r to fall below L_{crit}, and thus for convection to turn off: (1) in "giants", L_{crit} rises and meets L_r (due to the falling opacity as T increases toward 5×10^8 K);

or (2) in "supergiants", L_r falls and meets L_{crit} (as one moves in through the hydrogen-burning shell). TŻ also discovered that no smooth transition between these two classes of models was possible; mechanism (1) fails before mechanism (2) is ready to take over. In the "mass gap", there were no equilibrium models with degenerate neutron cores.

For an alternative view of the "giant"-"supergiant" dichotomy, consider starting at the degenerate neutron core and moving outward. In the hot, almost isothermal "halo" region, the gas-pressure scale height is typically of the order of a few meters, so the halo density decreases rapidly as one moves upward. In order for the object to possess an extended stellar envelope, the scale height must increase to something larger, of the order of the radius ($\sim$10 km). This happens in "supergiant" models at an abrupt "knee" where hydrogen-burning supplies a luminosity nearly equal to the Eddington critical luminosity, and the force of this luminosity on the plasma nearly counterbalances the huge local acceleration of gravity. In "giants", nucleosynthesis cannot provide the necessary luminosity to force the scale height to increase, but accretion and gravitational energy release by isothermal compression of the gas, in conjunction with increasing opacity as one moves outward, do the job.

C. Origin, Evolution, and Observational Evidence for Stars with Degenerate Neutron Cores

TŻ(L) suggested several ways in which stars with degenerate neutron cores might form in nature. One method might be by the collapse of the degenerate electron core of a normal massive, evolved star, if such a

collapse can take place without totally disrupting the envelope. Another method could be supercritical accretion onto a normal neutron star in a close binary system. A related procedure involves the coalescence of a neutron star and its ordinary companion; the neutron star might be able to spiral inwards and eat the core of its unfortunate neighbor, leaving an extended envelope. This scenario was later explored in detail by Taam, Bodenheimer, and Ostriker (1978). All of these mechanisms to form stars with neutron-star cores are rather speculative; a rigorous calculation is difficult or impossible to perform at this time.

TŻ discuss the probable evolutionary tracks of both "giant" and "supergiant" class models of stars with degenerate neutron cores. A "giant" converts accreted matter to luminosity at $\sim(GM_{core}/r_{core}c^2) \approx 0.15$ efficiency, as compared to the ~ 0.007 efficiency of hydrogen-burning in ordinary stars and in "supergiant" class models. The fundamental limit to a "giant" model's life is due to the upper mass limit on its central neutron star. After $\sim 5 \times 10^7$ years, a "giant" model's core will have accreted $\sim 1\ M_\odot$ and will probably have collapsed into a black hole. The abrupt change in boundary conditions at the center of the star may have a radical (if not catastrophic!) effect on the extended envelope. (Richard Flammang and Kip S. Thorne (private communications) are working on questions related to the structure of stars with black-hole cores.) A "supergiant" class model faces the limit imposed by exhaustion of the hydrogen in its envelope; that exhaustion occurs after $\sim 10^7$ years, and so a realistic lifetime for a "supergiant" is probably (a few) $\times 10^6$ years--comparable to the main-sequence lifetime for a star of this same total mass. (The time scale for accretion to add $1\ M_\odot$ to the core is $\sim 7 \times 10^8$ years.)

As its core mass changes, an evolving "giant" star with a neutron core moves along a path in the (photospheric temperature) versus (luminosity) plane that lies close to, but just barely on the stable side of, the Hayashi forbidden region. TŻ produced a sequence of equilibrium models, with constant total mass, that follow the evolution of a 5 $M_\odot$ "giant". They found that as the core mass increased from 0.4 $M_\odot$ to 1.625 $M_\odot$, and the core radius correspondingly shrank, their model's luminosity increased from ~25000 $L_\odot$ to ~63000 $L_\odot$ and its photospheric radius increased from ~700 $R_\odot$ to ~1160 $R_\odot$.

The external characteristics of TŻ's models of stars with neutron star cores are very nearly identical, in most respects, to the characteristics of ordinary red giant stars (which have white-dwarf-like cores). "Giant" class TŻ objects have a longer evolutionary time scale, and have imperceptibly lower photospheric temperatures than do normal red giants. These differences are not easily observable, however.

TŻ did find one possible distinguishing feature for their "supergiant" models: since convection links the hydrogen-burning shell and the surface, "supergiant" objects should rapidly develop quite exotic photospheric abundances as the products of nucleosynthesis are mixed upward. Spectroscopic observations, especially of molecules in the radio and infrared, can measure isotopic abundances in the atmospheres of red giant stars. One might thus hope that a massive star with a neutron-star core would display an unmistakable signature in its spectrum, a signature that would reveal the details of its internal organization.

D. Nucleosynthesis in the Original Thorne-Żytkow Models

The models of "supergiant" class stars with degenerate neutron cores calculated by TŻ used a simple set of equations to estimate the energy production due to hydrogen burning. TŻ considered the "normal" CNO cycle:

$$C^{12}\ (p,\gamma)\ N^{13} \xrightarrow{\beta^+} C^{13}\ (p,\gamma)\ N^{14}\ (p,\gamma)\ O^{15} \xrightarrow{\beta^+} N^{15}\ (p,\alpha)\ C^{12}\ .$$

Cox and Giulli (1968) give formulae (Eqs. (17.280)-(17.283)) for the energy generation rate due to this cycle, under the assumptions that: (1) the cycle has reached an equilibrium state, with the abundance of each isotope in the chain constant, (2) the limiting (slowest) reaction is $N^{14}\ (p,\gamma)\ O^{15}$, and (3) there are no significant alternative chains of reactions.

TŻ warned, however, that the "normal" CNO cycle might be a source of error in their models; their warnings were justified. All of the assumptions behind the Cox and Giulli (1968) formulae break down in the TZ "supergiant" models. Material is convected into and out of the hottest, densest zones, where the majority of (p,γ) and (α,p) reactions occur, on time scales short compared to the time needed to reach equilibrium, so one really must consider individual reaction rates and abundances within the cycle. The temperature is much higher than the (few) x 10^7 K where $N^{14}\ (p,\gamma)\ O^{15}$ is the slowest process. In addition, important alternative processes such as $N^{13}\ (p,\gamma)\ O^{14}$ take material out of the "normal" paths which dominate at lower temperatures.

A crucial limitation on the rate of CNO energy production at temperatures $T \sim 10^9$ K and densities $\rho \sim 10^2$ to 10^3 g cm^{-3} is the time required

for beta decays during the cycle. The half-lives of N^{13}, O^{14}, and O^{15} are 598 s, 70.5 s, and 122 s respectively. The most important strong interactions ((p,γ), (γ,p), (p,α), (α,γ), etc.) typically go to completion in a few microseconds. After that initial burst of activity, everything gets "hung up" waiting for beta decays to transform unusable isotopes into usable ones.

So, as was prophesized by TŻ, a more detailed treatment of nucleosynthesis in their "supergiant" models is required. I have begun this work, with much help on the nuclear physics and computational techniques from Michael J. Newman. I have built upon earlier ideas about the structure of the nuclear burning region, which are due to Kip S. Thorne, Anna Żytkow, and Michael J. Newman (private communications).

E. Nucleosynthesis--A Revised Approach for Thorne-Żytkow Models

The approach which I use to calculate nucleosynthesis in models of stars with neutron cores is straightforward. I first choose a mass and a radius for the central neutron star (typically 1 $M_\odot$ and 10 km) and a total mass for the model (typically 16 $M_\odot$). I also choose values for the envelope composition, typically $X = 0.7$, $Z = 0.03$. I then use a modified version of Paczyński's (1969) program for calculating static, extended stellar envelopes in order to determine the curve in the (photospheric temperature) versus (luminosity) plane along which a model may exist. Choosing a particular value of luminosity, I take the unique

envelope model thus determined.

I divide the envelope into two zones: a "diffusive zone" and a "burning zone". The "diffusive zone" extends from the photosphere down to a single pressure scale height above the bottom of the convective zone, at a radius I call r_o. The "burning zone" consists of that final scale height, a single convective cell, from r_o down to the "knee" at radius r_K, where the envelope ceases to be convective. The "knee" radius r_K lies at the outer edge of the "halo", a few meters above the degenerate neutron core. Typically r_o is 12.5 km in my models where the "knee" radius r_K is 10 km. The "burning zone" is the hottest, densest part of the convective envelope, and most of the nucleosynthesis which occurs in the star occurs in that zone.

Consider the "diffusive zone": Keith Despain (1976) derived a diffusion approximation for treating the convective mixing of the products of nucleosynthesis in a star. I take the values of turbulent velocity, scale height, and density as functions of radius from the chosen envelope model, plug them into the diffusion equations, and apply Despain's method to the "diffusive zone" above radius r_o. By numerically integrating the linear, ordinary differential equations of the diffusion approximation, I determine the equilibrium relationships between the photospheric abundances, the abundances at radius r_o, and the flux of each isotope across the sphere of radius r_o. I ignore the strong nuclear reactions which occur in only small amounts above r_o; I include, however, beta decays of unstable isotopes.

Consider next the "burning zone": I treat the single convective cell

comprising the "burning zone" as a conveyor belt, which carries material from radius r_o down to r_K and then back up to r_o. At r_o I assume that there is essentially complete mixing between the material at the bottom of the "diffusive zone" and at the top of the "burning zone". Thus, if an isotope comes up from the "burning zone" with abundance Y_{up} and is present at radius r_o of the "diffusive zone" with abundance Y_o, then the composition of the material going down for the next pass through the "burning zone" is simply $(Y_o + Y_{up})/2$.

Most of the mass in the "supergiant" class of models resides far out in the extended stellar envelope. Nuclear burning changes the isotopic abundances in this reservoir only slowly compared to the time scale for diffusion throughout the envelope. Hence, for long periods of time the star is in a "quasi-equilibrium" state, where smooth radial abundance gradients carry "fuel" down to the "burning zone" and transport "wastes" out to the photosphere. My models assume that the star has reached this quasi-equilibrium state.

The nuclear reactions which occur in the "burning zone" are computed using my adaptation of a program originally developed by Michael Newman. The program as used for this work treats a set of 24 low-atomic-number ($Z \leq 11$) isotopes; it considers 63 distinct reactions among those isotopes. No assumption of "equilibrium" condition or low temperature is imposed by the nucleosynthesis program. The reaction rate formulae are taken from Fowler, Caughlan, and Zimmerman (1975), Wagoner, Fowler, and Hoyle (1967), Wagoner (1969), and from Michael Newman and William A. Fowler (private communications).

The algorithm which I follow in order to generate a complete $T\dot{Z}$

"supergiant" model can now be described succinctly. Consider the list of abundances of each of the 24 isotopes of interest as a 24-dimensional vector $\vec{Y}$. The photospheric abundances $\vec{Y}_p$ are related to the abundances deep within the star by the Despain diffusion equations. The set of abundances $\vec{Y}_{up}$ coming up out of the "burning zone" are determined (via conveyor-belt nucleosynthesis plus the complete-mixing assumption) by the abundance $\vec{Y}(r_o) \equiv \vec{Y}_o$ at the base of the diffusive zone.

Given a particular envelope model (which assumes some luminosity L_{env}), the diffusion equations determine the relationship between $\vec{Y}_p$, $\vec{Y}_o$, and $\vec{Y}_{up}$. The task now remaining is only to adjust $\vec{Y}_o$ until the output $\vec{Y}_{up}$ from the nucleosynthesis network-solving program is such as to give some desired $\vec{Y}_p$.

For specificity, I consider the situation soon after the formation of a star with a neutron-star core, when the stellar structure has settled down to its quasi-equilibrium state, but before there has been time for nucleosynthesis to significantly alter the abundances of isotopes in the bulk of the stellar envelope. The photospheric abundances $\vec{Y}_p$ will have some standard set of values. (In this work, I have set $\vec{Y}_p$ equal to Cameron's (1973) "cosmic" abundances.) For a given model, I try various $\vec{Y}_o$ until a choice is found which produces the desired $\vec{Y}_p$. When that correct $\vec{Y}_o$ is found, the nucleosynthesis program tells me what the actual luminosity L_{nuc} produced by strong interactions and by beta decays is. If L_{nuc} is not equal to the L_{env} hypothesized initially in the construction of the stellar envelope model, I go back to the beginning,

guess another L_{env}, generate a new envelope, and repeat the rest of the process.

Ultimately, when a value of L_{env} is found which agrees with the calculated L_{nuc}, I have a self-consistent model. The values of $\vec{Y}_o$, $\vec{Y}_{up}$, and $\vec{Y}_p$ then imply a flow rate for each isotope, either out of the "burning zone" to the envelope reservoir, or down from the envelope into the "burning zone". These flow rates, and the envelope mass, give a time scale for the photospheric abundances to change; equivalently, they specify $\dot{\vec{Y}}_p$.

F. Results of Revised Nucleosynthesis Treatment of Thorne-Żytkow (1977) Models

Using a "conventional" network of low-Z nuclear reactions, I have tried and failed to produce enough nuclear luminosity L_{nuc} to make a self-consistent equilibrium model of a 16 $M_\odot$ "supergiant" star with a neutron core.

I have found three major sources of difficulty in my attempts to generate models. First, the structure of the stellar envelope, as deduced from integrations inward from the photosphere, is such as to hinder the mixing of material into and out of the hot, dense "burning zone" where most of the nuclear reactions occur. Near the bottom of the convective envelope, the isotopes of carbon, nitrogen, and oxygen which help catalyze the conversion of hydrogen to helium typically occur at abundances of under 2 per cent of their photospheric abundances. Contrariwise, the waste products of nucleosynthesis, beta-unstable species which cannot undergo further

strong interactions until after they decay, accumulate in large amounts at the bottom of the convective zone. They form the second big difficulty that faces these models: the need for several beta decays per cycle of the reaction chain that burns hydrogen to helium. In the standard "hot CNO cycle", the necessary decays of O^{14} and O^{15} take ~100 s each; the remaining reactions require a negligible time in comparison. The third hangup is the small volume (and small amount of mass contained in that volume) wherein nuclear reactions are mainly restricted to occur. Because of the rapid fall-off of density and temperature as one moves up from the surface of the neutron star, and because of the strong dependence of most reaction rates on density and temperature, the majority of nucleosynthesis occurs in the thin "burning zone" near the bottom of the convective envelope of the star. Within the other constraints imposed by the stellar structure, there is not enough mass present to allow nuclear reactions to provide more than a few per cent of the necessary luminosity to support an equilibrium "supergiant" model.

My failure to create self-consistent models maintained by nuclear energy generation does not, of course, prove the impossibility of such objects in nature. The magnitude of the deficit in generated luminosity (a factor of 20 to 100 short of requirements) does, however, suggest that significant modifications are needed to my "conventional" (low-Z) approach to the nucleosynthesis problem. Though my results are negative, I present the details of them here for several reasons.

First, there is a possibility that some fairly straightforward modification or extension of the methods described here can achieve success,

that is, self-consistent models of "supergiant" Thorne-Żytkow stars. One candidate approach is to enlarge the network of nuclear reactions under consideration. Stanford Woosley and Richard Wallace (private communications) are now exploring the details of nucleosynthesis in a hot, hydrogen-rich environment; much of their work, when completed, may be applicable to the conditions inside "supergiant" class models. There is reason to hope that the enlarged network may indeed produce the additional needed luminosity (see § VII for discussion).

Another, less attractive, possibility is that local collapses and explosions ("relaxation oscillations" in and near the burning zone) might be able to produce enough luminosity to support a star with a degenerate core, where an equilibrium model could not exist. There are, however, analytic suggestions (discussed in § VII) which cast doubt on this idea. In any case, the computational complexity of a time-dependent and possibly multi-dimensional dynamic model gives one reason to hesitate and examine other techniques first.

A major reason to write up the details of my efforts, of course, is to expose to other people the ideas behind this approach to modeling nucleosynthesis in stars with degenerate neutron cores. Possibly my failures will suggest improvements and will stimulate new assaults on this problem, which will ultimately lead either to successful models or to rigorous impossibility proofs.

II. STELLAR ENVELOPE STRUCTURE AND THE DESPAIN (1976) DIFFUSION APPROXIMATION

Given a total mass and luminosity for a star, and given a mass and a radius for a degenerate core, standard stellar modeling techniques (e.g., Paczyński, 1969) can clothe the core with an extended envelope of some desired composition. For models of stars with neutron cores, when the total mass (core + envelope) exceeds about 10 $M_\odot$ the resulting envelope is convective all the way down from the star's photosphere to near the core. In the 16 $M_\odot$ models which I have investigated, near the bottom of the convective envelope the temperature is typically $T \sim 1.5 \times 10^9$ K and the density $\rho \sim 500$ g cm^{-3}. Under these conditions, radiation pressure dominates gas pressure, and the equations governing the stellar structure have simple, accurate analytic solutions for the temperature and density as functions of radius.

The derivation of the analytic formulae for T(r) and $\rho(r)$ is straightforward, and the results will be useful throughout this paper. Consider the radiation-dominated convective region near the bottom of a TŻ "supergiant" envelope: the entropy per unit mass $s \approx 4aT^3/3\rho$ is very close to a constant. It is convenient, instead of using s, to express this adiabatic relationship between T and ρ in terms of the (small) quantity β_g, the fraction of the total pressure due to gas. It follows that $\beta_g \equiv P_{gas}/P_{total} \approx P_{gas}/P_{rad'n} = (\rho kT/\mu m_p)\ (aT^4/3)^{-1} = 4k/\mu m_p s$, where μ is the mean molecular weight of the gas. (A good approximation in a region of complete ionization where the abundance of elements beyond helium is small is $\mu \approx 2/(1+3X+0.5Y)$ (Clayton, 1968,

Eq. (2-15)); X and Y are the mass fractions [g g^{-1}] of hydrogen and helium, respectively.) The result for the density as a function of temperature is

$$\rho = \frac{\beta_g \mu m_p a T^3}{3 k} = 180 \text{ g cm}^{-3} \left(\frac{\beta_g}{10^{-2}}\right)\left(\frac{\mu}{0.6}\right)\left(\frac{T}{10^9 \text{ K}}\right)^3 . \quad (1)$$

The (Newtonian) equation of hydrostatic equilibrium is $dP/dr = -GM_r\rho/r^2$, where M_r is the mass inside radius r. To an exceedingly accurate approximation, $M_r = M_{core}$ in the region just above the degenerate neutron core; within 10^6 neutron-star radii of the center, the envelope contributes only 10^{-3} $M_\odot$ to the value of M_r. Since $P \approx P_{rad'n}$ in the region of interest, substituting $aT^4/3$ for P and using ρ from Eq.(1) gives $dT/dr = -GM_r\beta_g m_p/4kr^2$, which can be solved to yield, near r_o ($\equiv$ 12.5 km) and r_K ($\equiv$ 10 km)

$$T = \frac{G M_{core} \beta_g \mu m_p}{4 r k} = 2.4 \times 10^9 \text{ K} \left(\frac{M_{core}}{1 M_\odot}\right)\left(\frac{\beta_g}{10^{-2}}\right)\left(\frac{\mu}{0.6}\right)\left(\frac{10 \text{ km}}{r}\right). \quad (2)$$

(A constant of integration added to this solution becomes important at $r \gg r_o$, but is negligible at $r \lesssim r_o$.) The pressure scale height is $H_p \equiv -(d(\ln P)/dr)^{-1} \approx -(d(\ln(aT^4/3))/dr)^{-1} = r/4$.

The envelope models analyzed in this work were generated using Kip Thorne and Anna Żytkow's modified version of Paczyński's (1969) Newtonian program GOB. This program takes as inputs the star's total mass, luminosity (excluding neutrinos), photospheric temperature, and isotopic abundances (mass fractions X and Y). It then integrates the Newtonian equations of stellar structure inward, and stops when the density or temperature exceeds some preselected limit. GOB uses the

standard mixing-length theory to treat convection; it assumes a constant luminosity L_{env}, and thus does not calculate nuclear energy generation rates as it integrates inward. Opacities are interpolated within a table including H_2O effects (which are important near the photosphere), and the equation of state used is analytic and takes account of pressure due to gas, free electrons, and radiation, the ionization of H, He, and He^+, and the dissociation of H_2. A "gray atmosphere" model is used at optical depths of less than 2/3. (For more details of the program GOB, see TŻ, § II.c., and Paczyński (1969).)

By iterating, for a given choice of total mass it was possible to determine the curve in the L_{env}-T_p plane along which an inward-going integration by GOB left a 1 $M_\odot$ central core of 10 km radius. Choosing a particular point on this curve corresponds to choosing a particular envelope model. The actual equilibrium star in nature will be the model on the curve which generates the correct luminosity, by nucleosynthesis or accretion, to satisfy its envelope's demands.

In the models under consideration in this paper, gravity is exceedingly strong near the neutron-star core ($GM_{core}/r_K c^2 \approx 0.15$) and Newtonian results which are accurate at large radii give errors as large as a factor ~ 2 for effects near r_K. Nevertheless, for the calculations of this paper fully Newtonian models are sufficiently accurate; the ultimate failure of "conventional" nucleosynthesis described in § VI is so severe that general-relativistic corrections are unlikely to change the results significantly.

The standard subsonic mixing-length theory of convection used in the models calculated for this work is discussed in detail in Cox and

Giuli (1968, Chapter 14). In my models, the mixing-length ℓ was simply set equal to the pressure scale height H_p.

Along with the mixing-length theory of convection, a related theory used in the calculations reported here is the Despain (1976) diffusion approximation for convective transport of isotopic abundance inhomogeneities. This approximation replaces the turbulent bulk motions of material, which have length scales ranging from microscopic up to a scale height or so, with a single diffusion parameter D(r) and an ordinary differential equation. Given a mean turbulent velocity $\langle v \rangle$ for the largest convective cells at a given radius (as computed by GOB) and given their length scale ℓ (assumed equal to H_p), it is straightforward to derive the result that the abundance of a stable isotope Y_i [in units of moles g^{-1}] obeys the equation

$$\frac{\partial Y_i}{\partial t} = \frac{1}{\rho} \vec{\nabla} \cdot (\rho D \vec{\nabla} Y_i) \quad . \tag{3}$$

Here, the diffusion coefficient D is $D \equiv \langle v \rangle \ell$. This diffusion approximation is valid for times long compared to $\ell/\langle v \rangle$ and for lengths large compared to ℓ, and as written above does not include non-diffusive changes in Y_i (such as might be caused by nuclear reactions or beta decays).

The time-dependent diffusion equation (3) is more than was needed in this work. After going through some initial transients, depending on how the system was formed, a TŻ model of a star with neutron core should settle down into a "quasi-equilibrium" state. The hydrodynamic and thermal timescales for these "supergiant" objects are

of the order of a few years, and a similar time is required for convection (which transports isotopic inhomogeneities as well as energy) to smooth out the radial abundance gradients. The timescales for nuclear energy generation to alter the photospheric abundances of significant isotopes, however, are far longer--typically thousands to hundreds of thousands of years. Thus, for long periods of its life, the star will be in a state where smooth positive gradients of abundances drive steady flows of fresh material into the hot "burning zone" of the star below r_o (one scale height above the bottom of the convective region), and negative gradients propel waste products out to the photosphere. Only gradually do the abundances in the envelope reservoir change. In the meantime, to excellent accuracy, the abundances $Y_i(r)$ are time-independent at any chosen radius. The Despain diffusion equation for any species whose abundance Y_i is only governed by diffusion (no nuclear reactions or beta decays) reduces in this time-independent case to a simple relationship:

$$0 = \frac{d}{dr} \left(r^2 \rho D \frac{dY_i}{dr} \right) \quad . \tag{4}$$

In the more general case of a species "k" which undergoes beta decay at a rate $\beta_k \equiv 1/\tau_k$ (where τ_k is the e-folding lifetime) and which is produced by the decay of species "j" with beta decay rate β_j, the quasi-equilibrium abundance Y_k is governed by the linear inhomogeneous equation (Despain, 1976, § III.B., Eq.(21) and accompanying discussion)

$$Y_k'' + \frac{d}{dr}(\ln(r^2 \rho D))\, Y_k' - \frac{\beta_k}{D} Y_k = \frac{-\beta_j}{D} Y_j \tag{5}$$

where $Y_k' \equiv dY_k/dr$.

Note that as long as the diffusion approximation is only applied in regions where there is negligible strong-interaction nucleosynthesis, there are no complicated reaction-rate formulae in the system of equations; different isotopes are only coupled by simple beta decays. In the hottest, densest regions of the star, the "burning zone" between r_o and r_K, nuclear reactions can no longer be ignored. In that region, however, the diffusion approximation itself is a poor technique, since the details of bulk convective motions are important to the temperature and density that a given gram of matter experiences as a function of time. In place of the diffusion calculation, I use my conveyor-belt analysis from r_o down to r_K.

To summarize, the Despain (1976) diffusion approximation (Eq.(5)) is used in this work to treat the transport by convection of isotopes which are important in nucleosynthesis. The diffusion approximation is applied to the numerically-integrated stellar envelope between radius $r_o \equiv 12.5$ km and the photosphere. Between r_o and the bottom of the convective envelope at r_K a nucleosynthesis program, to be discussed in the following sections, calculates the local production of energy and the transformation of isotopes. Simple formulae (Eqs.(1),(2)) describe the temperature and density structure of the inner envelope quite accurately; these formulae are used in the nucleosynthesis program and in analytic estimation of effects in the stellar models.

III. NUCLEOSYNTHESIS ON THE BURNING-ZONE'S "CONVEYOR BELT"

Section I.B. reviewed the structure of TŻ models of stars with neutron cores. As Figure 1 shows, above the surface of the central degenerate object a hot, approximately isothermal "halo" extends up to an abrupt "knee" at radius r_K, where the temperature gradient becomes adiabatic.

Above the "knee" (which typically occurs only a few dozen meters above the degenerate core's surface) the envelope of a "supergiant" class object is convective all the way out to the photosphere, at $r_p \sim 7 \times 10^{13}$cm $\sim 10^3 R_\odot$. As discussed in § II above, most of this extended envelope can be accurately treated using the Despain (1976) diffusion approximation to describe the convective transport of the various isotopes of carbon, nitrogen, oxygen, etc. of importance to nucleosynthesis. The zone nearest to the "knee", however, where strong nuclear reactions proceed on timescales short compared to a convective cycle time H_p/v_t = (pressure scale height)/(turbulent velocity) $\sim$ 0.1 s, cannot adequately be described by a diffusion equation.

So, I divide the stellar model's convective envelope into two zones: a "diffusive zone" extending down from the photosphere (at r_p) to the radius r_o, and a "burning zone" which reaches from r_o down to the "knee" at r_K, where convection ceases. I choose the dividing radius r_o to be one scale height above the knee: $r_o \equiv r_K + H_p(r_K)$ = 10 km + 2.5 km = 1.25×10^6 cm. The "burning zone" thus consists of a single convective cell. For purposes of approximate model-building, I assume that the motion of

matter in the "burning zone" is in a simple, sinusoidal pattern ("conveyor-belt" motion):

$$r(t) = \left(\frac{r_o + r_K}{2}\right) + \left(\frac{r_o - r_K}{2}\right) \cos\left(\frac{2tv_t}{r_o - r_K}\right) . \qquad (6)$$

A single convective cycle requires time $t_c \equiv \pi(r_o - r_K)/v_t(r_o)$. (In typical models, $v_t(r_o)$ is of the order of 10^7 cm s^{-1} and $t_c \sim 0.1$ s.) At the beginning of each cycle around this convective loop, I assume that there has been essentially complete mixing between material that has come up from a previous cycle and material that has convected down from higher ("diffusion-analyzed") loops. This "complete mixing" hypothesis is in accord with the mixing-length conception of convection, in which a typical parcel of material retains its identity while rising or descending a distance $\sim \ell \sim H_p$, and then breaks up and blends with its surroundings. (If mixing with material coming down from above r_o is less efficient than I have assumed, it will be even harder for "fresh" catalyst isotopes to get down into the "burning zone", and even harder for the star to generate the luminosity it needs to hold up its envelope.) The implication of the "complete mixing" assumption is simple. For any given species, if the abundance coming up from the "burning zone" is Y_{up} and the abundance coming down to r_o from higher convective cells is Y_o, then the composition of the mixed material about to go down again is $(Y_o + Y_{up})/2$.

To fairly high accuracy, as derived in § II (Eqs.(1),(2)) the radiation-dominated matter near r_K has $T(r) = T(r_K)(r/r_K)^{-1}$ and $\rho(r) = \rho(r_K)(r/r_K)^{-3}$. At radius r_o, then, the temperature has fallen

to 0.80 $T(r_K)$ and the density to 0.51 $\rho(r_K)$. For a parcel of matter, the reaction rate (in units of reactions g^{-1} s^{-1}) for a two-body process involving distinct nuclei "1" and "2" is $\rho N_A^2 Y_1 Y_2 \langle 12 \rangle$ in the notation of Fowler, Caughlan and Zimmerman (1975, henceforth referred to as FCZ-II). The reaction rates "$\langle 12 \rangle$" themselves are typically strong functions of temperature; near 10^9 K the important reactions in the "hot CNO cycle" run at rates proportional to T^n with $n \approx 1.8$ to 5.1 . Thus, at r_o these reactions are down to between 33 % and 16 % [$= \rho(r_o)T(r_o)^n / \rho(r_K)T(r_K)^n$] of their rates at r_K, and it is a fairly good, though not extraordinarily accurate, approximation to ignore the reactions which occur above r_o in the "diffusive zone".

IV. NETWORK OF NUCLEAR REACTIONS USED

In my nucleosynthesis calculations, I adapted a computer program originated by Michael J. Newman. This program treats a set of 24 low-atomic-number ($Z \leq 11$) isotopes; it considers 63 distinct reactions among those isotopes. Tables 1 and 2 and Figure 3 summarize the nuclear species and reactions included in the program. The reaction rates are taken from Fowler, Caughlan, and Zimmerman (1975, "FCZ-II"), from Wagoner, Fowler and Hoyle (1967), from Wagoner (1969), and from Michael Newman and William A. Fowler (private communications). (Beta decay rates were also checked against a General Electric "chart of the nuclides" (1972).) Table 2 indicates the source of each reaction rate; Figure 3 illustrates, in the format of a Segrè chart, the isotopes and reactions of Tables 1 and 2.

The choice of isotopes and reactions included in the nucleosynthesis program was guided by two (somewhat contradictory) principles: completeness and computational efficiency. Completeness suggests that as many reaction rates as possible be in the program; each rate typically requires several floating-point arithmetic operations to evaluate, even if the rate is only being interpolated within a previously generated table. Completeness also pushes one toward the inclusion of as many distinct isotopes as possible. Each additional species, however, adds one unknown and one equation to the system of equalities which must be solved in order to follow the nucleosynthesis as time progresses.

As a compromise between completeness and computational efficiency,

Michael Newman and I chose the isotopes and reactions of Tables 1 and 2 and Figure 3. We included all the important isotopes and published reaction rates available involving nuclei with $Z \leqslant 11$; we believe that the network is therefore reasonably complete and applicable at temperatures of less than 2×10^9 K and densities less than 10^4 g cm^{-3}. (At higher temperatures or densities, reactions not included in the nucleosynthesis program may take material out of the pathways contained therein.) Stanford Woosley and Richard Wallace (private communications) have recently done work on ultra-high temperature nucleosynthesis in a hydrogen-rich environment. Their (unpublished) findings indicate that some reaction rates leading to nuclei with $Z > 11$ occur at rates significantly higher than those used in our calculations. Sections I.F. and VII discuss the work of Woosley and Wallace and its implications for models of "supergiant" class TŻ objects.

Of the 24 isotopes used in this work, 7 are "sinks", that is, isotopes away from which no reaction paths lead. The "sink" species are n, Ne^{20}, Ne^{21}, Ne^{22}, Na^{20}, Na^{21}, and Na^{22}. The presence of "sinks" is not necessary computationally, but does serve several useful purposes. The "sinks" among the Na and Ne isotopes terminate the reaction chains that might lead beyond the $Z \leqslant 11$ range. If products of nucleosynthesis begin to "pile up" to excess amounts in "sink" isotopes, it is a sign that further reactions may be important. (Such an accumulation in Ne^{20} is beginning to be visible in the $L_{env} = 89750\ L_\odot$, $T(r_K) = 1.76 \times 10^9$ K model of Table 4; it is discussed in detail in § VI.) Finally, the

omission of reverse reactions leading out of "sink" species saves some computer time and does not result in significant errors in the calculation of the luminosity produced by nuclear reactions. (Since most of the reaction paths away from the "sink" isotopes are endothermic, failure to include the reactions would at worst cause an overestimate of the luminosity; no such excess luminosity was seen in this work.)

The program which calculates nuclear reactions in TŻ "supergiants" takes as input $\vec{Y}(r_o)$, the vector of abundances for the 24 isotopes at radius r_o, and the values of v_t (turbulent velocity), ρ (density), and T (temperature) at r_o as computed by a stellar envelope integration. As discussed in §§ II and III above, accurate analytic expressions for T(r) and $\rho(r)$ permit the temperature and density to be calculated as functions of r, given their values at r_o. Equation (4) gives a simple, reasonable function r(t), which the nucleosynthesis program then uses to determine the run of temperature and density T[r(t)] and $\rho[r(t)]$ encountered by a one-gram parcel of material as it moves down from r_o to r_K and back up during one (sinusoidal) convective loop.

Taking $\vec{Y}(r_o) \equiv \vec{Y}_o$ as the initial set of isotopic abundances, the program solves the coupled system of 24 ordinary, first-order differential equations by stepping along in time. At time t_c after the beginning, r(t) is equal to r_o again and a single convective cycle has been finished; the resulting vector of abundances is called $\vec{Y}_{up}$. Under the hypothesis that there is complete mixing at r_o between material coming up from the "burning zone" and material coming down from the

"diffusive zone", the input abundance to the next cycle is $(\vec{Y}_o + \vec{Y}_{up})/2$. A parcel of matter beginning at r_o with that abundance vector is therefore sent down, a new $\vec{Y}_{up}$ comes out a time t_c later, and the process is repeated until $\vec{Y}_{up}$ ceases to change significantly. (Three iterations typically suffices to converge to within 10 %.)

The above summarizes my treatment of nuclear reactions. In the remainder of this section, I discuss a few details of the program which actually does the integration.

As described in FCZ-II, under astrophysical conditions the interaction between two nuclei, 1 and 2, is governed by the quantity $N_A\langle 12\rangle \equiv N_A\langle \sigma v\rangle_{12}$, in units of reactions per second per (mole cm^{-3}). The constant N_A is Avogadro's number (= 6.0222 x 10^{23} $mole^{-1}$) and the angle brackets denote an average over a Maxwellian velocity distribution of the cross section times velocity for the nuclei 1 and 2. The quantity $N_A\langle 12\rangle$ is a function of temperature only; all density dependence has been factored out.

The analogous quantity for a three-body reaction is $N_A^2\langle 123\rangle$. In the event that some of the reacting nuclei are identical, numerical factors must be introduced to prevent multiple-counting; see FCZ-II for details.

The equations which must be solved to determine the abundances of the various isotopes are simple, first-order, ordinary differential equations. For two distinct isotopes 1 and 2,

$$\frac{dY_1}{dt} = \frac{dY_2}{dt} = -\rho Y_1 Y_2 N_A\langle 12\rangle \qquad [\text{mole g}^{-1}\ \text{s}^{-1}] \qquad (7)$$

(Eq. (4) of FCZ-II). For the sometimes-important "triple-alpha" reaction $He^4(\alpha\alpha,\gamma)C^{12}$,

$$\frac{dY_{He^4}}{dt} = \frac{-1}{2} \rho^2 Y_{He^4}{}^3 N_A{}^2 \langle \alpha\alpha\alpha \rangle \text{ [mole g}^{-1} \text{ s}^{-1}\text{]}. \quad (8)$$

Many reactions, such as $C^{12}(p,\gamma)N^{13}$, proceed also in the reverse direction, as in $N^{13}(\gamma,p)C^{12}$. FCZ-II tabulates the function "REV RATIO" which is the ratio of (reverse reaction rate)/(forward reaction rate) as a function of temperature. The "reverse reaction" is assumed to begin with the ground state of the reacting nucleus; as FCZ-II caution, at high temperatures ($T \gtrsim 10^9$ K) it may become necessary to take into account the population of excited (but low-lying) nuclear states. Such effects, however, are typically small for the light nuclei used in the calculations here.

For increased computational efficiency, instead of reevaluating the reaction rates at every step during the convective cycle, my program interpolates within a table of logarithms of the reaction rates. (The rates "$\langle 12 \rangle$", etc. are functions of temperature only.) I take care in the interpolation scheme to avoid any discontinuities in the interpolated values.

The important nuclear reactions in models of stars with neutron cores proceed at vastly differing rates. A one-gram parcel of matter starting at radius r_o, which recently has had "fresh" envelope material mixed into it, finds the abundances of some of its constituent isotopes changing extremely rapidly, on timescales typically shorter than 10^{-8} s.

After a few of these fastest timescales, though, the most rapidly changing species will have approximately reached their equilibrium concentrations. Then, the overall rate of change of abundances will occur on a somewhat longer timescale, governed by another set of critical reactions. As these approach their equilibria, another set of yet slower reactions become the fastest things left changing. Ultimately, the convective motions of the fluid will define the relevant timescale for abundance variations; the isotopes will move smoothly from one equilibrium set of ratios to another as the temperature and density which they experience is modulated.

Systems of differential equations (such as the nucleosynthesis equations described above) which incorporate vastly differing timescales are termed "stiff" systems. A naive application of standard methods for the integration of systems of ordinary differential equations (e.g., the usual Runge-Kutta or predictor-corrector techniques) will not work well on a stiff system of equations (Gear, 1971; Acton, 1970). Conventional methods become unstable when their time-step size exceeds the shortest timescale in the problem, even when the terms in the solution varying at that timescale have apparently all died away or reached equilibrium. It would be both uneconomical and inaccurate to take 10^8 steps in order to integrate the system of reactions in the stellar model under consideration here; even if roundoff and truncation errors were tolerable, the final computer bill would not be!

So, to integrate this system of equations efficiently, it is important

to use a method which is well-adapted to stiff systems. There are many; I chose, for simplicity, the implicit midpoint Runge-Kutta method. (See Gear (1971), Chapter 11, for the details of the technique.) Since the algorithm has no built-in error determination facilities, every two integration steps my program compares the results it is calculating with the results from a double-length integration step. If the outcomes disagree by more than a chosen error limit, the steps are rejected, the step size is cut down, and the program goes back and tries again. If, on the other hand, the single and double step results agree too well, this suggests that the current time step is overly conservative, and so the program tries increasing the step size next time.

Within the program that integrates the nucleosynthetic equations there is included an energy-production calculation. At each integration step, the reaction rates are multiplied by their respective "Q" values and summed to give the luminosity being produced in the "burning zone" of the star. This luminosity mainly comes from strong-interaction processes, though some small amount of beta decays do contribute. The other component of the star's total luminosity is due to the complete beta-decay of all unstable isotopes which are produced in the "burning zone" and mix or diffuse outward through the "diffusive zone" toward the photosphere. Their total contribution to the stellar luminosity is simply their decay Q values (omitting the energy lost to neutrinos) times their net fluxes outward across radius r_o. The flux, for any species, is just

$$\mathcal{F} = \frac{M_b}{2\,t_c}\,(Y_{up} - Y_o) \qquad [\text{mole s}^{-1}] \qquad (9)$$

where M_b is the mass in the "burning zone" involved in the convective cycling, $t_c \equiv \pi(r_o - r_K)/v_t$ is the cycling time, Y_{up} is the abundance coming out of a cycle, and Y_o is the abundance at r_o, at the bottom of the "diffusive zone".

V. RESULTS OF DIFFUSION CALCULATIONS

A. Introduction and Definitions

The system of equations governing isotopic abundances in the "diffusive zone" above radius r_o is a system of linear, second-order ordinary differential equations. Equation (5) in § II above exhibits the general form for the equations in the system. Because of the linearity and the second-order structure of the equations, the 24-dimensional solution vector of abundances $\vec{Y}(r)$ can be written as a linear superposition of 48 independent solutions. There are many possible choices for the independent solutions; one of the most convenient can be found by writing

$$\vec{Y}(r) = \overleftrightarrow{A}(r) \cdot \vec{Y}_o + \overleftrightarrow{B}(r) \cdot \vec{Y}_{up} \qquad (10)$$

where, as before, $\vec{Y}_o$ is the vector of abundances at radius r_o, as given by the solution of the diffusion equation, and $\vec{Y}_{up}$ is the abundance vector coming out of a cycle through the "burning zone". This is convenient since $\vec{Y}_o$ and $\vec{Y}_{up}$ are natural input and output parameters for the nucleosynthesis program treating the "burning zone". The matrices $\overleftrightarrow{A}(r)$ and $\overleftrightarrow{B}(r)$ are simple to generate in principle: to get $A_{ij}(r)$, set $\vec{Y}_{up} = 0$ and $(Y_o)_k = \delta_{jk}$, solve the system of diffusion equations with that boundary condition, and read off $A_{ij}(r) = Y_i(r)$. To get $B_{ij}(r)$, follow the same prescription but with $\vec{Y}_o = 0$, $(Y_{up})_k = \delta_{jk}$.

The specific goal of this work is as was described in the introduction, § I.E.: for a given envelope model, adjust $\vec{Y}_o$ so as to produce

a desired photospheric abundance vector $\vec{Y}(r_p) \equiv \vec{Y}_p$. Soon after its formation, a TŻ "supergiant" will settle down into a "quasi-equilibrium" solution of the time-independent diffusion equations. The isotopic abundances $\vec{Y}_p$ in its envelope reservoir will not have had time to change much; I therefore have set $\vec{Y}_p$ equal to Cameron's (1973) "cosmic" abundances. After the appropriate $\vec{Y}_o$ has been determined which gives a chosen $\vec{Y}_p$ for a specific envelope model, the nucleosynthesis program tells how much luminosity L_{nuc} was produced. If the value L_{nuc} disagrees with the L_{env} hypothesized for the envelope model, then that model is not self-consistent and another model with a different L_{env} must be tried.

Since the photosphere, $r = r_p$, is the only radius at which the solutions $\vec{Y}(r)$ are directly observable, it is convenient to define $\overleftrightarrow{A} \equiv \overleftrightarrow{A}(r_p)$ and $\overleftrightarrow{B} \equiv \overleftrightarrow{B}(r_p)$. Before going ahead to grind out numerical solutions for the components of $\overleftrightarrow{A}$ and $\overleftrightarrow{B}$, a little analysis will reveal some valuable simplifications.

B. Solutions for First and Second Isotopes in a Decay Chain

First, consider the physics behind Eq.(5) for the diffusion of a beta-unstable isotope "k" ($\beta_k \neq 0$) which is not produced by the decay of any other beta-unstable species ($\beta_j = 0$; diffusion equation (5) is homogeneous). The second-order linear equation which governs the abundance of "k" as a function of radius will, in general, have one solution which "blows up" roughly exponentially at large r, and another which "dies" roughly exponentially at large r. The kth rows of $\overleftrightarrow{A}$ and $\overleftrightarrow{B}$ are all zeroes except for the elements A_{kk} and B_{kk}, since (by hypothesis) no other isotopes decay to make "k". Because the boundary values $(Y_o)_k$, $(Y_{up})_k$ used to get A_{kk} and B_{kk} are not precisely

such as to find the "dying exponential" solution for $Y_k(r)$, both A_{kk} and B_{kk} will be exceedingly large numbers. (Typical values are 10^{50} to 10^{200} or so, depending on the stellar model and on the value of β_k.) Physically, this says that to achieve $(Y_o)_k = 1$, $(Y_{up})_k = 0$, which implies a sizeable flux of "k" down through radius r_o, one must have an absolutely huge amount (A_{kk}) of the unstable isotope present in the photosphere in order to get a sufficient radial abundance gradient at r_o, after allowing for all the beta-decay losses along the way down. A huge negative value is assumed by B_{kk}, since to have $(Y_o)_k = 0$, $(Y_{up})_k = 1$ and therefore to "suck out" a sizeable flux of "k" from the "burning zone", one must have a (nonphysical) huge negative photospheric abundance of "k".

Really, the boundary conditions which one wishes to apply to any beta-unstable isotope's abundance are that $(Y_p)_k$ be equal to zero and that the radial solution be a "dying exponential" sort of function. In terms of A_{kk} and B_{kk}, the necessary condition at r_o is

$$\frac{(Y_{up})_k}{(Y_o)_k} \approx \frac{-A_{kk}}{B_{kk}} \qquad (11)$$

for unstable species with no parents, where the accuracy of the approximate equality is of the order of $1/A_{kk} \sim -1/B_{kk}$, typically $\sim 10^{-50}$ or better. In other words, a beta-unstable isotope in a "quasi-equilibrium" model must have a precise relationship between its abundance at r_o and its flux across r_o in order to match successfully onto a physically reasonable solution of the diffusion equation. The ratio $-A_{kk}(r)/B_{kk}(r)$ has already settled down to very near its

photospheric value at $r \ll r_p$ in typical models.

The couplings between isotopes in the system of diffusion equations are unidirectional; that is, in a beta-decay chain $j \rightarrow k \rightarrow \ell$, $Y_k(r)$ is independent of $Y_\ell(r)$, and $Y_j(r)$ is independent of "k" and "ℓ". One can therefore simplify the solution of a physical problem by solving "from the top down". Specifically, one may demand that an unstable species such as "j" have $(Y_p)_j = 0$; given that "dying" solution, one can plug it into the inhomogeneous diffusion equation for a decay product of "j" such as "k", and solve that equation with $(Y_o)_k = 0$, $(Y_{up})_k = 0$. The resulting solution of the inhomogeneous equation can then be superposed with the solutions of the homogeneous equation for $Y_k(r)$, which handle the flow of species "k" into or out of the "burning zone". [$(Y_o)_k \neq 0$, $(Y_{up})_k \neq 0$]. The inhomogeneous solution appears as matrix elements A_{kj} and B_{kj}; the linearly independent solutions of the homogeneous equation give the values of A_{kk} and B_{kk}.

When one solves for the elements of the $\overleftrightarrow{A}$ and $\overleftrightarrow{B}$ matrices using the "top down" approach, one is simply imposing a relationship upon the ratio $(Y_{up})_j/(Y_o)_j$. This means that is no longer necessary to solve separately for the matrix elements A_{kj} and B_{kj}, although such a separated solution remains valid. Provided the correct ratio $(Y_{up})_j/(Y_o)_j \equiv \lambda$ for the isotope at the top of the chain is attained, the results for all decay products down to the stable termination of the chain will be invariant under a linear transformation of matrix coefficients:

$$A_{kj}^{new} = \alpha A_{kj}^{old} + \lambda (1 - \alpha) B_{kj}^{old}$$

$$B_{kj}^{new} = \frac{1 - \alpha}{\lambda} A_{kj}^{old} + \alpha B_{kj}^{old} \quad .$$

In this transformation, the parameter α may be varied freely; the only important quantity, $A_{kj}^{new} (Y_o)_j + B_{kj}^{new} (Y_{up})_j$, is an invariant. One may choose α so as to force B_{kj} to be equal to zero, for example. That is the choice which I make. I solve the inhomogeneous diffusion equation (Eq. (5)) for $(Y(r))_k$ given boundary conditions $(Y_o)_i = \delta_{ji}$, $(Y_{up})_i = \lambda \delta_{ji} = - (A_{jj}/B_{jj}) \delta_{ji}$. The resulting abundance at the photosphere is $(Y(r_p))_k = A_{kj}$; B_{kj} is zero. The solutions of the homogeneous diffusion equation (which assumes the absence of a beta-unstable parent) may now be added to the inhomogeneous solution. The sum is a complete solution of Eq. (5), including both diffusive flows across radius r_o and beta decays of the parent isotope.

The linearity of the system of diffusion equations allows the above "top down" procedure to be generalized and applied to longer beta decay chains. Among the low-Z isotopes included in my nucleosynthesis network, however, there is only one chain as long as three isotopes: $Ne^{18} \rightarrow F^{18} \rightarrow O^{18}$. All other chains are composed of only a single beta-unstable parent species and its stable daughter. (The $\overleftrightarrow{A}$ matrix coefficient for the middle element of the triple chain, $A_{F^{18}Ne^{18}}$, is given at the end of Table 3, following the tabulation of the diagonal matrix elements A_{ii} and B_{ii} for the $L_{env} = 89750\ L_\odot$ "fiducial" $16\ M_\odot$ model.)

The "top down" approach for solving the system of coupled diffusion equations not only saves some computational labor; it also improves numerical accuracy. If the huge $\overleftrightarrow{A}$ and $\overleftrightarrow{B}$ coefficients generated by the obvious technique (described in the text immediately following Eq. (10)) were used, tiny roundoff or truncation errors would be amplified and make it essentially impossible to determine photospheric abundances for any species below the top of a beta-decay chain. Use of the reduced coefficients avoids the subtraction of two large, nearly equal numbers, and preserves maximum accuracy in all calculations.

C. Solution for the Stable Termination of a Decay Chain

The stable species which terminates each sequence of decays ("ℓ" in the chain $j \to k \to \ell$) can be treated by an even more straightforward technique, due to the simplicity of the diffusion equation in that case. To derive the solution, consider (for the next three paragraphs) a stable species "s" which has no parents. The diffusion equation (5) reduces to:

$$Y_s'' + \frac{d}{dr}\left(\ln(r^2 \rho D)\right) Y_s' = 0 \qquad (12)$$

which can be solved up to a single quadrature:

$$Y_s(r) = (Y_o)_s + C\, r_o \rho_o D_o \left((Y_o)_s - (Y_{up})_s\right) \int_{r_o}^{r} \frac{dr}{r^2 \rho D} . \qquad (13)$$

Here C is a numerical constant which describes the specific assumptions about the mixing at r_o between material in the "burning zone" and in the "diffusive zone"; that is, C gives the relationship between the flux across r_o of an isotope and the gradient dY/dr of that isotope at r_o.

The density and diffusion coefficient at radius r_o are denoted ρ_o and D_o respectively.

The precise value of the constant C is dependent on one's specific model for the mixing between the "burning zone" and the "diffusive zone" above it. One reasonable model follows from the assumption that total mixing means that the abundance $Y(r_o) \equiv Y_o$ of a species is the mean of Y_{up} and $Y(r_o + H_p(r_o)) = Y(5r_o/4)$. Working in terms of the logarithmic radial variable $x \equiv \ln(r/r_o)$, which simplifies the diffusion equation and makes the solutions smoother, the Taylor series expansion of the abundance near r_o is $Y(x) = Y_o + x\,(dY/dx)_o + \ldots$. If $x_1 \equiv \ln(5/4)$ is used to denote the value of x at one scale height above r_o, total mixing implies that

$$Y_o = (Y_{up} + Y(x_1)) / 2 = (Y_{up} + Y_o + x_1 (dY/dx)_o + \ldots) / 2.$$

Truncating the Taylor expansion gives $Y_o = Y_{up} + x_1 (dY/dx)_o$; compare this with Eq. (13), which says that $(dY/dx)_o = r_o (dY/dr)_o = C (Y_o - Y_{up})$. Thereby conclude that for this specific model of total mixing, $C = 1 / x_1 = 1 / \ln(1.25) \approx 4.48$. A rather slight variation of the above model expands Y(r) as a series in r instead of in $x \equiv \ln(r/r_o)$; it yields the value C = 4.

A rather different model of total mixing comes from the application of the diffusion equations all the way down to r_o. By equating the diffusive flux across the sphere of radius r_o,

$$\mathcal{F}_o \equiv - 4 \pi r_o^2 \rho_o D_o (dY / dr)_o \quad ,$$

to the "burning zone" flux

$$\mathcal{F}_b \equiv \frac{M_b \, (Y_{up} - Y_o)}{2 \, t_c}$$

from Eq. (9), one finds that $C = M_b / 8 \pi r_o \rho_o D_o t_c = 10 \ln(1.25) / \pi \approx$ ≈ 0.71 . In this work, I have used the value $C \equiv 1 / \ln(1.25) \approx 4.48$. A smaller value for C would reduce the derivative $(dY/dr)_o$ corresponding to a particular pair of values Y_o and Y_{up}, would reduce the flow of fresh CNO catalyst isotopes into the "burning zone", and would hinder the transport of useless waste products out of that zone. All reasonable choices for C are of comparable order of magnitude, and test runs which I made using $C = 0.71$ produced results which did not differ significantly from my results with $C = 4.48$.

After this digression on the solution (13) for a stable species with no parents, return to the bottom species of a beta-decay chain. The solution for it can be generated from (13): for the sample chain $j \to k \to \ell$, consider the definition $Y_s(r) \equiv Y_j(r) + Y_k(r) + Y_\ell(r)$. The quantity $Y_s(r)$ obeys Eq.(12) and has the solution given by Eq. (13); if one has previously demanded that $Y_j(r_p) = Y_k(r_p) = 0$ for the unstable members of the chain, then $Y_\ell(r_p) = Y_s(r_p)$. Physically, this is easy to understand: the members of the chain have the same atomic weight $Z + N$, and the sum of the separate abundances is conserved by the beta decay processes. Thus, suppose one writes (c.f. Eq. (13)):

$$A_{ss} = 1 + C \, r_o \rho_o D_o \int_{r_o}^{r_p} \frac{dr}{r^2 \rho \, D}$$

$$B_{ss} = - C\, r_o \rho_o D_o \int_{r_o}^{r_p} \frac{dr}{r^2 \rho D} \qquad (14)$$

for the A and B matrix elements for a stable isotope without parents. For the chain $j \rightarrow k \rightarrow \ell$, one may write $A_{\ell j} = A_{\ell k} = A_{\ell\ell} = A_{ss}$, $B_{\ell j} = B_{\ell k} = B_{\ell\ell} = B_{ss}$, and the resulting photospheric abundances implied for isotope "ℓ" by Eq. (10) will be correct if the beta-unstable isotopes "j" and "k" are truly following their only physically-reasonable path, their "dying exponential" solutions. Species j is forced to follow that path by the huge values of A_{jj} and B_{jj}. Similarly, species k sees huge values for A_{kk} and B_{kk}, and in addition has a comparably huge coupling to j in the form of A_{kj} and/or B_{kj}. The large coefficients which k sees in Eq. (10) therefore constrain the relationship between $(Y_o)_k$ and $(Y_{up})_k$ to match onto k's "dying exponential" solution. Finally, since all of the unstable parents of species ℓ have decayed away before they could find their way out to the photosphere, the observable abundance of ℓ is the same as if ℓ were a stable isotope, without parents, being produced in the "burning zone" at a rate equal to the sum of the actual outputs of j, k, and ℓ.

D. Results and Conclusions

To give concreteness to the above abstract discussion of the coupled diffusion equations and their solutions, some specific examples are in order. Figure 4 shows the structure, T(r) versus $\rho(r)$, of a typical 16 $M_\odot$ envelope model produced in the course of this work. The luminosity

which needs to be generated by nuclear reactions for this envelope model is 89750 $L_\odot$. The slope of the numerically-integrated $T(\rho)$ curve shows excellent agreement with the analytic, adiabatic, radiation-pressure dominated solution (Eq. (1)), from r_K out to beyond 100 r_K. Figure 5 presents the solution $A_{jj}(r)$ of the diffusion equation in this stellar model for a beta-unstable species with lifetime $\tau = 2$ s; Figure 6 graphs the ratio $- A_{jj} / B_{jj}$ for two representative isotopes with lifetimes of 2 s and 95 s.

The solutions of the diffusion equation (Eq. (5)) were calculated using a standard Adams-Bashforth-Moulton (predictor-corrector) algorithm. The first four points on the curves, beginning at r_o and moving upward, were calculated by a Runge-Kutta technique, since the predictor-corrector needs some points to get itself started. For numerical convenience, the diffusion equation was rewritten in terms of the independent variable $x \equiv \ln(r/r_o)$; step sizes of 0.1 to 0.5 in x were used, over the range from x = 0 out to x = 17 ($r = 1.25 \times 10^6$ cm to $r = 3.0 \times 10^{13}$ cm). Although the Adams-Bashforth-Moulton integration scheme is quite stable and generally safe to use, for a short-lifetime isotope the explosively growing exponential behavior of the solutions $A_{jj}(r)$ and $B_{jj}(r)$ eventually causes a loss of accuracy in the numerical integration results. The loss of accuracy occurs sooner for isotopes with shorter lifetimes and for larger integration step sizes. For example, the $\tau = 2$ s isotope of Figure 5 can be tracked to $r \sim 3 \times 10^8$ cm with fair precision (better than 20 %) when a step size of 0.5 in x is used; it can be followed to $r \sim 5 \times 10^9$ cm using a step of 0.1 in x. To the same accuracy, an isotope with $\tau = 95$ s can have its $A_{jj}(r)$ and $B_{jj}(r)$ coefficients determined

through $r \sim 10^{11}$ cm. At the maximum radius of x = 17, integrations of the diffusion equation for the 95 s isotope gave results which varied by 90 orders of magnitude!

The huge errors described above might seem to render nugatory the results of my numerical integrations. Such is not the case. As discussed in § V.B. above, only the ratio $- A_{jj}/B_{jj}$ is important for a beta-unstable isotope; the precise sizes of A_{jj} and B_{jj} are irrelevant, as long as they are large compared to the reciprocal of the accuracy being sought. As shown by Figure 6, $- A_{jj}/B_{jj}$ converges to a constant at radii much smaller than the photospheric radius; the ratio computed using a step size of 0.5 in x is accurate to better than a few tenths of a per cent, even for the isotopes with the shortest lifetimes.

Table 3 lists all of the isotopes used in the nucleosynthesis network and gives their lifetimes and the computed ratios $- A_{jj}/B_{jj}$ for each. Also tabulated are my computed values for the separate $\overleftrightarrow{A}$ and $\overleftrightarrow{B}$ matrix elements; they are included for completeness and to facilitate checking of my results. For the triple chain $Ne^{18} \rightarrow F^{18} \rightarrow O^{18}$ the significant ratio $A_{F^{18}Ne^{18}} / B_{F^{18}F^{18}}$ is listed. All of the data in Table 3 apply to the "fiducial" 16 $M_\odot$ envelope model with L_{env} = 89750 $L_\odot$. Figure 7 shows how the all-important ratio $- A_{jj} / B_{jj}$ varies with beta lifetime for a family of models, each with total mass 16 $M_\odot$ but with varying envelope luminosities.

An interesting effect is apparent in Fig. 7: the curves of $- A_{jj} / B_{jj}$ cross each other in the vicinity of lifetime τ = 50 s. Isotopes which live longer than 50 s find it easier to diffuse outward from r_o in models with larger values of L_{env}; those models have higher turbulent velocities

and their densities $\rho(r)$ fall off more slowly with increasing radius than is the case for envelopes with smaller L_{env}. Isotopes with beta decay lifetimes shorter than 50 s, on the other hand, can more readily escape from the "burning zone" of models with smaller L_{env}; such species mainly sample the regions just above r_o, where the envelopes with smaller values of L_{env} have high densities and are capable of absorbing a large influx of material.

Several significant conclusions emerge from the results of the diffusion calculations which I performed for envelope models of "supergiant" stars with neutron cores. The first (and probably the most important as far as nucleosynthesis is concerned) is that the stellar structure resembles a nozzle: between r_o and r_p there is a severe restriction in the flow of material into and out of the "burning zone". Figure 8 shows $A_{ss}(r)$ (defined in Eqs. (14)) for several 16 $M_\odot$ models. The "nozzle" effect is manifested by the large value of this function at $r = r_p$. A stable isotope which is a "fuel" for nuclear energy generation and which is completely destroyed in the "burning zone" ($Y_{up} = 0$) occurs with abundance $Y(r) = Y_o / A_{ss}(r)$ (if it is not produced by any beta decays). In other words, usable "fuels" are typically depleted at r_o to $\lesssim 1$ per cent of their "normal" (photospheric) abundances, and conversely, unusable "wastes" build up. This reduces the luminosity produced by nucleosynthesis. (Figure 8 also shows again that stable isotopes can more easily diffuse down from the photosphere in models with larger values of L_{env}.)

A second conclusion to be drawn from the results of the diffusion

calculations is that beta-unstable species with lifetimes of more than a few dozen seconds act about the same as do stable isotopes as far as their flows across radius r_o go. As Figure 7 shows, the ratio $-A_{jj} / B_{jj}$ does not change much until one gets down to rather short beta lifetimes. In physical terms, the hope that an unstable isotope might be able to diffuse outward, decay, and diffuse back down to provide significant amounts of extra "fuel" for the "burning zone" will be an unfulfilled hope unless the beta lifetime is exceedingly short. I estimate that important beta decays would have to proceed on time scales of less than 10 s for "wastes" to be efficiently recycled.

A third result of the diffusion model for the transport of nucleosynthesis products is that, among the beta-unstable isotopes included in my analysis, only Na^{22} has a sufficiently long lifetime to diffuse out to the photosphere where it might be observable. As Table 3 shows, the A_{jj} coefficients for all other decaying species, which have lifetimes of less than 10^4 s, are greater than 10^{40}. The size of the A_{jj} matrix elements reflects the speed with which the "blowing-up exponential" solutions are growing; numerical integrations and analysis confirm that the "dying exponential" solutions shrink at a comparable rate. All unstable isotopes at the photosphere are therefore dozens of orders of magnitude down from their abundances at r_o, with the exception of Na^{22}. Its $\sim 10^8$ s lifetime enables it to reach the photosphere at an abundance of the order of 1 per cent of the Na^{22} abundance at r_o, when it has had time to build up to equilibrium in the envelope reservoir. (Initially, however, Na^{22} presumably has a nearly zero abundance in the outer envelope, just as all other unstable isotopes have. It is therefore correct, when

the star is younger than $\sim 10^4$ years, to treat Na^{22} in the same way as the rest of the decaying species are being treated, according to the prescription of Eq. (11).)

VI. RESULTS OF NUCLEOSYNTHESIS CALCULATIONS

As discussed in § I.E. above, for each luminosity L_{env} within a reasonable range, a stellar envelope model may be constructed. The Despain (1976) diffusion equations, when applied to that envelope, determine how the photospheric abundances $\vec{Y}_p$ are related to the abundances $\vec{Y}_o$ at the bottom of the "diffusive zone" and to the abundances $\vec{Y}_{up}$ coming up out of the "burning zone". The diffusion equations are linear, and so these relationships may be stated in terms of matrices $\overleftrightarrow{A}$ and $\overleftrightarrow{B}$, defined according to Eq. (10) and the accompanying discussion in § V.A. To make a self-consistent model of a Thorne-Zytkow "supergiant" star with a neutron core, one must first adjust the abundances $\vec{Y}_o$ so as to achieve some standardized photospheric abundances $\vec{Y}_p$. (I have used Cameron's (1973) "cosmic" abundance ratios for my targets.) Once the abundances are correct, the nucleosynthesis program calculates how much luminosity is actually being liberated by strong interactions in the "burning zone" and by beta decays there and in the "diffusive zone". If this nuclear luminosity L_{nuc} is not equal to the envelope model's hypothesized luminosity L_{env}, it is necessary to go back, guess another L_{env}, and repeat the procedure.

If an envelope can be found which has the right conditions of density and temperature in the "burning zone", and which allows the right amount of diffusion of isotopes into and out of that zone, then one has found a self-consistent "supergiant" model. The diffusion equations then determine the slow evolution in time of the photospheric

abundances; that is, $\dot{\vec{Y}}_p$ is determined.

It is simple to estimate maximum and minimum time scales $\vec{Y}_p / \dot{\vec{Y}}_p$ for envelope abundance evolution. Suppose that hydrogen-burning is responsible for the bulk of the stellar luminosity. Conversion of hydrogen to helium yields $\epsilon_H \approx 6 \times 10^{18}$ erg g^{-1}. (Neutrino losses make this figure vary slightly for some reaction chains.) If the star's envelope mass is M_{env}, its luminosity is L, and the mass fraction of hydrogen is X, then a time scale for hydrogen exhaustion is

$$t_H \sim 10^7 \text{ years} \left(\frac{M_{env}}{15\ M_\odot}\right)\left(\frac{\epsilon_H}{6 \times 10^{18}\ \text{erg g}^{-1}}\right)\left(\frac{X}{0.7}\right)\left(\frac{10^5\ L_\odot}{L}\right) .$$

This is the longest possible time scale for the star's evolution.

If hydrogen-burning were catalyzed by a truly cyclic process, there would be no changes in catalyst isotope abundances. On the other hand, if mixing out of the "burning zone" meant that a catalyst nucleus (such as C^{12} or N^{14}) could only be used once, then each H^1 atom fused would destroy one atom of a catalyst. If one particular isotope "s" were chosen for all reactions, a time scale of $(Y_s/X)t_H$ would exist for consumption of "s" (where Y_s is a number fraction [mole g^{-1}] of "s"). Typical important "CNO" isotopes occur with cosmic abundances by number of a few times 10^{-4}, implying minimum time scales of thousands of years for their consumption. The actual evolutionary time scales for the envelope abundances will therefore lie between a few thousand and a few million years.

All of the above applies after a self-consistent model with $L_{env} = L_{nuc}$ has been found. I have not been able to find any such model for a 16 $M_\odot$

total mass "supergiant" class star with a neutron core, with reasonable ("cosmic") values for the photospheric abundances $\vec{Y}_p$. For the $L_{env} = 89750\ L_\odot$ envelope model of Figure 4, the results of the nucleosynthesis ($\vec{Y}_o$, $\vec{Y}_{up}$, and $\vec{Y}_p$) are given in Table 4. The luminosity L_{nuc} calculated falls far short of L_{env}!

An attempt to bring L_{nuc} up by reducing the L_{env} chosen for the model-building program (moving downward along the curve of acceptable envelope models in the L_{env}-T_p plane) failed. Table 5 shows the effects of changes in the assumed envelope luminosity L_{env} on the other parameters of the star: T_p (photospheric temperature), $T(r_K)$, $\rho(r_K)$, $\beta_g(r_K)$ (ratio of gas pressure to total pressure), t_c (cycle time in the "burning zone"), A_{ss} (ratio of photospheric abundance to abundance at r_o for a stable isotope without parents and which is completely consumed in the "burning zone"), and L_{nuc}. The entries in Table 5 were calculated using my standard set of programs, which do not include the effects of electron-positron pairs or neutrino losses. Unfortunately, above about 2×10^9 K, electron-positron pairs are produced in profusion, neutrino losses due to their annihilation and due to plasma processes are severe, and endothermic photodisintegration of heavy nuclei to alpha particles becomes significant. Other approximations used in the calculations become dubious or break down completely. It is probably fruitless to attempt to operate at temperatures above 2×10^9 K for the hottest part of the "burning zone".

Section V.D. above has already discussed one major cause of my low computed values of L_{nuc}: the convection (diffusion) restriction on the flow of fresh material into the "burning zone". A second problem,

due to another aspect of the star's structure, also exists. At the bottom of the convective region, the density and temperature of the gas are linked by the demands of stellar structure. It is impossible to raise the density, and thereby increase the nuclear energy generation, without raising the local temperature to unacceptably high values. This has several important consequences:

As derived in § II above (Eqs. (1), (2)), in the adiabatic, radiation-pressure dominated region between r_K and a few hundred r_K, the temperature increases proportionally to β_g. Density therefore increases proportionally to $\beta_g T^3 \propto \beta_g^4$. If at r_K one demands that $T < 2 \times 10^9$ K (to avoid numerous catastrophes), Eq. (2) implies that

$$\beta_g < 8 \times 10^{-3} \left(\frac{M_{core}}{1\ M_\odot}\right)\left(\frac{\mu}{0.6}\right)\left(\frac{10\ km}{r_K}\right)$$

and therefore that

$$\rho(r_K) < 1.2 \times 10^3\ g\ cm^{-3} \left(\frac{M_{core}}{1\ M_\odot}\right)\left(\frac{\mu}{0.6}\right)^2\left(\frac{10\ km}{r_K}\right) .$$

This means that the mass in the "burning zone" where most of the nucleo-synthesis occurs is rather small:

$$M_{burn} = \int_{r_K}^{r_o} 4\pi r^2 \rho\, dr = 4\pi r_K^3 \rho(r_K) \ln(r_o/r_K) < 1.7 \times 10^{-12}\ M_\odot .$$

Between 10^9 K and 2×10^9 K, the triple-alpha reaction ($He^4(\alpha\alpha,\gamma)C^{12}$) reaches its maximum rate; in the notation of FCZ-II, that rate is $N_A^2 \langle\alpha\alpha\alpha\rangle \lesssim 4.8 \times 10^{-10}$ reactions s^{-1} $mole^2$ cm^{-6}. The corresponding energy generation rate is $Q \rho^2 N_A Y_{He^4}^3 N_A^2 \langle\alpha\alpha\alpha\rangle / 6$ [erg g^{-1} s^{-1}]

where $Q = 1.17$ erg reaction^{-1}. Thus, the maximum triple-alpha luminosity to be expected from the "burning zone" is less than 9×10^{32} erg s^{-1} $\approx$ 0.2 $L_\odot$ for a star with number abundance of helium $Y_{He^4} = 0.07$ mole g^{-1} (mass fraction of 0.28 g g^{-1}).

If hydrogen-burning occurs and is catalyzed by "metals", one can derive another interesting upper limit on the energy generation rate. Suppose "metals" occur with mass fraction Z, and suppose that every "metal" nucleus in the "burning zone" could catalyze half of the process $4\ H^1 \rightarrow He^4$ before becoming a beta-unstable "noncatalyst". (For the standard "hot CNO cycle" the main beta-unstable noncatalysts are O^{14} and O^{15}, each of which requires $\sim$100 s to decay and become a catalyst again.) If the mean molecular weight of a catalyst is $\sim$14 atomic mass units, then the energy generation rate in the "burning zone" is limited to

$$\left(\frac{Z}{14 \text{ g mole}^{-1}}\right)\frac{M_{burn}\,\epsilon_H}{2\ t_c} = 2 \times 10^{38} \text{ erg s}^{-1}\left(\frac{Z}{0.03}\right)\left(\frac{\epsilon_H}{6 \times 10^{18} \text{ erg g}^{-1}}\right) x$$

$$x\left(\frac{M_{burn}}{3.4 \times 10^{21} \text{ g}}\right)\left(\frac{0.1 \text{ s}}{t_c}\right) ,$$

that is, almost 60 000 $L_\odot$. This in itself would be only 50 per cent below the required luminosity L_{nuc} to generate a self-consistent model, and one might hope that increasing the turbulent velocity v_t slightly (which decreases t_c, the cycle time) or increasing the metallicity Z would give satisfaction.

Unfortunately, as demonstrated in § V.D., the quasi-equilibrium solutions to the diffusion equation for typical models do not allow a

large fraction of the "metals" to be in the form of active hydrogen-burning catalyst isotopes. In fact, there can be only something of the order of one per cent of the isotopes in "useful" species; around 99 per cent of the material is inactive, generally in the form of beta-unstable isotopes awaiting decay. Catalyzed hydrogen burning cannot provide the requisite L_{nuc} for long, if energy generation is constrained to follow "conventional" (low-Z cycle) paths.

VII. SUGGESTIONS FOR FURTHER RESEARCH

If a star with total mass greater than about 10 $M_\odot$ is to survive with a degenerate neutron core inside it, TŻ found that the star had to have a significant amount of its luminosity produced by nucleosynthesis. I have not been able to generate enough energy using "conventional" reactions and stellar models. Here, I mention two other possibilities.

One step up in complexity from an equilibrium stellar model would be to a non-stationary model--one in which the regions near the neutron star were alternately collapsing and exploding, for example. Then, more violent mixing could occur, higher densities could be achieved in the "burning zone", and perhaps enough time-averaged luminosity would come out to support a massive extended envelope.

There are reasons to doubt this possibility, however. Presuming that the luminosity is provided by hydrogen burning, catalyzed by CNO isotopes as in the equilibrium models, one can estimate the change in internal energy of the gas when nucleosynthesis abruptly occurs. If a collapse is to be reversed and become an explosion, the change in specific internal energy $\delta\Pi$ should be a sizeable fraction of Π, since the ratio $\delta\Pi/\Pi$ gives an estimate for the acceleration of a mass element as a fraction of the local acceleration of gravity. Hydrogen burning converts approximately 7×10^{-3} of the mass of the input protons into energy, and two catalyst nuclei are required for each nucleus of He^4 output. If Z_{cat} denotes the mass fraction [g g^{-1}] of potential catalyst isotopes, one finds that a parcel of matter which abruptly

undergoes hydrogen burning experiences a change in its specific internal energy of $\delta\Pi \approx 7 \times 10^{-3}\ c^2\ (Z_{cat}/2)/14$, where 14 is the approximate mean atomic weight of the CNO catalysts. If a value of $Z_{cat} \approx 0.03$, comparable to the photospheric abundance, were possible (which it almost certainly is not), $\delta\Pi \approx 8 \times 10^{-6}\ c^2$. The specific internal energy of a radiation-dominated gas is

$$\Pi \approx \frac{a\ T^4}{\rho} = 0.084\ c^2 \left(\frac{T}{10^9\ K}\right)^4 \left(\frac{100\ g\ cm^{-3}}{\rho}\right) ;$$

the ratio, therefore, of $\delta\Pi$ to Π is small, typically 10^{-4} or less. This tiny fractional change in internal energy of the gas is unlikely to be able to turn a collapse around into an explosion and make a viable hydrodynamic model of the near-core regions of a "supergiant" type Thorne-Żytkow object.

A second important possibility to consider is a less-conventional network of nuclear reactions. Stanford Woosley and Richard Wallace (private communications) have done work on an "rp process" for rapid, very hot hydrogen burning. They find significant leakage out of the CNO isotopes at conditions of $T \gtrsim 5 \times 10^8$ K; by a series of (p,γ) reactions and beta decays, a nucleus of Ne^{19} can, for example, move up to the Fe^{56} area, liberating over 300 MeV in the process. Woosley has estimated that only about 10 s of beta decays are necessary along the way, and that these might in fact be replaced by (α,p) reactions at high enough temperatures and densities in a helium-rich environment. In the near future, when Woosley and Wallace finish development of their network of nuclear reactions, it will be interesting to try to use the

"rp process" to model "supergiant" TŻ objects.

If neither hydrodynamic nor "rp process" models succeed in producing $L_{nuc} = L_{env}$, and no other unforseen processes intervene, it seems likely that an envelope of $\gtrsim 10\ M_\odot$ around a degenerate neutron core will experience a catastrophic collapse, on a hydrodynamic time scale of a few years. As discussed in TŻ (§ VI) and in Zel'dovich, Ivanova, and Nadyozhin (1972), a temperature increase in the halo to much above 10^9 K can lead to increasing neutrino losses, which lead to further contraction and a further increase in the neutrino luminosity, etc. Such a runaway instability would soon push the central neutron-star core over the maximum allowed mass, and would thus leave one with a black hole surrounded by a still rapidly contracting envelope. The resulting system would be quite different from the models of stars with neutron cores which were the primary subject of this research!

ACKNOWLEDGEMENTS

I thank Michael J. Newman, Kip S. Thorne, and Anna N. Zytkow for many helpful conversations, letters, and computer programs related to this paper. I have also received support from the National Science Foundation [AST76-80801 A02] and from a Caltech graduate research assistantship.

REFERENCES

Acton, F. S., 1970, Numerical Methods that Work (Harper & Row, New York), esp. Chapters 5 and 6.

Cameron, A. G. W., 1973, Space Sci. Rev. 15, 121.

Clayton, D. D., 1968, Principles of Stellar Evolution and Nucleosynthesis (McGraw-Hill, New York), esp. Chapter 2.

Cox, J. P. and R. T. Giuli, 1968, Principles of Stellar Structure: Volume 1, Physical Principles (Gordon and Breach, New York), esp. Chapter 17.

Despain, K. H., 1976, Ph.D. dissertation, California Institute of Technology, Pasadena (unpublished).

Fowler, W. A., G. R. Caughlan and B. A. Zimmerman, 1975, Ann. Rev. Astron. Astrophys. 13, 69.

Gear, C. W., 1971, Numerical Initial Value Problems in Ordinary Differential Equations (Prentice-Hall, Englewood Cliffs, NJ), esp. Chapter 11.

General Electric Company, 1972, "Chart of the Nuclides", prepared by N. E. Holden and F. W. Walker, 11th edition (Schenectady, NY).

Paczynski, B., 1969, Acta Astron. 19, 1.

Taam, R. E., P. Bodenheimer and J. P. Ostriker, 1978, Ap. J. 222, 269.

Thorne, K. S., 1977, Ap. J. 212, 825.

Thorne, K. S., and A. N. Zytkow, 1975, Ap. J. (Lett.) 199, L19.

Thorne, K. S., and A. N. Zytkow, 1977, Ap. J. 212, 832.

Wagoner, R. V., 1969, Ap. J. Suppl. No. 162, 18, 247.

Wagoner, R. V., W. A. Fowler, and F. Hoyle, 1967, Ap. J. 148, 3.

Zel'dovich, Ya. B., L. N. Ivanova, and D. K. Nadyozhin, 1972, Astr. Zh. 49, 253 [English transl. Soviet Astr.--AJ, 16, 209 (1972)].

TABLE 1: Isotopes included in nucleosynthesis programs used in this work. For each unstable species, the e-folding lifetime to beta decay is given; for each stable species, the last column of the table presents Cameron's (1973) estimated "cosmic" abundance by number [mole g^{-1}]. See text, § IV.

TABLE 1

isotope	Z	e-folding lifetime s	"cosmic" abundance g^{-1} moles
n^1	0	918	--
H^1	1	--	0.70
He^4	2	--	0.070
C^{12}	6	--	3.86 E-4
C^{13}		--	4.33 E-6
N^{13}	7	863	--
N^{14}		--	1.20 E-4
N^{15}		--	4.39 E-7
O^{14}	8	102	--
O^{15}		176	--
O^{16}		--	7.07 E-4
O^{17}		--	2.65 E-7
O^{18}		--	1.45 E-6
F^{17}	9	95	--
F^{18}		9504	--
F^{19}		--	8.09 E-8
Ne^{18}	10	2.41	--
Ne^{19}		25.1	--
Ne^{20}		--	1.01 E-4
Ne^{21}		--	3.07 E-7
Ne^{22}		--	1.23 E-5
Na^{20}	11	0.642	--
Na^{21}		32.9	--
Na^{22}		1.18 E+8	--

TABLE 2: Complete list of nuclear reactions included in the nucleosynthesis program used in this work. Abbreviations for the sources of each reaction rate are:

F := FCZ-II [Fowler, Caughlan, and Zimmerman, 1975].

GE := General Electric "Chart of the Nuclides", 1972.

MJN := Michael J. Newman, private communication.

RVW := Wagoner, 1969.

WAF := William A. Fowler, private communication.

WFH := Wagoner, Fowler, and Hoyle, 1967.

Note that all beta decays, even if not contained in the nucleosynthesis program, were included in the diffusion equation program. (No beta decays of significant isotopes occurred at a fast enough rate to have any perceptible effect on the nucleosynthesis within the "burning zone".) Note also that no reactions taking material out of the "sink" species (n, Ne^{20}, Ne^{21}, Ne^{22}, Na^{20}, Na^{21}, Na^{22}) are included. As discussed in § IV, omitted reactions should have no significant effect on nucleosynthesis or energy generation calculations, as long as the low-Z network remains valid. See text, § IV, for additional comments.

TABLE 2

reaction	source	reaction	source
$C^{12}(p,\gamma)N^{13}$	F	$N^{13}(\gamma,p)C^{12}$	F
$C^{12}(\alpha,\gamma)O^{16}$	F	$O^{16}(\gamma,\alpha)C^{12}$	F
$C^{13}(p,\gamma)N^{14}$	F	$N^{14}(\gamma,p)C^{13}$	F
$C^{13}(\alpha,n)O^{16}$	F	$N^{13}(\ ,\beta^+\nu)C^{13}$	GE,MJN
$N^{13}(p,\gamma)O^{14}$	F	$O^{14}(\gamma,p)N^{13}$	F
$N^{13}(\alpha,p)O^{16}$	F	$O^{16}(p,\alpha)N^{13}$	F
$N^{14}(p,\gamma)O^{15}$	F	$O^{15}(\gamma,p)N^{14}$	F
$N^{14}(\alpha,\gamma)F^{18}$	F	$F^{18}(\gamma,\alpha)N^{14}$	F
$N^{15}(p,\gamma)O^{16}$	F	$O^{16}(\gamma,p)N^{15}$	F
$N^{15}(p,\alpha)C^{12}$	F	$C^{12}(\alpha,p)N^{15}$	F
$N^{15}(\alpha,\gamma)F^{19}$	F	$F^{19}(\gamma,\alpha)N^{15}$	F
$O^{14}(\alpha,p)F^{17}$	WFH	$F^{17}(p,\alpha)O^{14}$	WFH
$O^{14}(\ ,\beta^+\nu)N^{14}$	GE,MJN	$O^{15}(\ ,\beta^+\nu)N^{15}$	GE,MJN
$O^{15}(\alpha,\gamma)Ne^{19}$	MJN	$Ne^{19}(\gamma,\alpha)O^{15}$	MJN
$O^{16}(p,\gamma)F^{17}$	F	$F^{17}(\gamma,p)O^{16}$	F
$O^{16}(\alpha,\gamma)Ne^{20}$	F	$O^{17}(\alpha,n)Ne^{20}$	F
$O^{17}(p,\gamma)F^{18}$	F	$F^{18}(\gamma,p)O^{17}$	F
$O^{17}(p,\alpha)N^{14}$	F	$N^{14}(\alpha,p)O^{17}$	F
$O^{18}(p,\gamma)F^{19}$	F	$F^{19}(\gamma,p)O^{18}$	F
$O^{18}(\alpha,\gamma)Ne^{22}$	F	$F^{17}(\alpha,p)Ne^{20}$	WFH
$O^{18}(p,\alpha)N^{15}$	F	$N^{15}(\alpha,p)O^{18}$	F
$F^{17}(p,\gamma)Ne^{18}$	WFH	$Ne^{18}(\gamma,p)F^{17}$	WFH
$F^{17}(\ ,\beta^+\nu)O^{17}$	GE,MJN	$F^{18}(\alpha,p)Ne^{21}$	RVW
$F^{18}(p,\gamma)Ne^{19}$	RVW	$Ne^{19}(\gamma,p)F^{18}$	RVW
$F^{18}(\ ,\beta^+\nu)O^{18}$	GE,MJN	$F^{19}(p,\gamma)Ne^{20}$	F
$F^{18}(p,\alpha)O^{15}$	RVW	$O^{15}(\alpha,p)F^{18}$	RVW
$F^{19}(\alpha,p)Ne^{22}$	F	$Ne^{18}(\alpha,p)Na^{21}$	WFH
$F^{19}(p,\alpha)O^{16}$	F	$O^{16}(\alpha,p)F^{19}$	F
$Ne^{18}(\ ,\beta^+\nu)F^{18}$	GE,MJN	$Ne^{19}(p,\gamma)Na^{20}$	MJN
$Ne^{19}(\alpha,p)Na^{22}$	RVW	$Ne^{19}(\ ,\beta^+\nu)F^{19}$	GE,MJN
$He^{4}(\alpha\alpha,\gamma)C^{12}$	F,WAF	$C^{12}(\gamma,\alpha\alpha)He^{4}$	F,WAF
$O^{18}(\alpha,n)Ne^{21}$	F		

TABLE 3: Beta unstable isotopes included in the nucleosynthesis and diffusion equation programs. Following each decay and its e-folding lifetime the table gives the corresponding diagonal element of the $\overleftrightarrow{A}$ and $\overleftrightarrow{B}$ matrices defined in § V.A., Eq. (10) and the accompanying discussion. The values given are for a 16 $M_\odot$ total mass object, with core mass 1 $M_\odot$ and core radius 10 km, and with postulated luminosity L_{env} of 89750 $L_\odot$. The precise values of the A_{jj} and B_{jj} coefficients are highly sensitive to the numerical integration step size and to the radius at which the integration is terminated, as discussed in § V.D. For Table 3, the radial step size was 0.1 in $\ln(r/r_o)$ and the cutoff was at $r = r_o e^{17}$ (except for $Na^{20} \rightarrow Ne^{20}$, which had its integration terminated at $r_o e^{16.7}$ to avoid a numerical overflow). The values of A_{jj} and B_{jj} are not important, however, as long as they are large; the important quantity is the ratio $-A_{jj} / B_{jj}$, as discussed in § V.B. (Eq. (11) and accompanying text). That ratio, tabulated in the last column, is exceedingly insensitive to the details of the step size or integration cutoff. See text, § V.D., for more details.

TABLE 3

beta decay	e-folding lifetime s	A_{jj}	B_{jj}	$-A_{jj}/B_{jj}$
$Na^{20} \rightarrow Ne^{20}$	0.642	1.862 E308	-1.598 E308	1.1648
$Ne^{18} \rightarrow F^{18}$	2.41	6.620 E267	-6.141 E267	1.0780
$Ne^{19} \rightarrow F^{19}$	25.1	1.334 E180	-1.306 E180	1.0210
$Na^{21} \rightarrow Ne^{21}$	32.9	1.774 E171	-1.742 E171	1.0184
$F^{17} \rightarrow O^{17}$	95	6.846 E138	-6.766 E138	1.0118
$O^{14} \rightarrow N^{14}$	102	6.420 E136	-6.169 E136	1.0115
$O^{15} \rightarrow N^{15}$	176	4.881 E121	-4.834 E121	1.0098
$N^{13} \rightarrow C^{13}$	863	1.292 E+83	-1.283 E+83	1.0074
$n^{1} \rightarrow H^{1}$	918	5.951 E+81	-5.908 E+81	1.0074
$F^{18} \rightarrow O^{18}$	9504	1.233 E+40	-1.225 E+40	1.0067
$Na^{22} \rightarrow Ne^{22}$	1.18 E+8	181.1	-179.9	1.0066
[stable]	--	153.6	-152.6	1.0066

For triple chain $Ne^{18} \rightarrow F^{18} \rightarrow O^{18}$: $A_{F18Ne18} = -8.738$ E+38

$$A_{F18Ne18} / B_{F18F18} = 0.07133$$

TABLE 4: Results of the nucleosynthesis calculations for the 16 $M_\odot$ total mass, $L_{env} = 89750\ L_\odot$ model of Table 3 and Figure 4. For each isotope, the abundance Y_o [mole g^{-1}] at the bottom of the diffusive zone is given, followed by the resulting abundance Y_{up} which, in equilibrium, comes up out of the "burning zone". For a beta-unstable isotope "j", the ratio $(Y_{up})_j/(Y_o)_j$ should be very close to the ratio $-A_{jj}/B_{jj}$ of diffusion equation matrix elements. The two ratios are tabulated in columns 4 and 5; I stopped iterating when all of the abundance ratios were within a few parts per thousand of their targets. The remaining columns of the table give the computed photospheric abundances for the stable isotopes (Y_p) and the target abundances ($Y_{Cameron}$) based on Cameron's (1973) work. In most cases, I was able to hit Cameron's target values almost precisely; the largest errors occurred in N^{14} and Ne^{20}. More iterations could fine-tune these numbers, but there would be only a negligible effect on the total nuclear luminosity L_{nuc}. See § VI for discussion.

TABLE 4

isotope	Y_o mol g^{-1}	Y_{up} mol g^{-1}	Y_{up}/Y_o	$-A_{jj}/B_{jj}$	Y_p mol g^{-1}	$Y_{Cameron}$ mol g^{-1}
H^1	0.7000	0.7000	*	*	0.7000	0.70
n^1	8.420 E-08	8.482 E-08	1.0074	1.0074	*	*
He^4	0.06800	0.06799	*	*	0.06965	0.070
C^{12}	2.540 E-06	2.087 E-14	*	*	3.901 E-4	3.86 E-4
C^{13}	2.850 E-08	7.756 E-25	*	*	4.378 E-6	4.33 E-6
N^{13}	2.280 E-15	2.302 E-15	1.0096	1.0074	*	*
N^{14}	6.710 E-07	1.356 E-17	*	*	1.031 E-4	1.20 E-4
N^{15}	2.930 E-09	3.709 E-20	*	*	4.433 E-7	4.39 E-7
O^{14}	4.100 E-13	4.148 E-13	1.0117	1.0115	*	*
O^{15}	1.135 E-08	1.147 E-08	1.0104	1.0098	*	*
O^{16}	1.300 E-05	8.633 E-06	*	*	6.794 E-4	7.07 E-4
O^{17}	1.740 E-09	1.056 E-20	*	*	2.672 E-7	2.65 E-7
O^{18}	9.540 E-09	3.146 E-31	*	*	1.455 E-6	1.45 E-6
F^{17}	6.079 E-11	6.151 E-11	1.0118	1.0118	*	*
F^{18}	3.314 E-18	2.329 E-18	1.0067	1.0067	*	*
F^{19}	5.450 E-10	5.171 E-20	*	*	8.186 E-8	8.09 E-8
Ne^{18}	9.805 E-10	1.057 E-09	1.0780	1.0780	*	*
Ne^{19}	8.398 E-10	8.575 E-10	1.0210	1.0210	*	*
Ne^{20}	1.100 E-03	1.106 E-03	*	*	1.771 E-4	1.01 E-4
Ne^{21}	1.570 E-05	1.570 E-05	*	*	2.654 E-7	3.07 E-7
Ne^{22}	1.300 E-05	1.300 E-05	*	*	1.226 E-5	1.23 E-5
Na^{20}	1.406 E-07	1.638 E-07	1.1651	1.1648	*	*
Na^{21}	1.028 E-05	1.045 E-05	1.0164	1.0184	*	*
Na^{22}	1.026 E-04	1.033 E-04	1.0066	1.0066	*	*

TABLE 5: Results of the nucleosynthesis and diffusion equation programs for a family of models with total mass of 16 $M_\odot$, core mass of 1 $M_\odot$, core radius r_K of 10 km, and Cameron (1973) surface abundances. The model envelope luminosity L_{env} and photospheric temperature T_p (at the top of the atmosphere, optical depth 0) were input to a modified version of Paczyński's (1969) stellar envelope program GOB. GOB determined the structure of the extended envelope down to near the region of nuclear energy generation just above the central degenerate core. The quantities $T(r_K)$, $\rho(r_K)$, and $\beta_g(r_K)$ are the values of temperature, density, and (gas pressure)/(total pressure) calculated by GOB at radius r_K. The cycle time t_c is $\pi\,(r_o - r_K)/v_t(r_o)$, that is, the time required for the bottommost convective cell to turn over once. The envelope calculated by GOB was input to a program which numerically integrated the Despain (1976) diffusion equations and determined the matrices $\overleftrightarrow{A}$ and $\overleftrightarrow{B}$ defined in § V.A. (Eq. (10) and accompanying discussion). The diagonal element of the $\overleftrightarrow{A}$ matrix for a stable isotope, A_{ss}, gives the ratio of surface abundance to abundance at r_o for a stable isotope which is completely consumed by nuclear reactions in the "burning zone" and which is not produced by the beta decay of any product of nucleosynthesis. The matrices $\overleftrightarrow{A}$ and $\overleftrightarrow{B}$ from the diffusion

program, and the temperature, density, and cycle time of the "burning zone", are input to a program which calculates non-equilibrium nucleosynthesis. By adjusting the isotopic ratios at the bottom of the convective envelope, a set of abundances is obtained which produces Cameron (1973) surface abundances. The nucleosynthesis program computes L_{nuc}, the total luminosity produced due to nuclear reactions in the "burning zone" plus the energy released by beta decays of material in the "diffusive zone". If a stellar envelope could be found which had L_{env} equal to L_{nuc}, it would be a self-consistent model of a Thorne-Żytkow "supergiant" object. See text, § VI, for further discussion.

TABLE 5

L_{env} / $L_\odot$	T_p / K	$T(r_K)$ / 10^9 K	$\rho(r_K)$ / g cm^{-3}	$\beta_g(r_K)$	cycle time t_c / s	A_{ss}	L_{nuc} / $L_\odot$
90 000	2448.39	1.32	224	0.00511	0.050	112.3	940
89 750	2449.27	1.76	710	0.00679	0.073	153.6	1900
89 500	2450.14	2.21	1770	0.00852	0.099	193.4	2590
89 250	2451.01	2.69	3860	0.0102	0.127	233.0	3490

FIGURE 1: The structure of stars with degenerate neutron cores; figure adapted from Thorne and Zytkow (1977). As discussed in § I.B., an abrupt "knee" at radius r_K, density $\rho \sim 1$ g cm^{-3} separates the convective stellar envelope above from the almost-isothermal halo and degenerate core below. Distances away from r_K are given in meters on the right edge of Fig. 1; the left edge presents the corresponding local density of rest-mass. The specific figures shown are for a typical 5 $M_\odot$ total mass "giant" class model. In the more massive "supergiant" objects which are the subject of this paper, gravitational energy release provides only a few per cent of the stellar luminosity; the hydrogen-burning region marked "H Shell" overlaps the knee, and convection carries the products of nucleosynthesis out to the photosphere. See text, § I.B., for further discussion.

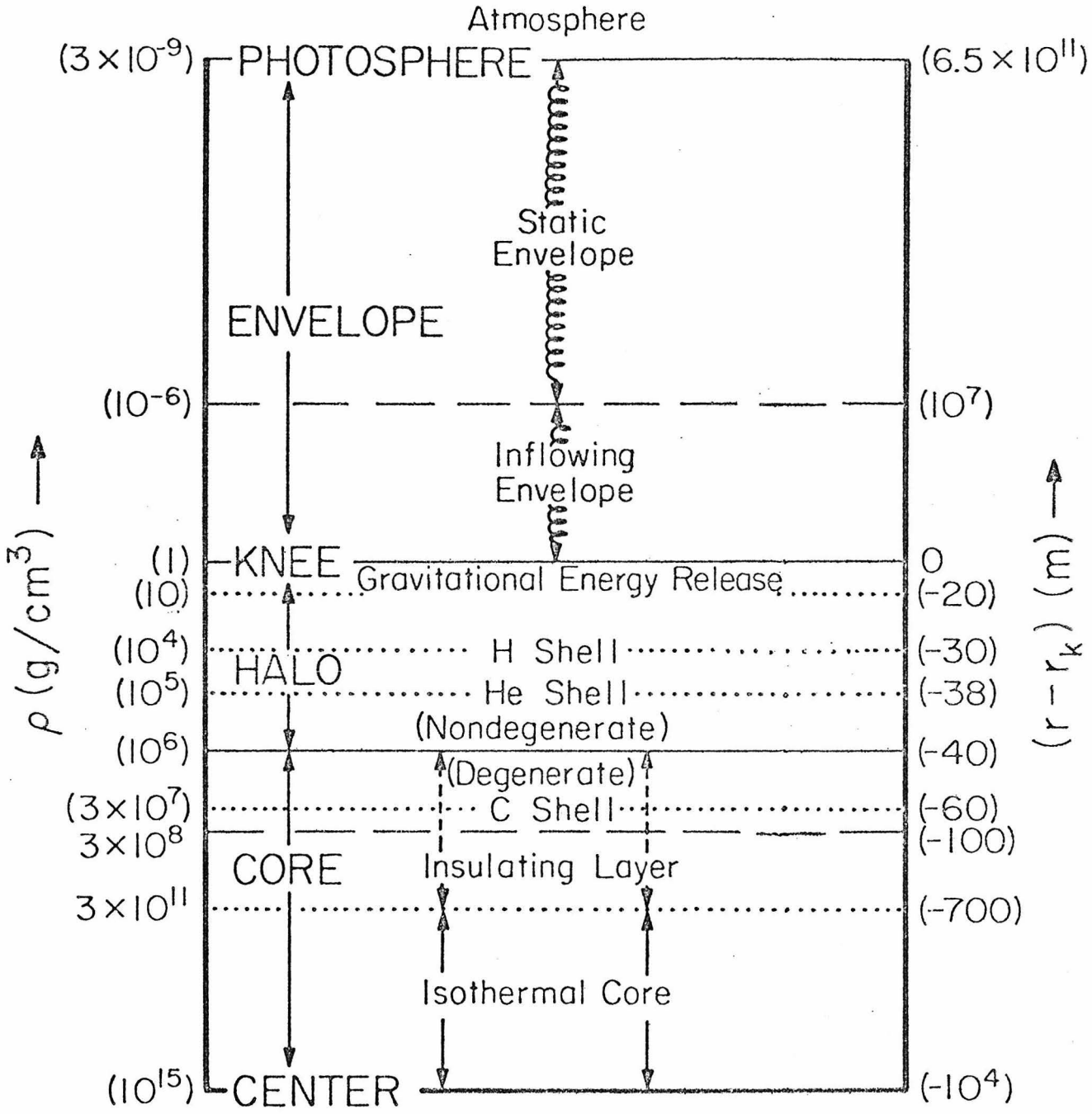
Atmosphere
(3×10⁻⁹)
PHOTOSPHERE
(6.5×10¹¹)
Static
Envelope
ENVELOPE
(10⁻⁶)
(10⁷)
Inflowing
Envelope
ρ (g/cm³)
(1)
KNEE
0
(10)
Gravitational Energy Release
(-20)
(10⁴)
H Shell
(-30)
HALO
(10⁵)
He Shell
(-38)
(Nondegenerate)
(10⁶)
(-40)
(Degenerate)
(3×10⁷)
C Shell
(-60)
3×10⁸
(-100)
CORE
Insulating Layer
3×10¹¹
(-700)
Isothermal Core
(10¹⁵)
CENTER
(-10⁴)
(r - r_k) (m)

Fig. 1

FIGURE 2: Density versus temperature for a typical "giant" (5 $M_\odot$) and a typical "supergiant" (12 $M_\odot$) model; figure taken from Thorne and Żytkow (1977). Dotted lines divide the plane into regions of radiation dominance versus gas dominance, degenerate versus nondegenerate, relativistic versus nonrelativistic, etc. Compare this figure with Fig. 1, and see the discussion in § I.B. for more detailed comments on the structure. Note, in particular, the overlap of the hydrogen-burning region (marked "H") with the convective zone above the "knee" in the "supergiant" model. This overlap allows the products of hot, nonequilibrium nucleosynthesis to be carried out to the photosphere, where they may be observed.

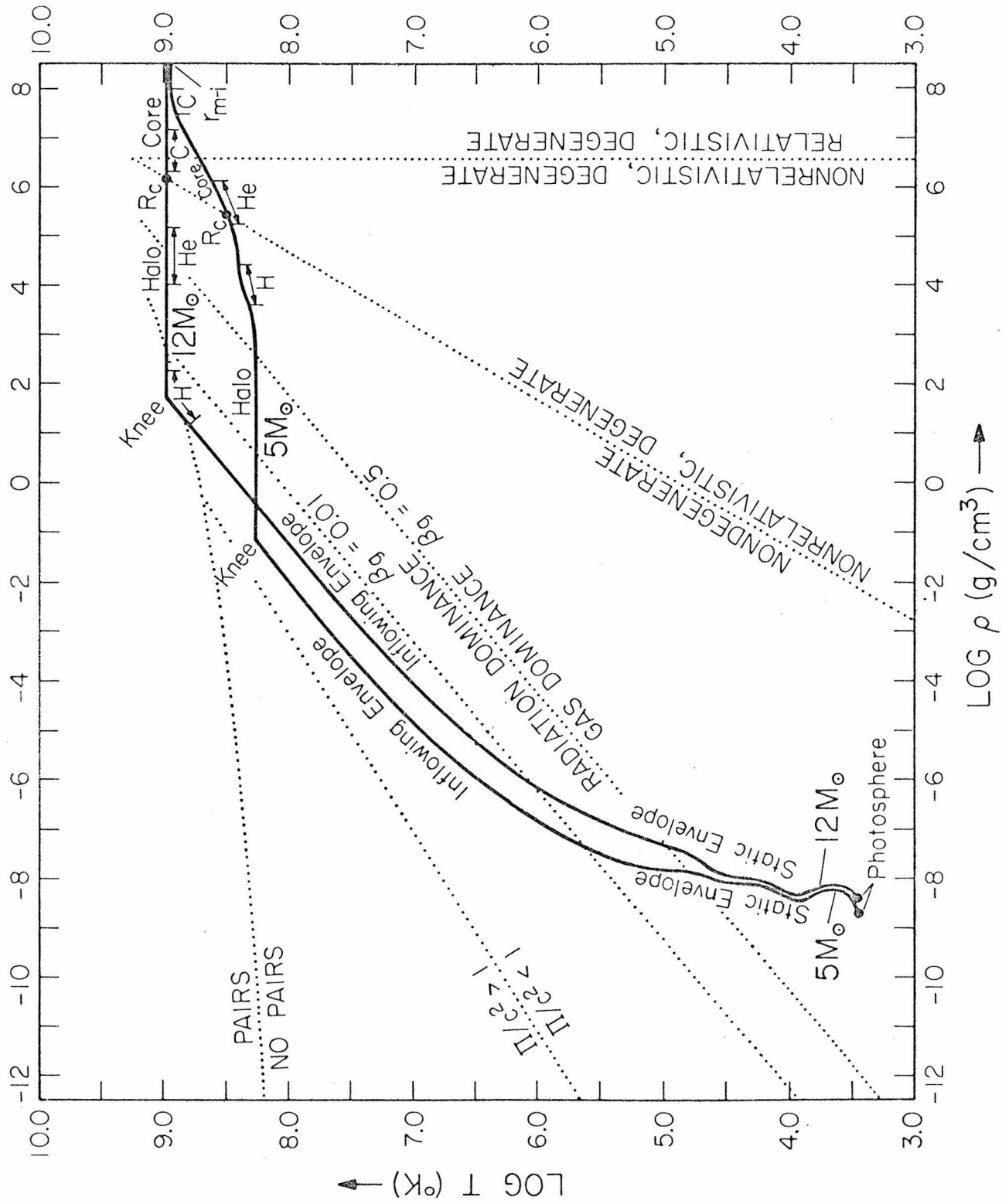
LOG T (°K) ⟵
LOG ρ (g/cm³) ⟶
NONRELATIVISTIC, DEGENERATE
RELATIVISTIC, DEGENERATE
NONDEGENERATE
NONRELATIVISTIC, DEGENERATE
RADIATION DOMINANCE Pg = 0.5
GAS DOMINANCE Pg = 0.01
PAIRS
NO PAIRS
Core
Halo
Knee
Infiowing Envelope
Static Envelope
Photosphere
12M⊙
5M⊙
H
He
C
Rc

Fig. 2

FIGURE 3: Chart showing the 24 isotopes included in the low-Z nucleosynthesis network used in this work. Arrows mark the (α,γ) [diagonally, right 2 cells and up 2 cells, as in $O^{18}(\alpha,\gamma)Ne^{22}$], (γ,α) [as in $O^{16}(\gamma,\alpha)C^{12}$], (α,n) [a move like a keima in go, or a knight in chess, up 2 and right 1, as in $C^{13}(\alpha,n)O^{16}$], and triple-alpha [as in $He^{4}(\alpha\alpha,\gamma)C^{12}$] reactions. Not shown are the possible beta decays [arrows diagonally rightward and down] and the (p,γ) [arrows up 1 cell], (γ,p) [arrows down 1], (p,α) ["keima", left 2 down 1], and (α,p) ["keima", right 2 up 1] reactions among the 24 species, since essentially all of those reactions are included in the program, and the forest of arrows would render the diagram illegible. As discussed in § IV, the reactions not included in the network are ones which would take nuclei away from the "sink" isotopes n^{1}, Ne^{20}, Ne^{21}, Ne^{22}, Na^{20}, Na^{21}, Na^{22}. Beta decays out of these isotopes are included in the diffusive zone. The missing reactions would not be expected to have a significant effect on nucleosynthesis or energy generation at temperatures of less than 2×10^{9} K. By omitting them, one both saves computer time and has a warning, if large abundances begin to accumulate in the "sink" species, that nuclei beyond $Z = 11$ may be needed in the reaction network. See § IV. for further discussion.

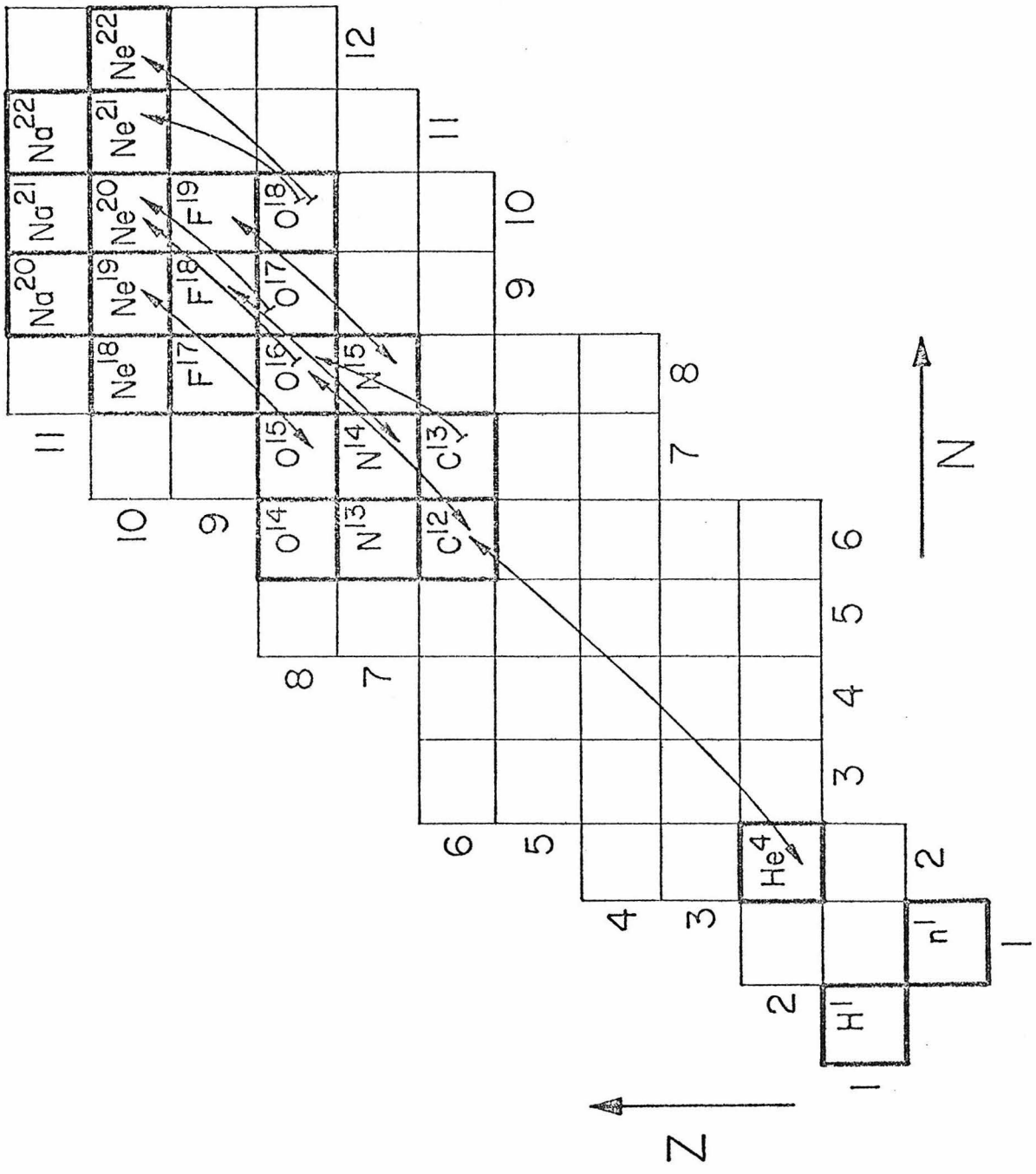
Ne22
Na22 Ne21
Na21 Ne20 F19 O18
Na20 Ne19 F18 O17
Ne18 F17 O16 N15
O15 N14 C13
O14 N13 C12
He4
n1
H1
12
11
10
9
8
7
6
5
4
3
2
1
N
Z

Fig. 3

FIGURE 4: Temperature versus density structure of the 16 $M_\odot$ total mass, L_{env} = 89750 $L_\odot$ envelope model used in Fig. 5, Fig. 6, Table 3 and Table 4. The curve is parameterized by radius in centimeters. The nearly-constant slope of the graph inside radius 10^9 cm corresponds to the adiabatic, radiation-pressure dominated region deep within the stellar envelope. The analytic formulae for temperature and density discussed in § II, Eqs. (1) and (2), fit the numerically computed stellar structure accurately in that region. See § V.D. for additional discussion.

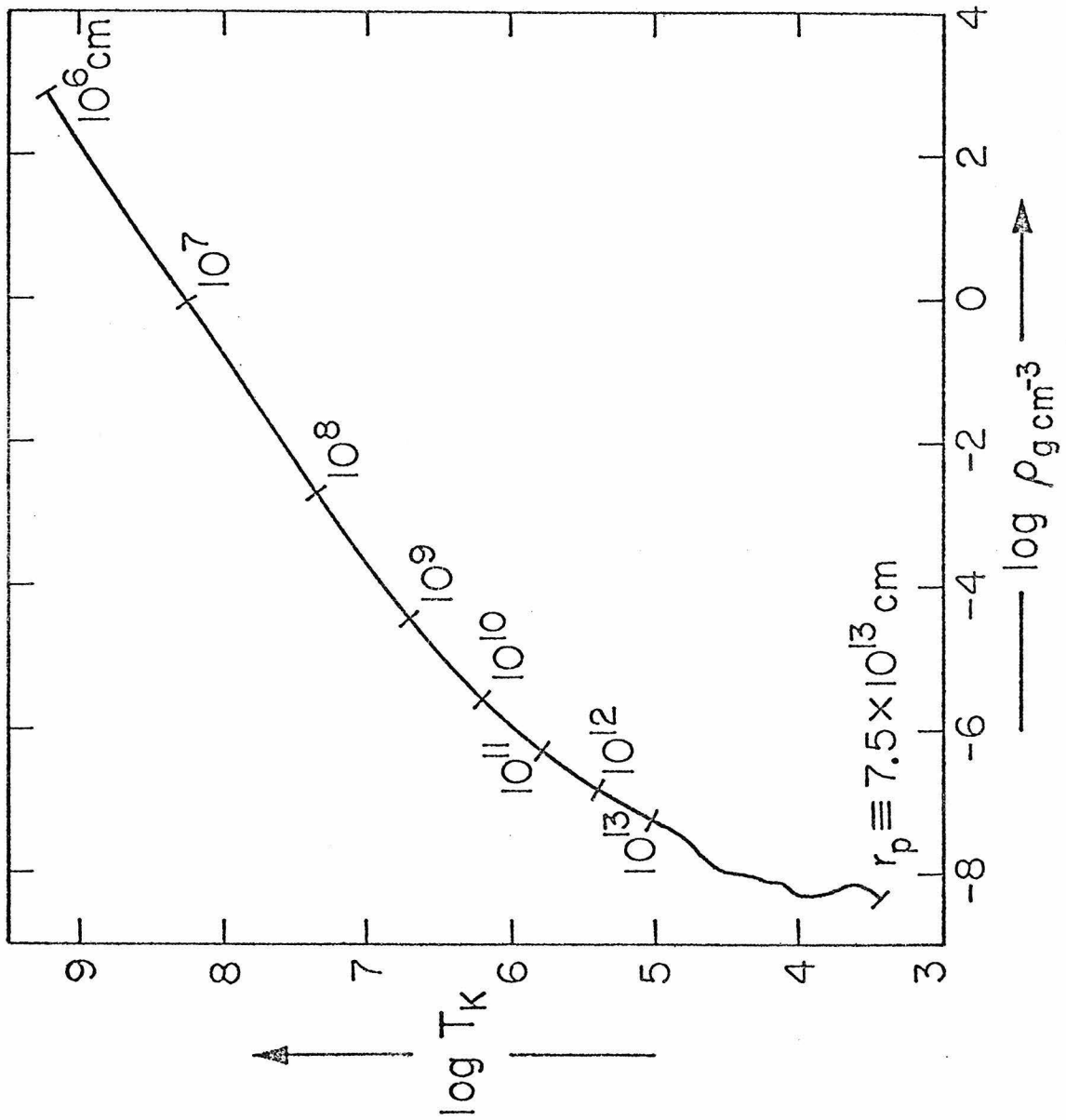
10^6cm
10^7
10^8
10^9
10^{10}
10^{11}
10^{12}
10^{13}
$r_p \equiv 7.5\times10^{13}$ cm
log T_K
log $\rho_{g\,cm^{-3}}$
9
8
7
6
5
4
3
4
2
0
-2
-4
-6
-8

Fig. 4

FIGURE 5: Diffusion equation solution $A_{jj}(r)$ and $\log_{10}A_{jj}(r)$ for an unstable isotope with e-folding lifetime of 2 s in a 16 $M_\odot$, L_{env} = 89750 $L_\odot$ envelope model. The numerical integration graphed in Figure 5 used a step size of 0.1 in $\ln(r/r_o)$. The huge magnitude of $A_{jj}(r)$ at the stellar photosphere is due to the presence of a growing exponential (or worse!) solution of the second-order diffusion equation. To avoid an unphysically large photospheric abundance of an unstable isotope, the abundance and its derivative must be carefully adjusted at r_o, at the bottom of the "diffusive zone". See § V.B. and § V.D. for additional discussion.

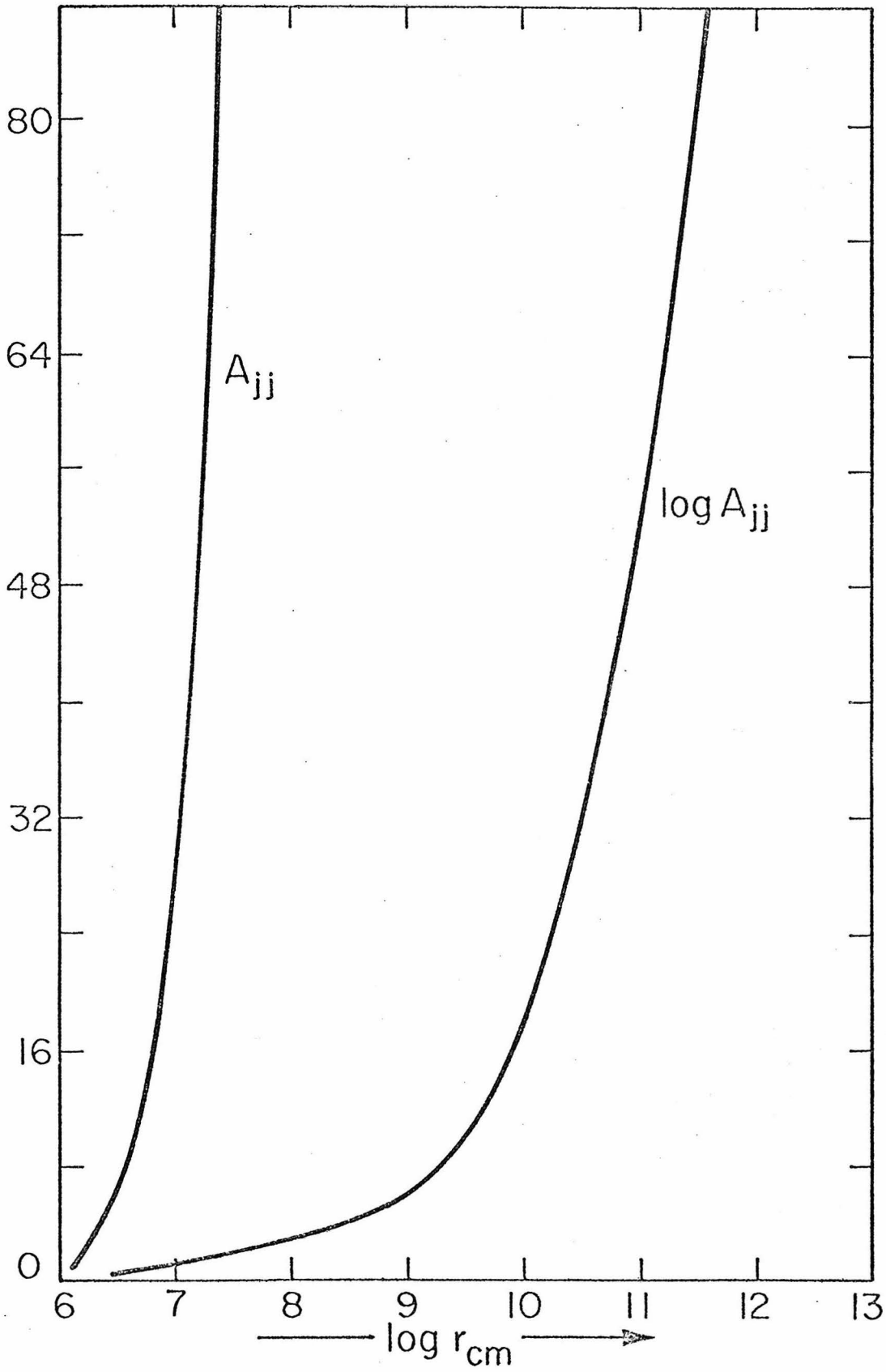

Fig. 5

FIGURE 6: Ratio - $A_{jj}(r) / B_{jj}(r)$ versus $\log_{10} r$ for isotopes with e-folding lifetimes of 2 s and 95 s, in the 16 $M_\odot$, $L_{env} = 89750\ L_\odot$ model of Fig. 4. As discussed in the text, § V.B., the ratio - $A_{jj}(r_p) / B_{jj}(r_p)$ determines the boundary condition to be imposed on the abundance of an unstable isotope at the bottom of the "diffusive zone" of the star. Note that the ratio as a function of r approaches its photospheric value rapidly, at $r \ll r_p \approx 8 \times 10^{13}$ cm. (The ratio is infinite at $r_o \equiv 12.5$ km, where $B_{jj}(r_o) \equiv 0$.) See § V.D. for additional discussion.

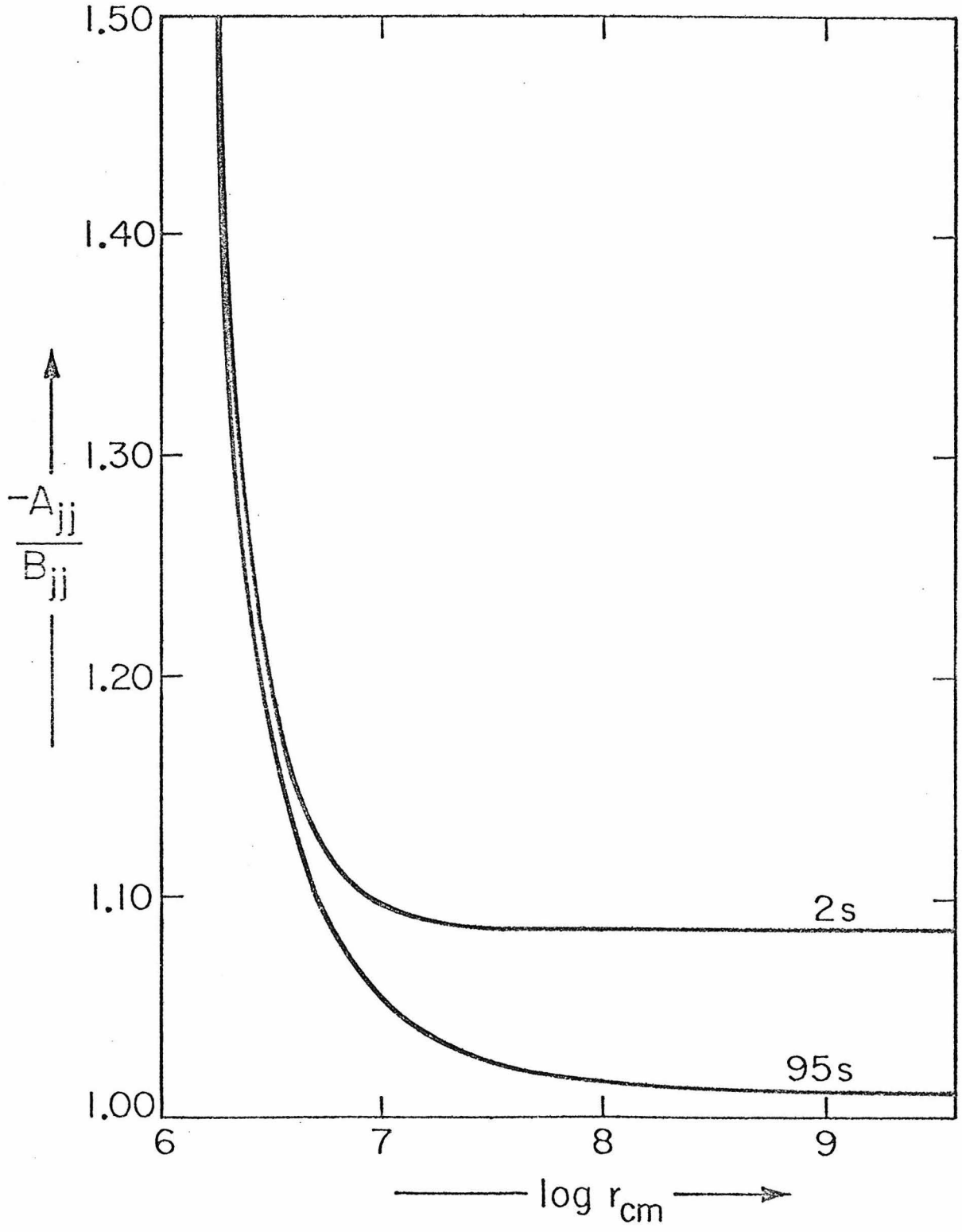

Fig. 6

FIGURE 7: Ratio - $A_{jj}(r_p)$ / $B_{jj}(r_p)$ versus (1 s)/lifetime for the 16 $M_\odot$ total mass envelope models with luminosities L_{env} of 89500 $L_\odot$, 89750 $L_\odot$, and 90000 $L_\odot$. As discussed in § V.B. (Eq. (11) and accompanying text), the ratio of the abundance of an unstable isotope "j" coming up out from the "burning zone", $(Y_{up})_j$, to the abundance at the bottom of the "diffusive zone", $(Y_o)_j$, is constrained to be exceedingly close to - A_{jj} / B_{jj} in order to match onto the physically-reasonable dying exponential solution of the diffusion equation. Note that over the whole range of lifetimes shown, from 0.7 s to infinity, the ratio - A_{jj} / B_{jj} remains within 20 per cent of unity. This fact implies that to reach equilibrium, an unstable species must build up its concentration at the bottom of the "diffusive zone" until almost as much is present as is coming out of the "burning zone" each cycle. In other words, transport by diffusion of unstable products of nucleosynthesis is not very efficient in removing "wastes" from the region in which they are produced. It follows that diffusion will not be able to bring in usable "fuel" with much efficiency either, and the production of luminosity by nuclear reactions will be hindered. Note also that the curves for various L_{env} cross each other in the vicinity of lifetime τ = 50 s. See § V.D. for discussion.

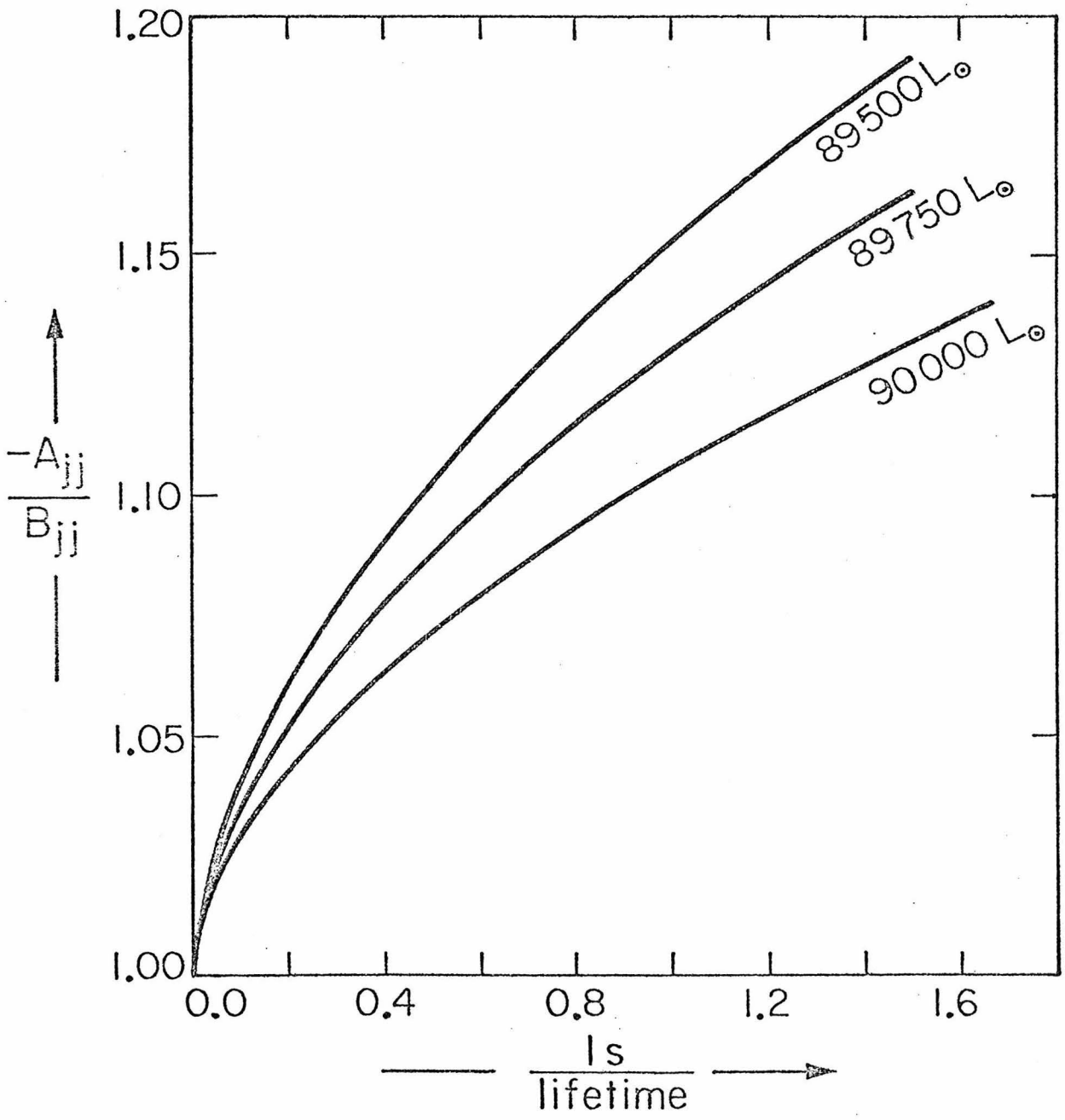
1.20
1.15
1.10
1.05
1.00
$-\frac{A_{jj}}{B_{jj}}$
89500 L⊙
89750 L⊙
90000 L⊙
0.0
0.4
0.8
1.2
1.6
$\frac{1s}{\text{lifetime}}$

Fig. 7

FIGURE 8: Graph of $A_{ss}(r) \equiv 1 + C\, r_o \rho_o D_o \int_{r_o}^{r} (r^2 \rho D)^{-1}\, dr$,

for envelope models with L_{env} of 89500 $L_\odot$, 89750 $L_\odot$, and 90000 $L_\odot$. $A_{ss}(r)$ was defined in § V.C., Eqs. (14); it is equal to the relative abundance at radius r of a stable isotope which is completely consumed in the "burning zone" and which has no beta-decaying parents. Note that long before the photosphere has been reached, $A_{ss}(r)$ has settled down to a constant value. This shows that the outer envelope is indeed a "reservoir" or material for the "burning zone" to draw upon. See § V.D. for additional discussion.

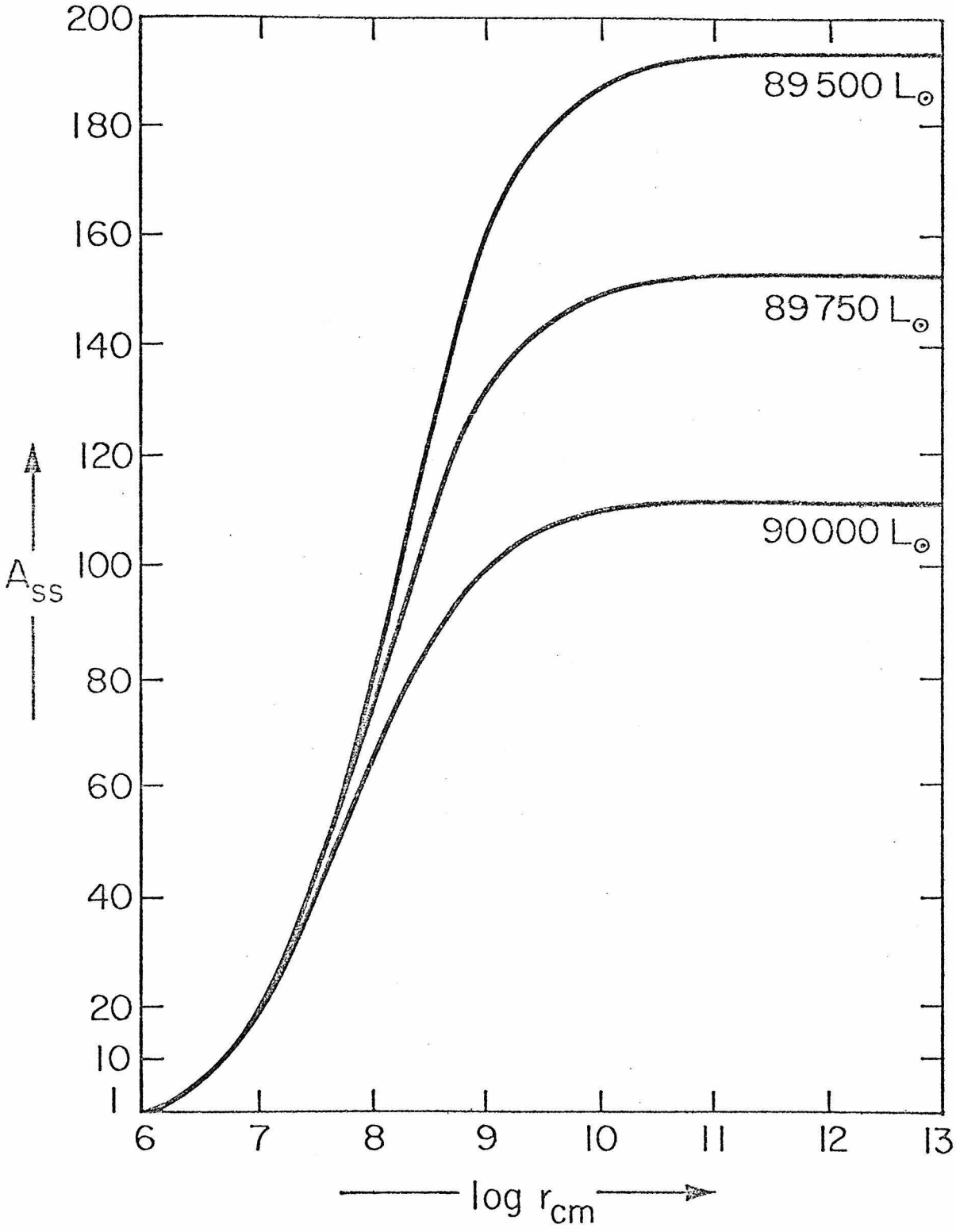
200
180
160
140
120
100
80
60
40
20
10
1
A_{ss}
89 500 $L_\odot$
89 750 $L_\odot$
90 000 $L_\odot$
6
7
8
9
10
11
12
13
log r_{cm}

Fig. 8